Biochemical characterisation of the cyanobacterial Hik2-Rre1 two-component regulatory system

Iskander Mohamed Ibrahim

School of Biological and Chemical Sciences

Queen Mary, University of London

A thesis submitted for the degree of Doctor of Philosophy

February 2013

Statement of originality

I certify that this thesis and the research it describes are entirely the product of my own work. Any ideas or quotations from the work of other people published or otherwise, are fully acknowledged in accordance with the standard referencing practices.

Iskander Mohamed Ibrahim

February 2013

Abstract

Two-component signal transduction systems (TCS) consist of a sensor histidine kinase and a response regulator. TCS are ubiquitous in prokaryotes, but found only in some eukaryotes. TCS mediate adaptation to various environmental changes in bacteria, plants, fungi, and protists. Histidine kinase 2 (Hik2) is a sensor histidine kinase found in all cyanobacteria. The Hik2 homologue known as Chloroplast Sensor Kinase is found in algae and plants, where it is encoded by the nuclear genome and it is targeted to chloroplasts. CSK couples the redox state of the photosynthetic electron transport chain to chloroplast gene transcription. This thesis describes biochemical characterisation of the signal transduction mechanism of Hik2 and its response regulator (Rre) partners in order to clarify the Hik2-Rre two-component signal transduction pathway. Results presented in this thesis illustrate that the autophosphorylation activity of the full-length Hik2 protein is specifically inhibited by sodium ions. An autophosphorylation event of a histidine kinase is the result of homodimerisation and is followed by trans or cis-autophosphorylation of each monomer on its conserved histidine residue. Chemical crosslinking revealed that the Hik2 protein exists predominantly as a phosphorylated (autokinase active) monomer, tetramer, and higher-order oligomeric complexes. The functions of these different oligomeric states of Hik2 are also discussed. From a previous study, which was based on an observation from a yeast two-hybrid assay, Hik2 was proposed to form a two-component pair with Rre1 and RppA. However, no further evidence was presented to support either direct interaction or direct phosphotransfer activity of the Hik2-Rre pair. This thesis confirms interaction of Hik2-Rre1 and Hik2-RppA two-component

pairs using an *in vitro* pull-down assay and phosphotransfer kinetics. Finally, a model is proposed for the Hik2 based two-component signal transduction pathway.

This thesis is dedicated to my family

Acknowledgments

I want to thank my supervisor professor John Allen for allowing me to conduct an interesting undergraduate final year project at his lab, which then followed with a PhD position. I am practically thankful to professor Allen for his inspirational scientific philosophies, and for give me the freedom to embark on the research that led me to write this thesis. I am grateful to Carol Allen for her support and encouragement.

I thank Dr. Sujith Puthiyaveetil for introducing me to the world of two-component signal transduction during my final year undergraduate project thesis and for his continues advices and supports during the course of my PhD. I thank Mr. Wilson de Paula for his valuable discussions and for his generous supports. I am grateful to Christine Ramsey for her help on the ATP-binding activity of CSK as part of her final year project at Queen Mary, University of London. I am thankful to Dr. Norbert Krauss, Dr. Soshichiro Nagano, Dr. Kristina Zubow, and Dr. Jon Nield for their helps on crystallisation and electron microscopy for determination of CSK and Hik2 structures. I want to thank Mrs. Brenda Thake, Dr. Brendan Curran, Dr. Mulugeta Worku, and Mr. Costas Zacharias for their encouragements and supports throughout my PhD research.

I am grateful to my family; my mother, Selam Bekel; my sister, Sara Ibrahim; my brothers, Ilyas Ibrahim and Abraham Ibrahim; and my cousins, Brook Zeramichael, Hana Feysa, and Abera Cheru for their patients, supports and encouragements when I most needed it. I acknowledge Queen Mary, University of London for a postgraduate teaching assistant research studentship.

Abbreviations

ADP	adenosine 5'-diphosphate
ATP	adenosine 5'-triphosphate
DBMIB	dibromothymoquinone
BSA	bovine serum albumin
Ca^{2+}	calcium
DNA	deoxyribonucleic acid
FAD	flavin adenine dinucleotide
GTP	guanosine triphosphate
kDa	kiloDalton
L	litre
Mg^{2+}	magnesium
Mn^{2+}	Manganese
μg	microgram
μCi	microcurie
μL	microliter
μM	micromolar
mL	millilitre
mM	millimolar
nL	nanolitre
nm	nanomolar
NADH	nicotinamide adenine dinucleotide
NADPH	nicotinamide adenine dinucleotide phosphate
PMSF	phenylmethanesulfonylfluoride
PCR	polymerase chain reaction
RNA	Ribonucleic acid
rpm	rotation per minute
SDS-PAGE	sodium dodecyl sulfate polyacrylamide gel electrophoresis

ycf	hypothetical chloroplast open reading frame

Table of contents

Chapter 2: Methods and materials

Chapter 3: Phylogenetic distribution of Hik2

Chapter 4: Signal perception by Hik2

Chapter 5: oligomeric state of Hik2

List of figures

Chapter 1

Chapter 2

Chapter 3

Chapter 4

Chapter 5

Chapter 6

Chapter 7

Chapter 8

Chapter 9

List of tables

Chapter 2

Chapter 1
Introduction

1.1. Two-component signal transduction

Unicellular microorganisms – bacteria and algae, and also some complex multicellular organisms such as plants have little ability to change their surrounding environments. Therefore, in order to enhance their chances of survival, they must possess mechanisms that allow them to continuously monitor and to rapidly acclimate to ever-changing environmental conditions.

Sensor-response circuits known as 'two-component systems' (TCSs) are utilised to mediate adaptations to various environmental changes in prokaryotes as well as in plants, fungi, protozoa, and archaea. The simplest form of TCS consists of two conserved proteins, a sensor histidine kinase (component 1) and a response regulator (component 2) protein (see figure 1.1.A). The second form of TCS consists of a multicomponent sensor histidine kinase known as a hybrid histidine kinase, a histidine phosphotransfer protein, and a response regulator protein (see figure 1.1.B).

1.2. Reactions that are catalysed by two-component systems

Three basic phosphotransfer reactions are catalysed by two-component signal transduction systems. The first reaction involves an autophosphorylation of histidine kinase on its conserved histidine (His) residue. The second reaction involves the transfer of phosphate from phospho-His to a conserved aspartate residue of the response regulator protein. Finally, the phosphate is released from

the response regulator as inorganic phosphate by addition of a water molecule in a hydrolysis reaction catalysed either by RR alone or with the help of histidine kinase (Stock *et al*, 2000).

1.3. Domain architecture of typical histidine kinase

Most histidine kinases are membrane proteins. But some exist as water-soluble cytoplasmic, sensor proteins. Membrane bound and soluble histidine kinases are homodimeric in their functional forms. Each monomer of histidine kinases contains a variable N-terminal sensor domain that is unique to each histidine kinase. The sensor domain is linked to a conserved C-terminal core kinase domain that is further divided into two functional domains. The first is the dimerisation and phosphoacceptor domain (DHp domain), also annotated as HisKinase_A domain in the Pfam database (Finn *et al*, 2006). The second domain is the catalytic and ATP-binding (CA) domain, also referred to HATPase in the Pfam database. The DHp domain contains the conserved phosphoryl-accepting histidine residue that is a site for autophosphorylation. The CA domain contains an ATP binding cavity, which, upon binding an ATP molecule, catalyses the transfer of γ phosphate group from the ATP molecule to a conserved histidine residue.

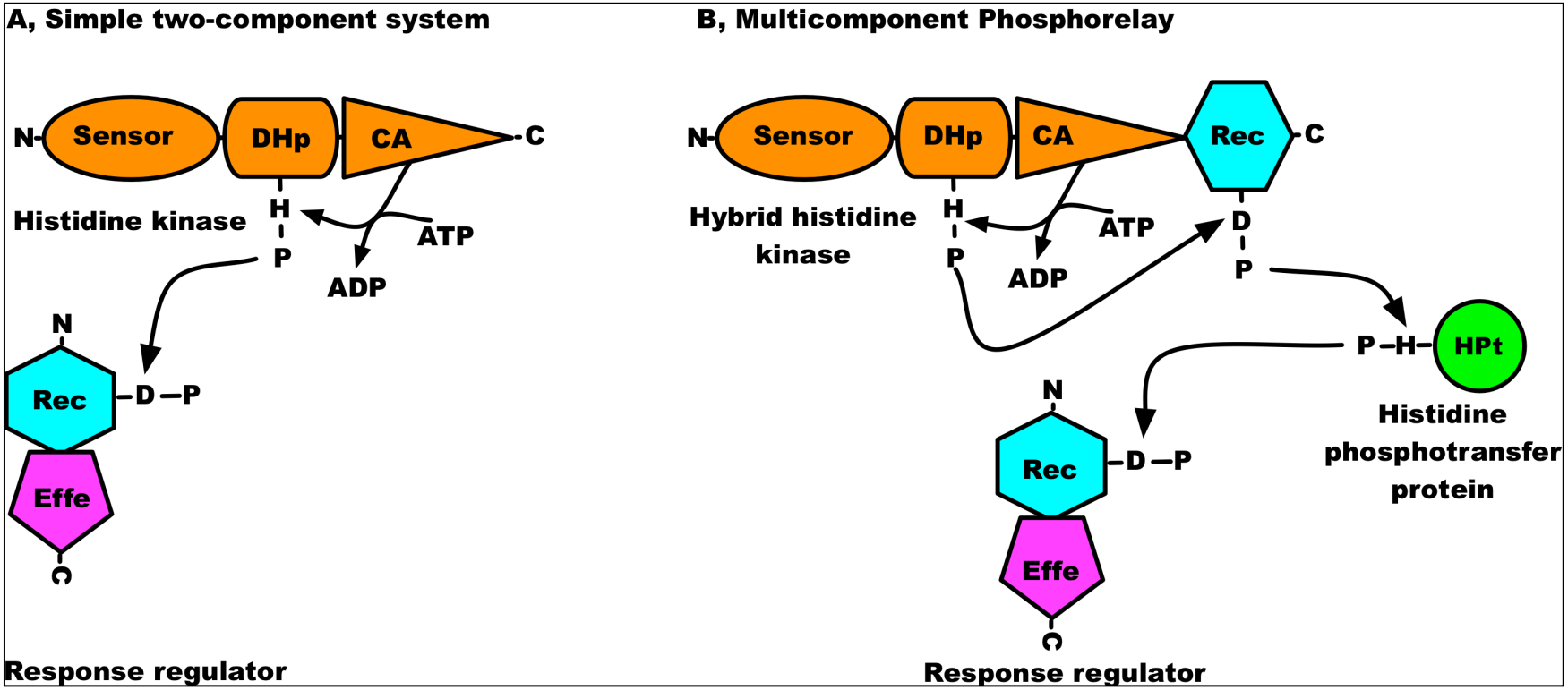

Figure 1.1 Domain architecture of two-component system. A) a simple two-component system and B) a multicomponent phosphrelay. The sensor domain is indicated by oval; the dimerisation and phosphoaccepting (DHp) domain by a cylinder; the catalytic and ATP-binding (CA) domain by a triangle; receiver (Rec) domain by a hexagon; effector (Effe) domain by a pentagon; and histidine phosphotransfer protein (HPt) by circle.

1.4. Diversity of sensor domains of histidine kinases

A sensor domain of HK is the non-conserved region that is located at the N-terminal region of HK polypeptide. Based on topology, sensor domains are categorised into three major classes. i) HKs which have their sensor domain located in periplasmic space of the cell; ii) HKs which are able to perceive signal(s) using their transmembrane region; iii) and finally, those HKs which have sensing domain confided to their cytoplasmic region (Gao & Stock, 2009; Mascher *et al*, 2006).

Signal perception by periplasmic-sensor domains of HK is achieved by direct interaction between the signalling molecule and the sensory domain. For example, the *Salmonella entrica* PhoQ HK directly binds divalent cations such as Mg^{2+} and antimicrobial peptides (Chakraborty *et al*, 2010). The sensory domains of *Klebsiella pneumonia* CitA, *Sinorhizobium meliloti* DctB, *Vibrio cholerae* DctB, and the *Escherichia coli* Dcus are known to bind small metabolites such citrate and C_4-dicarboxylates such as fumarate, succinate, and malate (Sevvana *et al*, 2008; Zhou *et al*, 2008).

Sensor domains that are involved in signal perception from the periplasmic or extracellular space are distinguished by their N-terminal

periplasmic sensing region, which is flanked by a transmembrane domain at either end of the sensor domain. The prototypical periplasmic space sensor HK has a "linker" region that connects the sensory domain to the C-terminal kinase domain. Various forms of linker regions are found, such as HAMP (named after their first discovery in Histidine kinase, Adenylyl cyclase, Methyl-accepting protein, and Phosphatases) and PAS (named after three proteins, Per-Arnt-Sim) domain (Gao & Stock, 2009; Mascher *et al*, 2006).

Based on recently solved structures, the periplasmic space sensor domains are further categorised into three classes; class 1 contains alpha-beta folds and they were given the term PDC (PhoQ, DcuS, and CitA) (Cheung & Hendrickson, 2010). PDC forms central five-stranded anti-parallel β-sheet scaffold. The second class of periplasmic-sensing domain has all-alpha folds that form four-helix bundles such as those found in NarX (see figure 1.2). The third class contains sensor domains that show a similar fold to periplasmic ligand binding proteins (Cheung & Hendrickson, 2010).

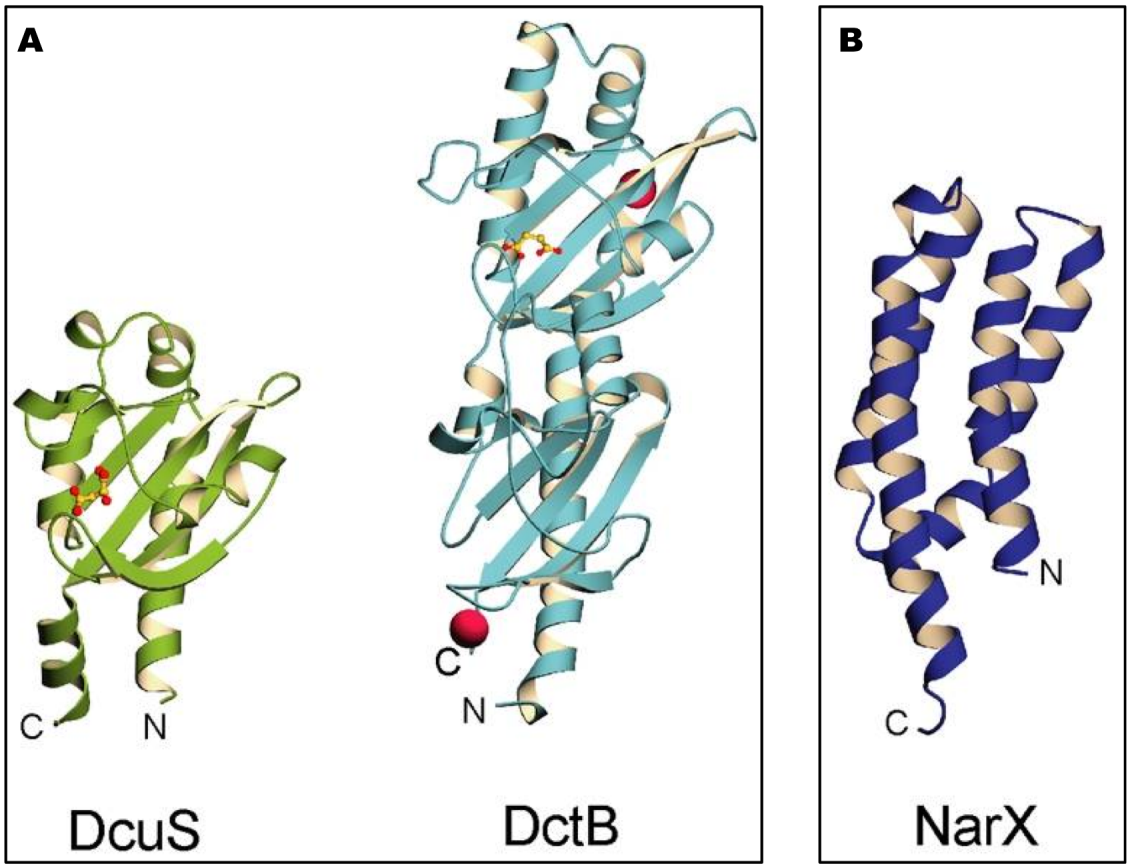

Figure.1.2 Architectures of periplasmic space sensor domains. A ribbon diagram showing sensor domains with: A) PDC folds (D-malate- bound DcuS and succinate and calcium bound DctB). None protein moieties are represented by ball-and-stick; carbon atoms are shown in yellow, oxygen in red, and calcium in magenta. B) All-alpha folds (NarX). Figure adapted from (Cheung & Hendrickson, 2010)

Representative histidine kinases

Domain architecture of histidine kinases

Phosphotransferase and histidine kinases without a sensor domain

Spo0B

Hik2-ike

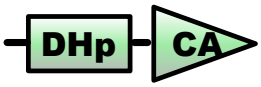

CheA

Histidine kinases with soluble sensor domain

Hik34-like

Hik2-like

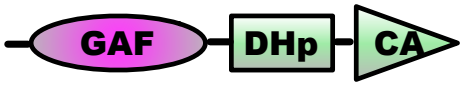

NtrB like

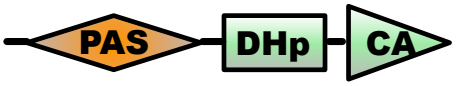

Phytochrome-like

ArcB

FixL like

Hik33-like

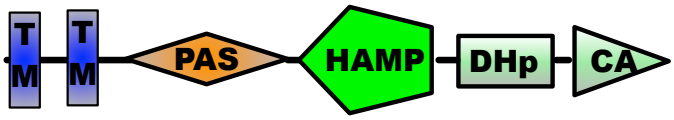

Histidine kinases with soluble sensor domain

PhoQ/Vir-like

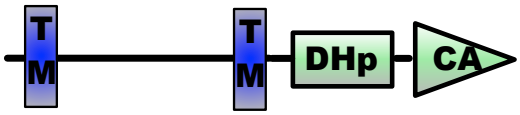

CitA-like

BvgS-like

Histidine kinases with transmembrane sensor domain

Desk, CorS-like

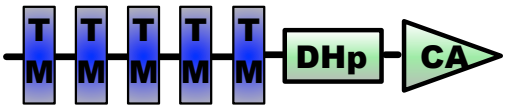

RegB, ArgC, ComD-like

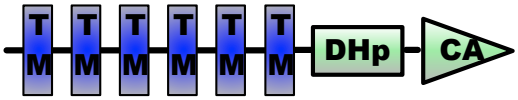

CamP-like

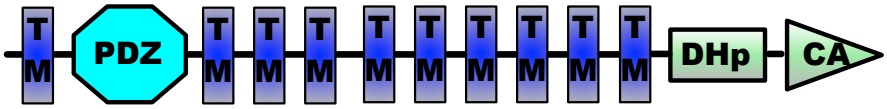

AtETR1

Figure 1.3 Diversity of domain architecture of histidine kinases. Domain architectures of histidine kinases were modified from graphical output of SMART database (Schultz et al, 1998). The conserved DHp and CA domains are depicted by green rectangle and triangle, respectively. The sensor domain GAF (named after its present in cGMP-specific phosphodiesterases, in certain adenylyl cyclases, and in transcription factor FhlA) domain is depicted by magenta oval shape; the PAS (named after three proteins, Per-Arnt-Sim) domain is shown by orange parallelogram; the PAC domain is shown by cyan triangle shape; TM (transmembrane) domains are shown by blue rectangle; HAMP (named after its present in Histidine kinases, Adenyl cyclases, Methyl- accepting proteins and Phosphatases) domain is shown by green pentagon; PBPs (bacterial periplasmic solute-binding proteins) domain is shown by purple hexagon; PDZ domain is shown by cyan octagonal shape; CHASE domain is shown by yellow rectangle. A receiver domain is depicted by red hexagon; HPT (histidine phosphotransferase) is depicted by gray rectangle; Chew (Chemotaxis W like adaptor domain) is shown by yellow parallelogram.

Sensing mechanisms that are embedded into the transmembrane region of histidine kinase polypeptide utilises the transmembrane (TM) domain for signal perception and transduction. HKs with this type of sensing mechanism usually have multiple TM domains and lack an obvious extracellular domain. The temperature sensor DesK, for example has five TM domains that are essential for its temperature sensing activity (Mascher et al, 2006). The *Arabidopsis* Etr1 histidine kinase detects ethylene via its hydrophobic N-terminal TM domain (Bleecker & Schaller, 1996). Finally, the redox sensor, SenS interacts with heme binding protein HbpS via its N-terminal TM domain (Ortiz de Orue Lucana & Groves, 2009).

Histidine kinases with cytoplasmic sensing domain are either entirely cytoplasmic soluble proteins, such as phytochrome (Moglich *et al*, 2010), CSK (Puthiyaveetil *et al*, 2008), NtrB, DosS (Ioanoviciu *et al*, 2007); or they are membrane bound HKs with their cytoplasmic sensing domain located at the N-terminus, just before the first TM or after the last TM domain, just before the kinase domain. For example, the K^+ or salt stress sensor KdpD (Steyn *et al*, 2003) (Heermann & Jung, 2010) has its sensory domain located before the transmembrane domain. Also, the redox sensor ArcB histidine kinase possesses a PAS domain found just after the last TM, just before the kinase domain (Malpica *et al*, 2004).

Many histidine kinases with cytoplasmic sensing domains adopt a true PAS-fold that is similar to that found in ArcB, but differ from that found in PDC-fold described above. A PAS domain is formed of 5-stranded anti-parallel *β*-sheets that are flanked by *α*-helices. PAS domains are known to bind small cofactors such as heme, FAD, and NADH. HKs with PAS domains are therefore excellent reduction-oxidation (redox) sensors (Allen, 1993). Indeed, the FixL histidine kinase from *Rhizobium meliloti* contains a heme-cofactor for sensing the redox state of O_2 gas (Miyatake *et al*, 2000). The *Klebsiella pneumonae* two-component system NifL is another example of a redox sensor. NifL contain a FAD-cofactor that is again a sensor of the redox state of O_2 gas (Grabbe & Schmitz, 2003).

1.5. Structure and function of kinase domain of histidine kinases

The core kinase domain of a histidine kinase has two conserved domains – the DHp and the CA domains, which have characteristic conserved motifs that are also referred to as boxes, play important roles in the autokinase and substrate dephosphorylation activities of histidine kinases. These are H, N, G1, F, G2, and G3 boxes. The H-box of HK is characterised by the conserved histidine residue. The conserved histidine residue serves as the site for autophosphorylation. The DHp domain is formed of a four-helix bundle, with two helices from each monomeric histidine kinase polypeptide. As well as being an autophosphorylation site and dimerisation domain, the DHp domain plays an important role in

conferring specificity between the sensor histidine kinase and its conjugate response regulator partner.

The overall structure of the CA domain is formed of layered α/β sandwiched fold (see figure 1.4.B), composed of three helices and five stranded β-sheets. The overall fold of the CA domain is distinct from that of Ser/Thr or Tyr kinases. But it has a strong similarities with the ATP binding domain of DNA topoisomerase II (Roca & Wang, 1992), Gyrase B (Ali *et al*, 1995), the chaperone Hsp90 (Panaretou *et al*, 1998), and the DNA repair enzyme MutL (Ban *et al*, 1999). The CA domain is characterised by its conserved sequence motifs; N, F, G1, G2, and G3 boxes that are important for stabilisation of an ATP molecule and for the hydrolysis of the γ-phosphate. The N-box and G1-box are involved in the stabilisation of an adenine ring of an ATP molecule. In particular, a conserved aspartic residue found within the G1-box forms a hydrogen bond with the amino N6 of an adenine base (Marina *et al*, 2001; Trajtenberg *et al*, 2010). This interaction is crucial for conferring specificity to an ATP molecule and to prevent the binding of other nucleotides such as GTP. CA domains discriminate nucleotides such as GTP based on the fact that they lack the amino group required to forming a hydrogen bond with the carboxyl group of the conserved aspartic acid found in the G1-box. The F-box, which is the less conserved region CA domain and the G2-box together forms a flexible loop that acts as the ATP-lid and controls the entry of the ATP-Mg^{2+} complex and the release of the ADP-Mg^{2+} complex. Conserved glycine residues the G2-box facilitates the flexibility of the ATP-lid (Marina *et al*, 2001).

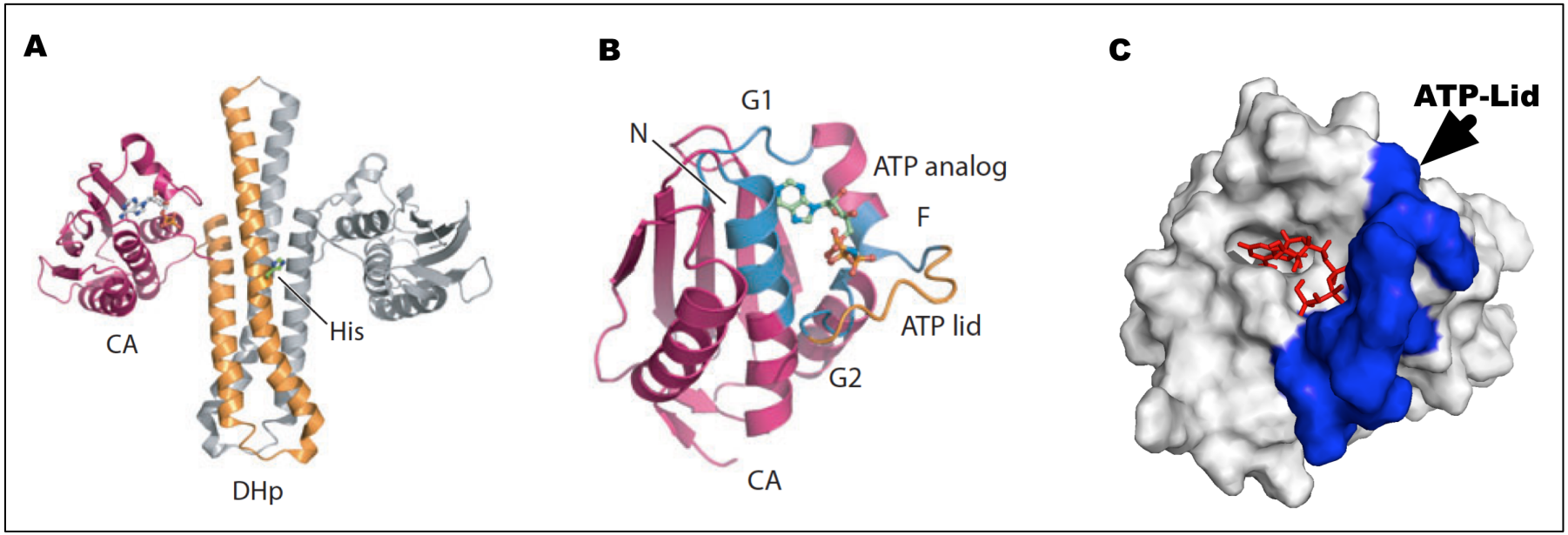

Figure 1.4 Architecture of core-kinase domain of histidine kinase. A) Ribbon representation of kinase core domain of histidine kinase, the DHp (dimerisation and phosphoacceptor) domain is coloured orange; the CA (Catalytic and ATP-binding) domain is coloured magenta. **B**) Ribbon representation of CA domain. The conserved motifs (N, G1, F, and G2) are indicated. ATP analogue, AMP-TNP (5′-Adenylylimidodiphosphate) is represented by ball-and-stick (A,B) renderings in each case. **C**) Molecular surface of CA domain (PDBID: 1id0). AMP-TNP molecule is represented by stick in red; the ATP-lid is represented in blue. Figure adapted from (Gao & Stock, 2009).

1.6. Response regulator

The second component in two-component system is a response regulator (RR) protein. Response regulators usually contain a helix-turn-helix DNA binding domain that function as transcriptional activators or repressors. However, some RRs do not have a DNA binding domain, and do not take part in transcriptional control (figure 1.5). Instead, about 15 % of receiver domains are not attached to an output domain and function by interacting with other proteins. And others participate in enzymatic activities such as: methylesterase (Anand *et al*, 1998), diguanylate cyclase (Ryjenkov *et al*, 2005), protein phosphatase (Shi, 2004). The CheB response regulator from *E.coli* has a typical response regulator receiver domain that is coupled to C-terminal methylesterase domain. The inactive form of CheB inhibits the active site of methylesterase domain. Inhibition of CheB is removed upon phosphorylation on receiver domain by the CheA histidine kinase. Like CheB, the PelD response regulator of *Caulobacter crescentus* has non-DNA binding domain, instead it has diguanylate cyclase activity (Chan *et al*, 2004).

RRs have a conserved input (receiver) domain and a highly variable effector domain. A receiver domain catalyses a phosphoryl transfer from phosphorylated histidine kinase to its conserved aspartic acid (Volz & Matsumura, 1991). The overall structure of a receiver domain is formed of conserved α/β folds, consisting of five-stranded parallel β-sheets that are surrounded by five amphipathic helices (Volkman *et al*, 1995). The catalytic cleft of a receiver domain has conserved acidic residues termed D2 with a conserved

motif "DDD/E" which serves as a dication-binding site for Mg^{2+} or Mn^{2+} (Stock *et al*, 1989). The second conserved acidic region is termed D1 and has a conserved aspartic acid that is a site for phosphorylation. The receiver domain exists at equilibrium between active and inactive conformations. Phosphorylation thus stabilizes the active conformation and thereby shifts the equilibrium toward the active RR.

Phosphorylation plays an important role in linking the signal from the input domain to the effector domain. This role involves phosphorylation-induced conformational changes that control the structure of α4-β5-α5 of the receiver domain. For many receiver domains, α4-β5-α5 are crucial for protein-protein interactions and are involved in dimerisation of RR. Thus phosphorylation-induced dimerisation seems to be the mechanism of response regulator activation. Although phosphorylation stabilizes an active RR, and facilitates promoter binding, it will not always lead to transcriptional activation. Transcriptional initiation is governed by many factors, such as interaction with other activators or repressors, and the location of DNA that RR binds (Maris *et al*, 2002).

Although phosphorylation plays an important role in promoter binding, it has been reported that some RRs can bind promoters even in their dephosphorylated form; however, phosphorylation seems to be required for transcriptional initiation. Moreover, a response regulator can act both as a transcription initiator or repressor. The dual activity of RR is governed by the

location of its promoter-binding site. If the RR is bound upstream to the target gene, it usually has a transcriptional activation role, whereas if it is bound downstream to the target gene, then it has a transcriptional repressor role.

Representative response regulators	Domain architecture of response regulators
Stand-alone receiver domain	
CheY and Spo0F like	
Response regulators with helix-turn-helix (HTH) DNA binding domains	
NarL like HTH	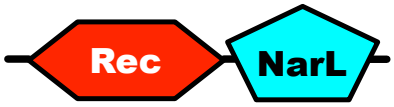
AraC like HTH	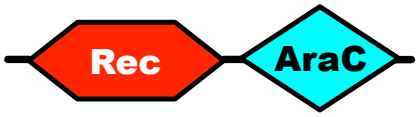
Fis like HTH	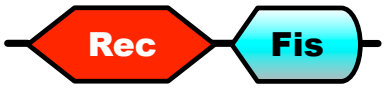
LytR-like HTH	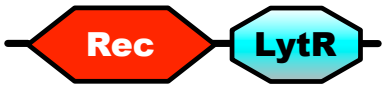
NtrC like	
Response regulators with Enzamatic activity	
PleD-like	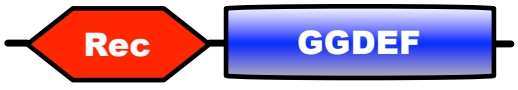

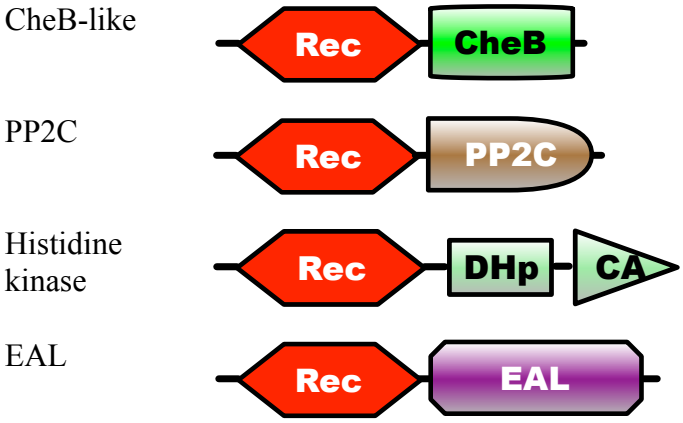

Figure 1.5 Diversity of domain architecture of response regulators. Domain architectures of response regulators were modified from graphical output of SMART database (Schultz et al, 1998). Based on the role of effector domain, representative response regulators are divided into three categories: stand-alone receiver domain depicted by red hexagon; response regulators with helix-turn-helix DNA binding domain, such those belong to NarL, AraC, Fis, LytR, or NtrC families are depicted. The third category contains an effector domain that contains enzymatic activity such as GGDEF (Diguanylate cyclase), CheB (chemotactic methylestrase), PP2C (protein phosphatase 2C), DHp and CA (histidine kinase core kinase domain), and EAL (c-di-GMP phosphodiesterase).

1.7. Photosynthesis

Oxygenic photosynthesis converts light energy from the sun into useful chemical energy. This important biological process takes place in some prokaryotes and in chloroplasts, – bioenergetic organelles of eukaryotic plants and algae. In photosynthesis in chloroplasts and cyanobacteria, light-driven primary electron transfer is carried out by the photochemical reaction centers of two photosystems, photosystem II (PS II) and photosystem I (PS I). A mobile electron carrier – plastoquinone (PQ) – in the thylakoid membrane is a link in the electron transport chain that connects these two reaction centres in series via the cytochrome b_6f complex. The reduction-oxidation (redox) state of the pool of PQ molecules determines the distribution of excitation energy between photosystem II and I by controlling the reversible phosphorylation of polypeptides of light harvesting complex II (LHC II) (Allen, 1992; Allen *et al*, 1981) in chloroplasts; however, the exact mechanism that govern the redistribution of phycobilisome in cyanobacteria and algae is yet to be determined.

The redox state of the PQ pool also plays an important role in controlling transcription of chloroplast DNA, regulating expression of genes that encode reaction-center proteins of photosystem II and I, and thus initiating a long-term acclimatory process known as photosystem stoichiometry adjustment (Pfannschmidt *et al*, 1999). In cyanobacteria, prokaryotes from which chloroplasts

originated, a similar redox control of photosystem stoichiometry is observed (Fujita, 1997; Murakami *et al*, 1997).

The PS II is a large homodimeric complex that functions as a light-driven water:plastoquinone oxidoreductase (figure.1.4A). The PS II complex of higher plants and cyanobacteria is composed of 22 and 17 polypeptides, respectively. The PSII complex comprises a chlorophyll pigment antenna, a P680 reaction centre, and the water splitting complex. Each monomer of PS II RC core complex includes one oxygen-evolving complex (OEC), two pheophytin (Pheo) molecules, two chlorophyll a (Chl a) molecules, two plastoquinone (Q_A and Q_B) molecules, and two heterodimer subunits, D1 and D2 (the letter 'D' is for a 'diffuse' appearance on the SDS-PAGE) that contain five transmembrane helices each. D1 and D2 polypeptides are products of the chloroplast *psbA* and *psbD* genes, respectively. The D1 polypeptide binds one molecule of Pheo, one molecule of Chl a, and Q_B. The D2 polypeptide binds one Chl a molecule, one Pheo molecule, and Q_A molecule. Both D1 and D2 polypeptides bind a P680 reaction centre and a conserved redox active tyrosine 161 that is found in the D1 polypeptide transfers electron from the OEC to the P680 RC. The CP47 and CP43 proteins are core antenna subunits of PSII, with each subunit containing six transmembrane helices.

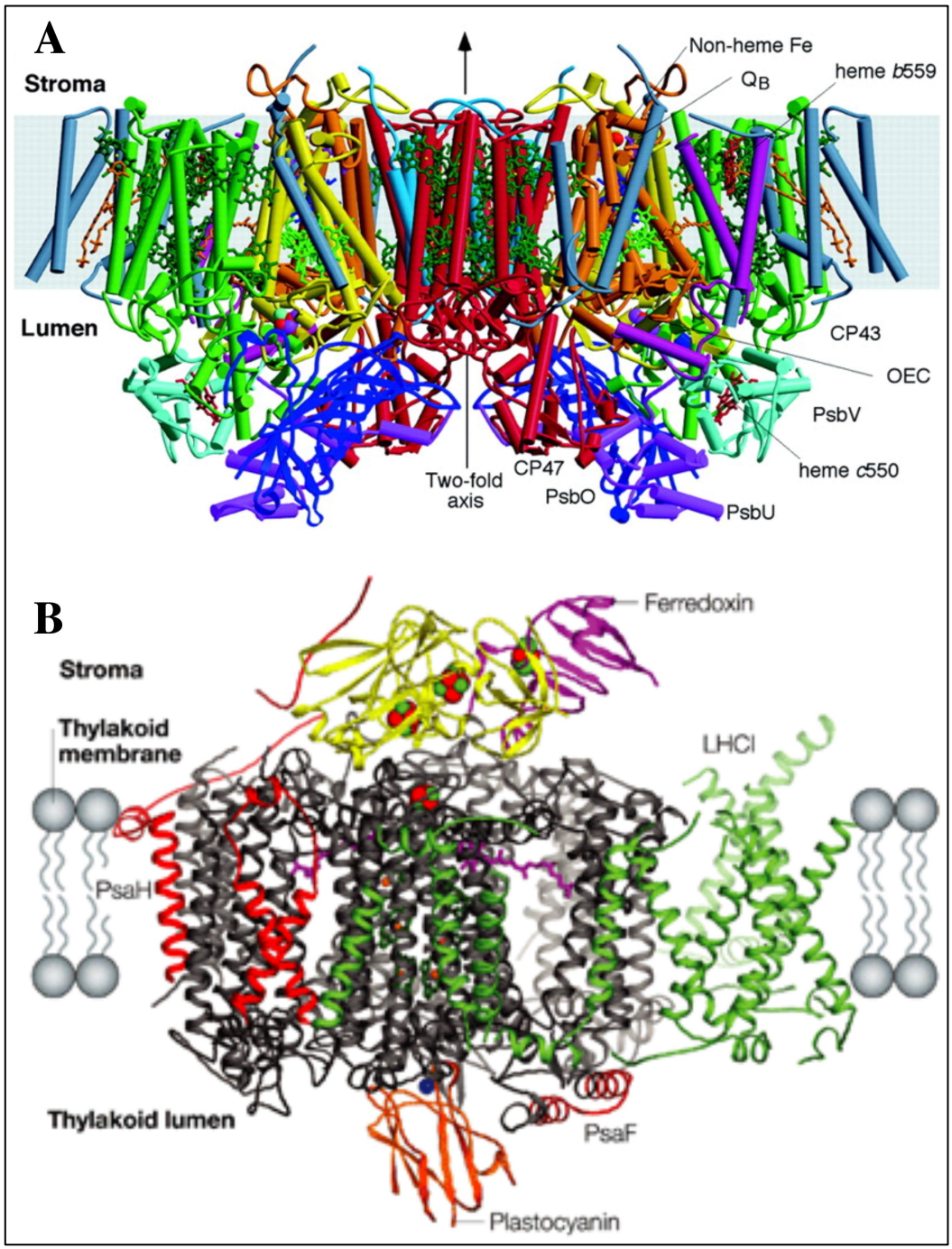

Figure 1.6 Architectures of photosystem II and I. A) Crystal structure of photosystem II dimer complex from cyanobacterium, *Thermosynechococcus elongatus* viewed parallel to the membrane plane (Ferreira *et al*, 2004). α-helices are represented as cylinders. B) Ribbon representation of structure of chloroplast photosystem I complex from plant, *Pisum sativum*, as viewed parallel to the membrane plane (Nelson & Ben-Shem, 2004).

Figure 1.7 Architectures of cytochrome b_6f complex and ATPase. A) Crystal structure of cytochrome b_6f complex from *Chlamydomonas reinhardtii* viewed parallel to the membrane plane. The porphyrin rings of heme are shown in red and chlorin ring of the chlorophyll is shown in green. B) Model of chloroplast ATPase. *α*-helices are represented as cylinders; C-ring is represented by orange colour; *γ*-subunit with red; and F_1 subunit with green, gray, and blue (Nelson & Ben-Shem, 2004).

Cytochrome b_6f (cyt b_6f) is a large complex is formed of heterodimer (see figure.1.5.A). Each monomer of cyt b_6f is composed of four large subunits that includes the redox active protein subunits: cyt b_{563} (also known as b_6), cyt *f*, and Rieske iron-sulfur proteins, as well as subunit IV; in addition, each monomer contains four small hydrophobic subunits: PetG, PetL, PetM, and PetN (Cramer *et al*, 2008; Kurisu *et al*, 2003). In higher plants and algae, with the exception to the Rieske iron-sulfur and PetM, all the other subunits are encoded by the chloroplast genome. Cyt b_6f function as a plastoquinone:plastocyanin oxidoreductase, and mediates electron transfer between PS II and I. The transfer of one electron from the doubly reduced plastoquinone (PQH_2) to the high potential electron transfer chain, consisting of Rieske iron-sulfur cluster and cyt *f* results in the release of two protons to the lumen phase. Subsequently, the transfer of second electron from PQH_2 to b_6 hemes results in the removal of a proton from the stromal phase, which results in the proton motive force used to catalyse ATP synthesis.

PS I catalyses the second step in light-induced transmembrane charge separation (See figure 1.4.B). The PS I is a monomeric complex in algal and plant chloroplasts. However, in cyanobacteria, PS I is found as a trimeric protein complex. Each monomer of PSI consists of 12-13 protein subunits and 127 cofactors that are non-covalently attached. PS I contains 96 chlorophyll, 22 carotenoids, 4 lipids, 3 4Fe4S clusters, 2 phylloquinones, and 1 Ca^{2+} ion. The core complex of PS I is formed of a heterodimer of PsaA and PsaB subunits. PsaA/B proteins are encoded by the chloroplast genome. PsaA/B proteins have structural homologies to D1/D2 subunits of PSII and the L and M subunits of the purple

bacterial reaction centre. Furthermore, the N-terminal region of PsaA/B shows homologies to the core antenna proteins CP43/47 of PS II. This observation led to the suggestion that PsaA/B subunits evolved by gene fusion of an ancient reaction centre protein with antenna proteins. Upon photon absorption by a pair of chlorophyll a molecules (an P700 pigment), the excited, strongly reducing P700 transfers an electron to a chlorophyll monomer, which then passes the electron to to a primary electron acceptor (phyloquinone), and onto an iron sulfur cluster (Kraus, 2008). Upon binding of Ferredoxin to PS I from stromal the phase, the electron moves to the reduced iron-sulfur cluster and reduces $NADP^+$ to NADPH in a reaction catalysed by the enzyme ferredoxin-$NADP^+$ reducatase.

Proton translocating ATP synthases (H^+ ATPases) from different sources have a similar over all structure. A hydrophilic part designated F_1 (factor 1), has ATPase activity and the capable of binding ADP and P_i, for the synthesis of an ATP molecule. The F_1 complex can also catalyse the hydrolysis of an ATP molecule to ADP and P_i. The chloroplast F_1 complex consists of five subunits that are designated by Greek letters α, β, γ, δ, and ε. The β-subunit of F_1 adopts three different conformations, two of which ADP and Pi or ATP is bound.

The second part of ATPase is the hydrophobic complex known as F_o or C-ring (Figure 1.5.B). The F_o was discovered after F_1. The F_o functions as a proton pump from high proton gradient to lower proton gradient. Binding of a proton to the C-ring of F_o results in rotation of the ring, this mechanical force is used to

drive the rotation of γ subunit of a F_1, which in turn alters conformation of subunits of F_o and results the synthesis of ATP in the ATP synthesis. In chloroplasts, the F_o transports protons from the lumen to stromal space; in mitochondria, it transports protons from inner membrane space to the matrix; and from the periplasmic space of bacteria to the cytoplasm (Bottcher & Graber, 2008).

1.8. Mechanisms of short-term and long-term adaptation of photosynthetic apparatus

Photosynthesis is optimal when the environment meets species-specific requirements. However, environmental condition fluctuates on the time-scale of minutes to days, which creates unwanted redox imbalance in a linear electron transfer chain (ETC) (Ibrahim, 2009; Pfannschmidt, 2003). Imbalance of redox state of ETC created from uneven light distribution between PSII and PSI has negative effects on the photosystems. For example, reduced PQ promotes the electron to transfer back to PSII, thus leading to the production of the free radical superoxide. Oxygen radical is harmful because of its high rate of reactivity with biological molecules. In case of the chloroplasts, the reactive free radical causes photo-inactivation as well as accumulative chloroplast DNA damage, which may results in incorrectly functional enzymes. Therefore, chloroplasts must have a mechanism(s) to prevent and sequester free radicals.

In chloroplasts, the redox state of ETC is controlled in several ways. In the

short term, pH change within the lumen activates a mechanism known as non-photochemical quenching that allows LHCII to dump about 80 % of the solar energy absorbed as a heat and fluorescence (Muller et al, 2001), thus resulting in the decrease of excitation of reaction centres. However, this mechanism dramatically reduces the efficiency of photosynthesis. The second pathway by which the electron flow between PSII and PSI is maintained at a constant rate is through light transition switch between light state 2 that favours PSI and light state 1 that favours PSII (Allen, 2003a). In the event of high light intensity, the rate of electron flow from PSII will be faster and therefore PSI will become saturated. This imbalance of redox state activates a specific membrane bound enzyme, a protein kinase (Allen, 1992; Allen et al, 1981), termed Stt7/Stn7 (Bellafiore et al, 2005; Depege et al, 2003; Rochaix, 2007). The activation of Stt7/Stn7 leads to phosphorylation of LHCII, which results in the dissociation of LHCII from PSII. Phosphorylated LHCII is no longer bound to PSII and diffuses into the stromal where it associates with PSI and in doing so the work load of each specific photosystem is decreased and the electron flow between them is balanced (see figure 1.8).

In the event of long-term redox imbalance of PQ pool, for example, from hours to days, redox regulation of gene expression will be activated to regulate the relative amount of PSII and PSI supercomplexes (Pfannschmidt et al, 1999). This long-term acclimation process was proposed to utilize a bacterial-type sensor-response circuit for sensing the redox state of PQ-pool and to control the transcription rate of genes coding for core component of photosystems (Allen,

1993; Allen, 2003b). Recently, Puthiyaveetil and Allen discovered a bacterial type sensor kinase termed CSK (Puthiyaveetil et al, 2008). The CSK conveys the redox state of PQ-pool to chloroplast transcription regulators (figure 1.8) (Puthiyaveetil et al, 2010; Puthiyaveetil et al, 2008).

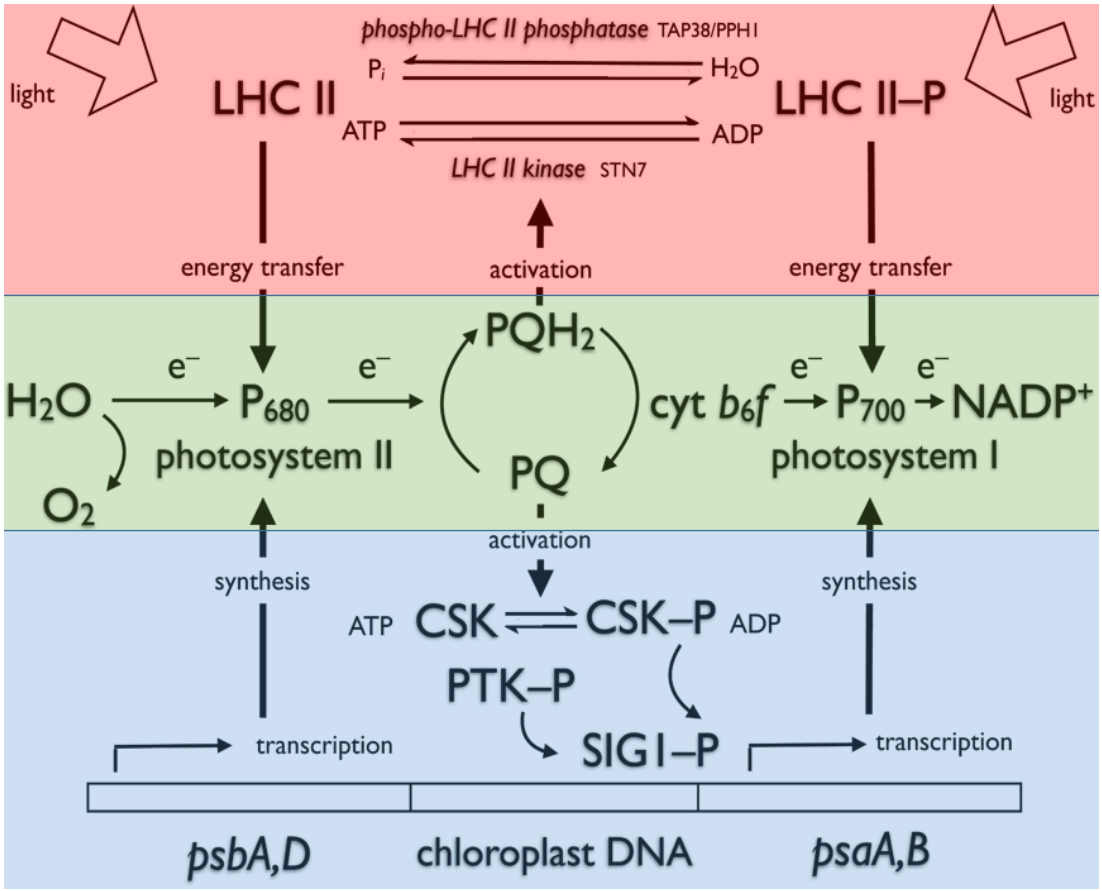

Figure 1.8 Discrete redox signalling pathways controls state transition and photosystem stoichiometry adjustment (figure adapted from (Allen et al, 2011). State transition (red) and redox control of transcription (blue) are controlled by two independent redox states of PQ pool (green). The reduced form of plastoquinone (PQH_2) controls state transition by acting on LHCII kinase, whereas the oxidised form of plastoquinone (PQ) controls the long-term acclimatory process by activating CSK as a protein kinase. The active CSK controls transcription by phosphorylating SIG1, thus phosphorylated SIG1 (SIG-P) inhibits transcription of *psaA,B* genes, while transcription of *psbA,D* genes are unaffected.

1.9. My PhD research

My PhD research aims to elucidate molecular mechanisms of the autophosphorylation and phosphotransfer activities of a conserved two-component system of chloroplasts and cyanobacteria. My research explores how different signals, including redox, are perceived by *Synechocystis* Hik2 and by its homologue, CSK of chloroplasts. This work also explores different oligomeric forms of Hik2 and deduces their autophosphorylation mechanism. Finally, the thesis presents results on functional partners of Hik2 and CSK, deducing functional models on the Hik2-RR and CSK-RR two-component systems using bioinformatics, molecular biology and biochemical techniques.

Chapter 2
Materials and methods

2.1. Purification of nucleic acid

2.1.1. Plasmid DNA

Plasmid DNA was purified from 5 ml *E.coli* cell culture using Qiagen mini-prep plasmid extraction kit. Plasmid DNA was eluted in 50 μL of RNase free water for DNA sequencing or in 50 μL of Tris-HCl (pH 8) buffer for other down stream procedures.

2.2. Quantification of nucleic acid

DNA samples were quantified using a Nanovue Plus (GE Healthcare) spectrometer. An optical density of 1.0 at 260 nm corresponds to a 50 μg mL^{-1} DNA.

2.3. Cloning

2.3.1. Polymerase Chain Reaction (PCR)

Amplification of Synechocystis sp. PCC6803 Hik2 gene – The full-length *Synechocystis* sp. PCC 6803 *hik2* gene (slr1147) encoding for amino acids 1-434 and the truncated form of *hik2* gene encoding for amino acids 175-434 were amplified from *Synechocystis* sp. PCC 6803 genomic DNA (*Synechocystis* sp. PCC 6803 genomic DNA was kindly donated by Mr. Dennis Nuernberg, Queen

Mary, University of London). Primer pairs used for PCR are listed on table 2.1. Primers were purchased from Eurofins MWG Operon, Germany.

Amplification of genes coding for the receiver domain of Rre, RppA, RpaA, and RpaA proteins – Genes coding for the receiver domain of Rre1 (slr1783), RppA (sll0797), RpaA (sll0797), and RpaB (slr0115) were amplified from *Synechocystis* sp. PCC 6803 genomic DNA using the primer pair given in table 2.1 (Synechocystis sp. PCC 6803 genomic DNA was kindly donated by Dr. Luning Liu, Queen Mary, University of London).

Amplification of Arabidopsis CSK gene – The full-length *Arabidopsis thaliana csk* gene (*At1G67840*) (coding for amino acids 1-611) and the truncated version of CSK gene (coding for amino acid 301-611) were amplified from template DNA, the CSK_GFP plasmid construct that was kindly donated by T.A Kavanagh at Cambridge University. The primer pair given in table 2.1 was used.

Table 2.1 Primers used for cloning

– Hik2_F_His (cloned in pET-21b)
Forward: GCGCGCcatatgGCCGGTTCCATCTCA
Reverse: GCGCGCctcgagCACTTGTTCTCCAGAGCG

– Rre1_Receiver_His (cloned into pET-30a+)

Forward: GCGGCGggatccATGGTGGGCTTGAGTTTG

Reverse: GCGGCGctcgagCTAGACGATCGCCTCCAATTC

– RppA_Receiver_His (cloned into pET-30a+)

Forward: GCGGCGggatccATGCGAATTTTGCTGGTG

Reverse: GCGGCGctcgagCTACAGTCTTGCTAATAGCTC

– RpaA_Receiver_His (cloned into pET-30a+)

Forward: GCGGCGggatccATGCCTCGAATACTGATC

Reverse: GCGGCGctcgagCTACACCCGGGCTAACATTTC

– RpaB_Receiver_His (cloned into pET-30a+)

Forward: GCGGCGggatccATGGTGGTCGATGACGAG

Reverse: GCGGCGctcgagCTAGATTCTAGCTTCCAATTC

-CSK-F_His (cloned into customized pJC20)

Forward: GCCGTGcatatgCTTCTTT CTGCAATCGCTTC

Reverse: CGAggatccCTATGCTTCATTGGCTTC

– CSK_T_ His (cloned into customized pETG-10A)

Forward: CACCATGCAGTCATCTTGGCAAAAC

Reverse: CTATGCTTCATTGGCTTC

Note: base pairs in lower case are restriction site overhangs.

Polymerase chain reaction was performed in a total reaction volume of 50 μL containing each deoxynucleoside triphosphates (Fermentas) at a final concentration of 200 μM, 1 X HF Phusion DNA polymerase reaction buffer, 1 μM primer pair, 5 ng of template DNA, and 0.012 units of Phusion DNA polymerase (New England BioLabs). RNase free water was added to a final volume of 50 μL. PCR amplicon DNA was purified from enzymatic reaction buffers using Fermentas gel extraction kit and DNA sample was eluted in 50 μL of Tris-HCl (pH 8).

2.3.2. Restriction endonuclease digest

Double digestion reaction was carried out for the PCR DNA product or for plasmid DNA in a total volume of 50 μL. Each digestion reaction mixture included: 8 μg of PCR product or 4 μg of plasmid, 40 units of the appropriate endonuclease (NEB), 100 μg μL^{-1} BSA (NEB), and 10-fold concentrated NEB-buffer. Volume was adjusted to 50 μL by adding RNase free water. Reactions were incubated at 37 ºC for 3 hours. Digested DNA was mixed with 1 X DNA loading dye (Invitrogen) and loaded onto an agarose 1 % gel. DNA fragments were separated on agarose gel. DNA bands in the gel was cut and purified from the gel using Fermentas gel extraction kit. DNA was eluted from the column in 50 μL of Tris-HCl (pH 8).

2.3.3. Ligation

Ligation reaction was carried out in a total reaction volume of 20 μL. Reaction was prepared by mixing the double digested plasmid and PCR product in 1:3 molar ratios respectively, 0.5 mM of ATP (Sigma), 20 units of T4-ligase (New England Bio Labs), and 2 μL of 10 X T4 ligase buffer (1 X final). Volume was adjusted to 20 μL using RNase-free water. Reaction was incubated at 25 ºC for 15 minutes or at room temperature over night.

2.3.4. Recombinant transformation

2 ng of DNA was transformed into One Shot TOP10 chemical competent cells (Invitrogen) for plasmid amplification, or transformed into BL21-(DE3) chemical competent cells (Invitrogen) for protein over-expression.

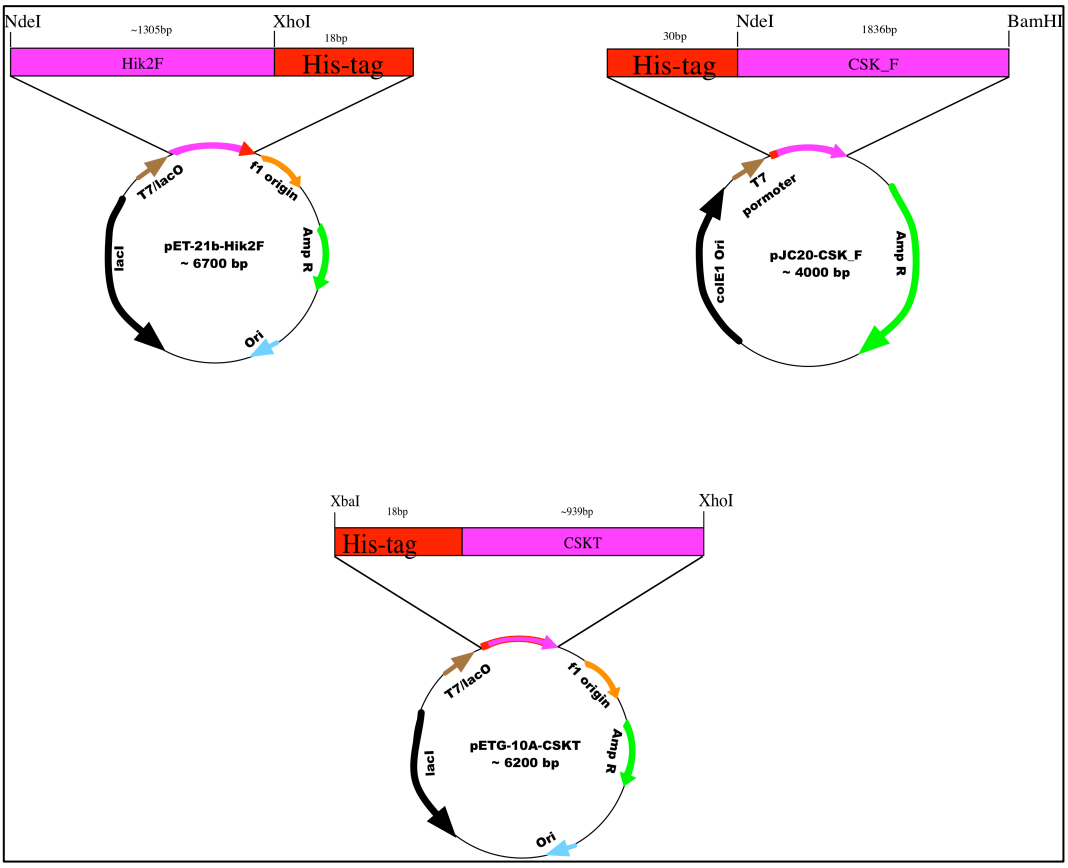

Figure 2.1 Recombinant vectors containing Hike2 and CSK genes. The full-length Hik2 (Hik2F), the full-length CSK (CSK_F), and truncated form of CSK (CSKT) genes are shown by magenta and the C or N-terminal poly-histidine tags (His-tag) are shown by red. Orange and blue arrows show the f1 and Ori origins of replication, respectively; an ampicillin resistant gene is shown by green arrow; black and brown arrows show the lacI and T7/lac promoters, respectively. The direction of arrow indicates the direction of translation of genes.

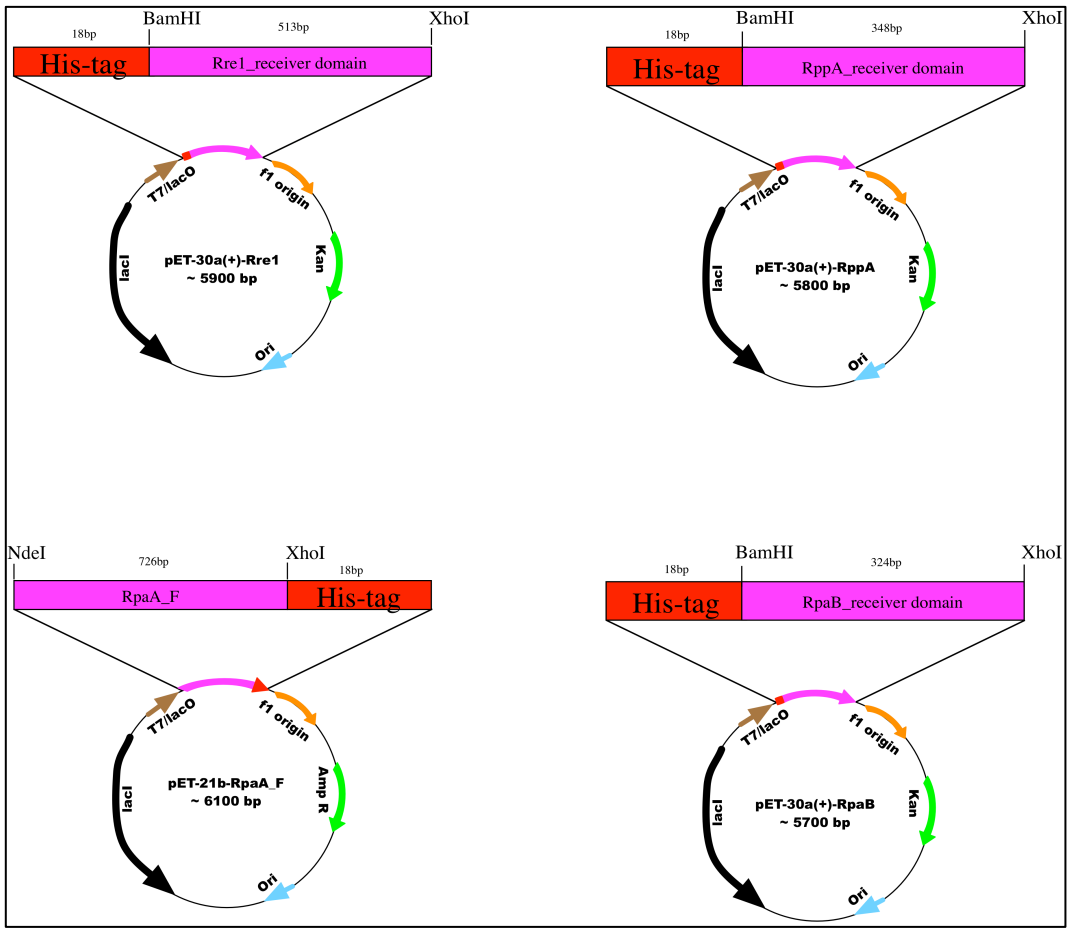

Figure 2.2 Recombinant vectors containing receiver domain of response regulators. Genes coding for receiver domain of Rre1, RppA, RpaA, and RpaB are shown by magenta arrow. The C or N-terminal poly-histidine tags (His-tag) are shown by red arrow. Orange and blue arrows show the f1 and Ori origins of replication, respectively; an ampicillin resistant gene is shown by green arrow; black and brown arrows show the lacI and T7/lac promoters, respectively. The direction of arrow indicates the direction of translation of genes

2.3.5. Site-directed mutagenesis

Site-directed mutagenesis was made using Stratagene Quick Change site-directed mutagenesis kit. Mutagenic primers listed on table 2.2 were designed using PrimerX (Lapid & Gao, 2011) (a web-based program), and primers were purchased from Eurofins MWG Operon, Germany. Mutagenesis was confirmed by sequencing and clones were transformed into BL21-(DE3) chemical competent cells.

Table 2.2 Primers used for site-directed mutagenesis

For H-box
–H185Q
Forward: CTGACCTCTTGCAGCAACTCCGCAATC
Reverse: GATTGCGGAGTTGCTGCAAGAGGTCAG
For G1-box
– G359A
Forward: CGCCGACACGGCTTATGGCATTC
Reverse: GAATGCCATAAGCCGTGTCGGCG
– G361A
Forward: GATCGCCGACACGGGTTATGCGATTCCCCCGGAGGATCAAC
Reverse: GTTGATCCTCCGGGGGAATTGCATAACCCGTGTCGGCGATC

For G2-box

– G386A

Forward: CGAGGCTCCATTAATGCGACTGGTTTGGGTTTG

Reverse: CAAACCCAAACCAGTCGCATTAATGGAGCCTCG

– G388A

Forward: CATTAATGGCACTGCGTTGGGTTTGGCGATC

Reverse: GATCGCCAAACCCAACGCAGTGCCATTAATG

– G390A

Forward: CACTGGTTTGGCATTGGCGATCGTG

Reverse: CACGATCGCCAATGCCAAACCAGTG

.

2.4. Protein over expression and purification

A colony grown on an agar-LB plate was used to inoculate an overnight starter culture in 10 ml Luria Broth (LB) [9] that was supplemented with ampicillin at a final concentration of 100 μg ml^{-1} or with Kanamycin at a final concentration of 35 μg ml^{-1}. The overnight culture was diluted to 1:100 in LB media containing the appropriate antibiotic and grown at 37 ºC to an optical density at 600 nm of 0.55 before initiating protein over-expression with 0.5 mM isopropyl β-D-1-

thiogalactopyranoside (IPTG) (Melford) and then grown for a further 16 hours at 18 ºC. Cells were harvested by centrifugation at 6000 rpm for 10 minutes at 4 ºC and the pellet was re-suspended in lysis buffer (300 mM NaCl, 50 mM NaH_2PO_4 pH 7.4, 25 mM imidazole, and 1 mM PMSF) and lysed with an EmulsiFlex-C3 homogenizer (Avestin). Lysate was separated by centrifugation at 39,000 g for 20 min. The supernatant was applied to Ni^{2+} affinity chromatography (GE Healthcare) and His-tagged recombinant proteins were purified from the column as instructed by the manufacturer. The above proteins were further purified using Superdex 200 gel filtration.

2.5. *In vitro* autophosphorylation assay

2.5.1. Autophosphorylation assay

Autophosphorylation assay was performed with 2.5 μM of purified recombinant Hik2 protein in kinase reaction buffer (50 mM Tris-HCl (pH 7.5), 50 mM KCl, 10 % glycerol, and 10 mM $MgCl_2$) in a final reaction volume of 25 μL. Autophosphorylation reaction was initiated by adding 5 μl of 5-fold concentrated ATP mix containing 2.5 mM ATP and 2.5 μCi [γ^{32}-P]-ATP (6000 Ci $mmol^{-1}$) (PerkinElmer). Reactions were incubated for 15 seconds at 22 ºC. Autophosphorylation reaction was stopped with 6 μL of 5-fold concentrated Laemmli sample buffer (Laemmli, 1970). Proteins were resolved on a 12 % SDS-PAGE (sodium dodecyl sulfate polyacrylamide gel electrophoresis). Once proteins were separated, the gel was rinsed with SDS running buffer and

transferred into a plastic bag and the completely sealed bag was exposed to a phosphor plate overnight. The incorporated γ^{32}-P was visualized using autoradiography and the band intensity from the autoradiograph was quantified using ImageJ version 1.44 (Schneider et al, 2012).

2.5.2. Autophosphorylation assay in the presence of salt

2.5 μM recombinant Hik2 protein was pre-treated with 5 μl of 5-fold concentrated, low potassium reaction buffer (250 mM Tris-HCl (pH 7.5), 25 mM KCl, 50 % glycerol, and 50 mM $MgCl_2$) and water or with the following salts: NaCl (0.3M final), Na_2SO4 (0.25 M final), $NaNO_3$ (0.3 M final) or KCl (0.375 M final) in a total volume of 20 μL. Reaction mixtures were then incubated at room temperature (22 ºC) for 30 minutes. Autophosphorylation reaction was assayed as above (section 2.5.1).

2.5.3. Autophosphorylation assay in the presence of redox agents

2.5 µM of recombinant Hik2 or CSK proteins were treated with kinase reaction buffer and the following redox agents: 2 mM $K_3Fe(CN)_6$, 6 mM DTT, 0.5 mM benzoquinone, and 0.5 mM hydroquinone and incubated at room temperature for 30 minutes. Auophosphorylation reaction was assayed as above (section 2.5.1) except that CSK was incubated at 30 ºC for 1 hour.

2.5.4. Acid-base stability assay

Four replicates of autophosphorylation reactions of Hik2 were prepared as in section 2.5.1. Proteins were then resolved on a 12 % SDS-PAGE and blotted to a PVDF membrane. Each lane containing the autophosphorylated Hik2 protein was cut and incubated in 50-100 mL of 50 mM Tris-HCl (pH 7.4) (neutral), 1 M HCl (acidic), or 3 M NaOH (basic). The membranes were then incubated for 2.5 hours at 55 ºC while being agitated. The presence or hydrolysis of γ^{32}-P was analysed using autoradiography.

2.6. Phosphotransfer kinetics

The autophosphorylation reaction was carried out by mixing 30 μM of Hik2 in a total reaction volume of 375 μL containing kinase reaction buffer (50 mM Tris-HCl (pH 7.5), 50 mM KCl, 10 % glycerol, 25 mM $MgCl_2$, and 2 mM DTT) and ATP mix (2.5 mM ATP and 37.5 μCi [γ^{32}-P]-ATP (6000 Ci mmol^{-1})). The reaction mixture was incubated at 30 for 10 minutes. Meanwhile, 25 μM of the following response regulators: Rre1, RppA, RpaA, or RpaB were diluted in the above kinase reaction buffer, in a total volume of 62.5 μL. A control sample lacking response regulator was prepared in the same way, except that response regulator protein was substituted with water. For each phosphotransfer reaction, 62.5 μL of autophosphorylated radiolabeled Hik2 protein was mixed with 62.5 μL of the above response regulators or a control with water alone. Kinase and response regulator were present at 1 μM and 5 μM, respectively. Reactions were

mixed and incubated at 30 ºC. 25 μL was removed at 0, 20, 40, 60, and 90 minutes, and stopped by addition of Laemmli sample buffer. Proteins were resolved on 15 % SDS-PAGE and the presence of γ^{32}-P was analysed using autoradiography. The incorporated γ^{32}-P was visualized using autoradiography and the band intensity from the autoradiograph was quantified using ImageJ.

2.7. Chemical crosslinking

The full-length Hik2 protein was desalted into crosslinking reaction buffer (25 mM HEPES-NaOH (pH 7.5), 5 mM KCl, and 5 mM $MgCl_2$) using PD-10 desalting column (Amersham Biosciences). Chemical crosslinking was carried out in a total reaction volume of 20 μL containing varying concentration of Hik2 protein in crosslinking reaction buffer. Crosslinking agent dithiobis (succinimidylpropionate) was added to a final concentration of 2 mM from 24.73 mM stock solution in dimethyl sulfoxide. Reactions were incubated at 23 ºC for 4 minutes. Reactions were stopped by addition of 50 mM Tris-HCl (pH 7.5) and 10 mM glycine. The above reaction was also repeated with 2 μM Hik2 and varying concentration of DSP. 2 μg of crosslinked proteins were resolved on 10 % SDS-PAGE and followed staining with Coomassie Brilliant Blue.

2.7.1. Autophosphorylation followed by crosslinking

Autophosphorylation reaction of Hik2 was prepared as in section 2.5.1 and followed by crosslinking as above. Proteins were resolved on 10 % SDS-PAGE and the incorporated γ^{32}-P was visualized using autoradiography.

2.8. Fluorometric titration of Arabidopsis CSK with DBMIB

Binding of plastoquinone analogue, 2,5-dibromo-3-methyl-6-isopropyl-p-benzoquinone (DBMIB) to recombinant CSK protein was examined by tryptophan quenching of CSK. DBMIB titration was prepared in 1 cm X 4 cm quartz cuvette containing 0.1 μM of CSK in 20 mM HEPES (pH 7.6) in a total volume of 3 mL. Varying concentration of DBMIB was added and the total volume of DBMB added never exceeded 0.05 % of the total sample volume. Fluorescence measurement was carried out using Perkin-Elmer LS55 spectrofluorometer with excitation wavelength set to 295 nm and emission wavelength was set at 280-450 nm. Excitation and emission monochromators were set to 5 nm and 10 nm, respectively. Fluorescence emission was monitored at 342 nm. In equation 1, $F_{corrected}$ and $F_{observed}$ are the corrected and observed fluorescence intensities, respectively, and A_{ex} and A_{em} are the respective observance values of DBMIB at excitation (295 nm) and emission (340 nm) wavelengths (Moxley et al, 2011).

$$F_{corrected} = F_{observed} \text{ x anti log } \left(\frac{A_{ex} + A_{em}}{2}\right) \quad (1)$$

An equilibrium dissociation consistence (k_d) for CSK-DBMIB complex was determined by nonlinear fitting of data using Prism 5 (Motulsky & Christopoulos, 2003) to equation 2.

$$X = \frac{n[DBMIB]}{K_d + [DBMIB]_{free}} \quad (2)$$

Fractional saturation X of CSK was calculated using equation 3, where X is the fraction of DBMIB bound and the corrected fluorescence with (F), without ($F_{[DBMIB]0}$), and saturation ($F_{[DBMIB]max}$) DBMIB concentrations.

$$X = \frac{F_{[DBMIB]0} - F_{observed}}{F_{[DBMIB]0} - F_{[DBMIB]max}} \quad (3)$$

The concentration of unbound DBMIB ($[DBMIB]_{free}$) was calculated by equation 4.

$$[DBMIB]_{free} = [DBMIB]_{total} - X[CSK]_{total} \quad (4)$$

2.9. TNP-ATP binding assay

TNP-ATP binding assay was carried out in a total volume of 3 mL containing 2 μM of CSK_T, 1 μM of TNP-ATP, and ATP binding buffer (10 mM NaCl and 10 mM Tris-HCl (pH 8)). Samples were prepared in 1 cm X 4 cm quartz cuvette. Fluorescence measurement was carried out using Perkin-Elmer LS55 spectrofluorometer with excitation wavelength set to 410 nm and emission wavelength was set at 500-650 nm. Excitation and emission monochromators

were set to 5 nm and 10 nm, respectively. TNP-ATP was excited at 410 nm and emission was scanned in the rage of 500-650 nm.

TNP-ATP binding titration was carried out by successive addition, to give varying concentrations of TNP-ATP, to 2 μM CSK diluted into ATP binding buffer. Control titration without protein was performed in the same way. Fluorescence emission intensity increase at 540 nm was monitored. Correction for buffer fluorescence was made. The total volume of TNP-ATP never exceeded 0.001 % of the total volume.

TNP-ATP displacement was carried out by successive addition of varying concentrations of ATP to a sample containing 2 μM CSK, 1 μM TNP-ATP in the above ATP-binding buffer. Decrease in fluorescence emission intensity at 540 nm was monitored. Total volume of ATP added never exceeded 0.05 % of total sample volume.

2.10. Sequence Analysis

Sequence similarity search was carried out with blastP and blastn (Altschul et al, 1990) using public databases, Cyanobase (http://genome.kazusa.or.jp/cyanobase) and Joint Genome Institute (JGI) (http://www.jgi.doe.gov/). Domain prediction was carried out using SMART database (http://smart.embl-heidelberg.de/smart/set_mode.cgi?NORMAL1⁄41) (Schultz et al, 1998). Multiple alignment was

generated with ClustalW (Chenna et al, 2003) and alignment was edited with Jalview (Clamp et al, 2004). Phylogenetic tree was reconstructed using a web-based program Phylogeny.fr (http://www.phylogeny.fr/version2_cgi/index.cgi) (Dereeper et al, 2008) and tree was edited using FigTree version 1.3.1.

Chapter 3
Phylogenetic distribution of Hik2

3.1. INTRODUCTION

Like all prokaryotes, cyanobacteria utilises two-component systems to monitor and adapt to their surrounding environment. In 1996, the first complete genemic sequence for *Synechocystis* sp. PCC 6803 was made available (Kaneko et al., 1996). Since then, genomes of most cyanobacterial species were sequenced and their complete genomic sequences can be accessed through the public databases, Cyanobase (http://genome.kazusa.or.jp/cyanobase) and Joint Genome Institute (JGI) (http://www.jgi.doe.gov/).

Cyanobacterial genomes encode a large number of two-component proteins for their genomic size, even more than *E.coli* genomes (Ashby and Houmard, 2006). But distribution of two-component systems varies between different cyanobacterial species. For example, the genome of the filamentous cyanobacterium *Nostoc punctiforme* encodes 146 histidine kinases and 168 response regulators. In contrast, some *Prochlorococcus* species have a very small number of genes for two-component systems. *Prochlorococcus* MED4 and *Prochlorococcus* SS120 genomes encode only five histidine kinases and six response regulators. Furthermore, out of the five histidine kinases of MED4, Histidine kinase 3 (His03) contains stop codons and frameshift, and therefore it is possible that the mRNA of hik03 is not be translated (Mary and Vaulot, 2003). Five histidine kinases are conserved in all cyanobacteria (Ashby and Houmard, 2006), one of which is Hik2. The ortholog of Hik2 that is also annotated as Hik01 in the genome of *Prochlorococcus* MED4 is present in all cyanobacterial species and almost in all chloroplasts as a Chloroplast Sensor Kinase (CSK)

(Puthiyaveetil et al., 2008, Ashby and Houmard, 2006). This implies that the Hik2 is an essential protein that plays an important role in cyanobacteria and chloroplasts. The role of CSK in chloroplasts of higher plants is already known (Puthiyaveetil *et al*., 2008, Puthiyaveetil *et al*., 2012, Puthiyaveetil *et al*., 2010); while the role of Hik2 in cyanobacteria has yet to be demonstrated.

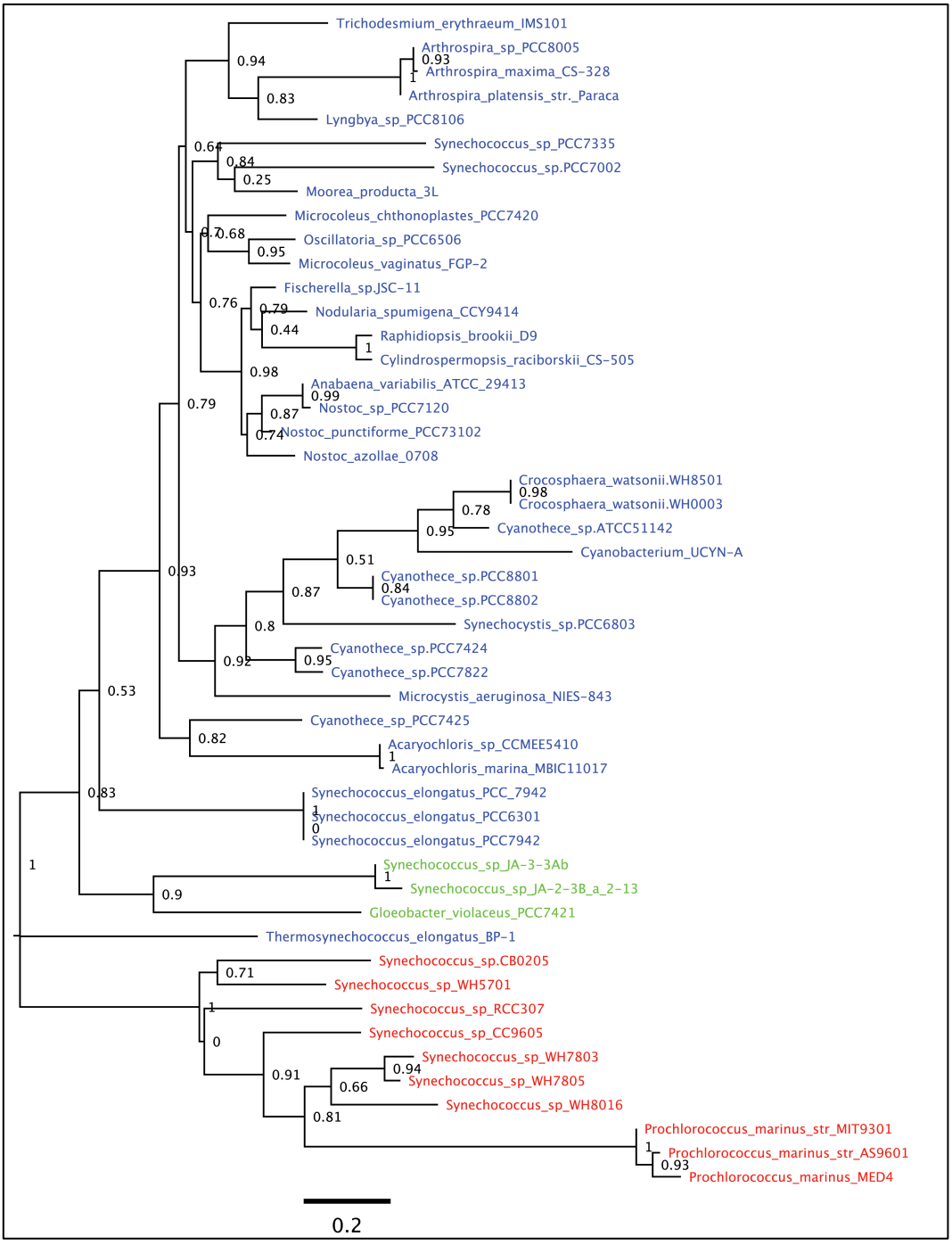

Figure 3.1 Phylogenetic distributions of Hik2 proteins. Unrooted tree for orthologues of Hik2 proteins in 49 cyanobacteria genomes was constructed from amino acid sequences by the neighbour-joining method. Bootstrap consensus tree is inferred from 1000 replicates. The colour corresponds to different forms of Hik2 proteins. Clade coloured blue corresponds to cyanobacteria containing the type I Hik2 protein; Clade coloured red corresponds to those containing the type II; Clade coloured green corresponds to those containing the type III

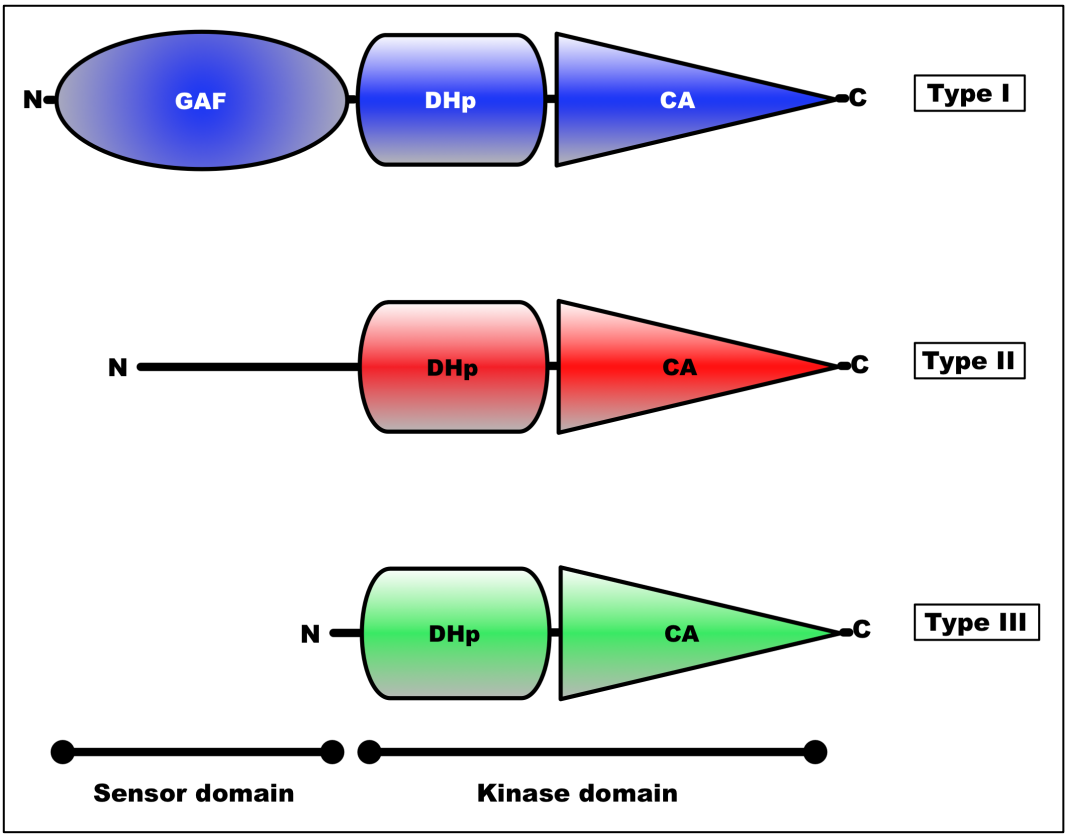

Figure 3.2 Domain Archtechare of Hik2 Proteins. The amino (NH_2) and the carboxyl (COO) termini are shown at each end, respectively. Domain architecture of Hik2 was peridicted using SMART database (Schultz *et al*., 1998). The predicted sensor domain is shown as GAF or where it is undefined it is shown as a line. The kinase core contains the DHp and CA domain. The colour corresponds to different forms of Hik2 proteins; i.e blue representing the full-length, type I Hik2 protein; red representing type II Hik2 proteins; and green representing type III Hik2 proteins.

3.2. Distribution, function and evolution of Hik2 Protein

Histidine kinase contains a conserved kinase core domain and a variable sensor domain. The Hik2 protein is present in all cyanobacterial species with its conserved kinase core domain, consisting of DHp and CA domains (for further information see chapter 6). Interestingly, the sensor domain of Hik2 is not fully conserved in cyanobacterial species. From sequence alignment and domain prediction, it appears that there are three types of Hik2 proteins and only one form is present within each cyanobacterium. As shown in figure 3.1 and 2, type I Hik2 protein contains a GAF domain as its sensor domain. The majority of cyanobacteria have this type of Hik2 protein. Type II Hik2s have a truncated form of GAF domain. The third type of Hik2 has no recognisable sensor domain. This finding is also consistent with earlier report by (Ashby and Houmard, 2006).

The presence of different forms of Hik2 proteins is intriguing because it implies that the Hik2 has multiple functions that are probably species specific. The type I Hik2 protein, which is found in freshwater and terrestrial cyanobacteria, has fully conserved GAF domain, and therefore will have all the sensing functional abilities. Whereas type II and III Hik2s are only found in marine cyanobacteria have either a truncated form of GAF domain or non-at all (figure 3.1 and 3.2).

The type II Hik2s probably had lost the ability to perceive some types of signals. This is probably because the signal is now sensed by another histidine kinase or those cyanobacteria are no longer exposed to such a signal. Therefore, there is no selective pressure to retain such motif. It is even more intriguing to find the type III Hik2s has lost their sensor domains completely.

Type III Hik2 is found only in three cyanobacterial species; *Gloeobacter violaceus* PCC 7421, *Synechococcus* sp. JA-2-3B'a(2-13), and *Synechococcus* sp. JA-3-3Ab. These three cyanobacteria diverged very early from other cyanobacteria (Gupta, 2009). Therefore, it is possible that the ancestral Hik2 protein lacked a sensor domain and later Hik2 acquired the new GAF sensor domain through gene fusion. Alternatively, it is possible that the sensor domain of Hik2 in those three cyanobacteria was lost after they diverged from other cyanobacteria.

Gloeobacter violaceus is unusual in that it lacks the orthodox thylakoid membrane that houses the photosynthetic machinery, as is found in all other oxygen-evolving cyanobacteria. *Gloeobacter* still performs oxygenic photosynthesis that unusually takes place on the plasma membrane. *Gloeobacter* also lacks *psaI*, *psaJ*, *psaK*, and *psaX* genes encoding for Photosystem I complex (Inoue *et al*., 2004). The loss of GAF-sensor domain from *Gloeobacter* Hik2 could be linked to the fact that photosynthesis does not take place in the thylakoid membrane.

The CSK protein in chloroplasts of *Arabidopsis thaliana* couples the redox signal from the thylakoid membrane to chloroplast transcription (Puthiyaveetil *et al*., 2008). Like Hik2, CSK does not have a predicted transmembrane domain. However, the CSK protein is capable of receiving signals from the thylakoid membrane (Puthiyaveetil *et al*., 2010, Puthiyaveetil *et al*., 2008), and can directly bind quinone (see chapter 8). Therefore, the GAF domain of CSK and Hik2 might have the ability to loosely associate itself to the thylakoid membrane so that it can receive a signal from the photosynthetic electron transport chain. There are examples of soluble histidine kinases that receive signals that are located in the membrane. The CikA (Circadian Input Kinase A) from *Synechococcus elongatus* PCC 7942 is a soluble histidine kinase that contains a GAF domain as its sensor domain. The CikA was reported to sense the redox state of plastoquinone pool (Ivleva *et al*., 2006). The regulator of N_2-fixation genes – NifL histidine kinase from *Azotobecter Vinelandii* again contains soluble PAS sensor domain, yet it can still receives signal from the quinone pool (Grabbe and Schmitz, 2003).

The orthodox view of the signal sensing mechanism of histidine kinases is that it takes place in the sensory domain, where the signal is then transduced to the kinase domain via signal-induced conformational change. Conformational change eventually leads to regulation of histidine kinase autophosphorylation. However, a recent study by Wang *et al* challenges this view of the signal perception mechanism of histidine kinases. Their finding showed that histidine kinase EnvZ signal sensing abilities is not restricted to its sensor domain. Wang *et al* study showed that the truncated form of EnvZ that only contains the core

kinase domain was perfectly capable of sensing an osmotic signal (Wang *et al*., 2012). They showed that NaCl was required for stabilisation of the four-helix bundle; thereby promotes stable conformation that facilitates an autophosphorylation event of EnvZ (Wang *et al*., 2012).

Response regulator 1 (Rre1) is a putative response regulator partner of Hik2 and Hik34. (Paithoonrangasarid *et al*.; 2004) Hik34-Rre1 controls expression of nineteen genes in response to hyperosmotic shock (Paithoonrangsarid *et al*., 2004). Furthermore, Rre1 controls five more genes that are not under the control of Hik34. In order to determine the histidine kinase that is upstream to Rre1, Paithoonrangsarid et al screened histidine kinase mutant libraries; however, they could not identify potential histidine kinase that controls those five genes. However, their yeast-two hybrid screening identified Hik2 as potential partner Rre1. It is therefore likely that Hik2-Rre1 controls the five genes that are under the Rre1 control, but not under Hik34 controls. If Hik2 perceives an osmotic signal, it is likely that it may employ EnvZ type mechanism. Therefore, one can assume that the full-length and the truncated form of Hik2 perceive an osmotic signal. The GAF domain of Hik2 that is found in type I and II Hik2s in addition might be involved in perceiving an additional signal such as redox signal or might bind small ligands required to regulate its autophosphorylation activity.

Chapter 4
Signal perception by Hik2

4.1. INTRODUCTION

Signal transduction by a two-component system (TCS) begins when a histidine kinase undergoes an autophosphorylation in an ATP-dependent manner. This autophosphorylation is then coupled to a histidine-to-aspartate phosphotransfer event from a conserved histidine residue on the histidine kinase to a conserved aspartic residue of a response regulator (see chapter 7 for an account of the His-Asp phosphotransfer reaction). The autophosphorylation event of a full-length histidine kinase is governed by environmental signal. Thus upon stimulation by signalling molecule(s), histidine kinases undergo conformational changes that result in the activation or inactivation of their autophosphorylation. Therefore, it is crucial to identify the signalling molecule(s) that regulate the activity of any histidine kinase.

As described in detail in chapter 1 section 1.4, histidine kinases possess diverse sensory domains that are capable of recognising various types of signal. One signal molecule that modulates the autophosphorylation activity of the histidine kinase is redox. Reducing agents donate electron(s) or hydrogen atom(s) to an acceptor molecule, whereas oxidising agents accept electron(s) or hydrogen atom(s) from a donor molecule. Redox reactions are key post-translational modulator for several enzymes involved in electron transport chains and metabolic pathways.

Redox sensor histidine kinases utilise a redox signal to modulate their autokinase activity (Allen, 1993). For example, the RegB-RegA two-component

system in *Rhodobacter capsulatus* is a global regulator that controls a wide range of oxygen-responsive processes such as respiration, photosynthesis, and nitrogen fixation. The autophosphorylation activity of RegB and phosphotransfer to an aspartic acid residue of RegA is controlled by the redox state of an electron carrier – ubiquinone (Wu & Bauer, 2010). Another well-studied quinone pool redox sensor is the *Arc* (Aerobic Respiratory Control) two-component system of *E. coli*. The ArcA-ArcB TCS consists of a membrane bound ArcB sensor histidine kinase and the ArcA response regulator (Georgellis *et al*, 2001; Malpica *et al*, 2004). ArcB is a ubiquinone sensor that uses cysteine residues for its redox sensing mechanism. Upon shifting from anaerobic to aerobic growth conditions, the ubiquinone pool in the *E. coli* respiratory membrane becomes oxidised. Electrons from cysteines on the ArcB are then transferred to the ubiquinone pool, which leads to formation of an intermolecular disulfide bond between each monomer of ArcB polypeptide. This results in the inhibition of ArcB autophosphorylation (Malpica *et al*, 2004).

Salt stress also controls the activity of some histidine kinases by directly stabilising or destabilising their tertiary structure (Wang *et al*, 2012). Although salt and hyperosmotic stresses are often regarded as the same signal, however, there is a clear distinction between them. Hyperosmotic stress results in efflux of water from the cytoplasm of cell, which causes a decrease of cytoplasmic volume and an increase in the concentration of solutes. In contrast, salt itself has a small effect on the cytoplasmic volume. However, intracellular concentration of Na^+

and Cl^- ions can rapidly increase through influx of NaCl via Na^+/K^+ and Cl^- channels (Los *et al*, 2010).

In *E. coli*, salt stress is sensed by a designated histidine kinase EnvZ. No homologue of EnvZ is encoded in cyanobacterial genomes. Instead, in cyanobacteria, salt and hyperosmotic stresses are monitored by multifunctional histidine kinases, namely Hik34, Hik10, Hik16, Hik33 and a putative sensor Hik2 (Marin *et al*, 2003; Paithoonrangsarid *et al*, 2004). In addition to salt, these histidine kinases have been reported to perceive other signals. For example, Hik34 functions as a temperature sensor (Surette *et al*, 1996); the Hik33 was reported to sense redox (Mary & Vaulot, 2003).

Paithoonrangasarid *et al* suggested that Hik2 could be involved in hyperosmotic sensing. However, there is no genetic or biochemical evidences to support this suggestion. Therefore, the function of Hik2 was extrapolated from its putative response regulator, the Rre1.

In this chapter, I describe results of an investigation of the autophosphorylation activity of Hik2 in the presence of salt. The homologue of Hik2 in chloroplasts is involved in PQ pool redox sensing, it is therefore likely that the Hik2 also perceives a redox signal. The role of redox sensing activity of Hik2 will be explored.

4.2. RESULTS

4.2.1. Overexpression and purification of full-length recombinant Hik2 protein

In order to elucidate the signalling molecule(s) that modulate the autophosphorylation activity of the Hik2 protein, I cloned *Synechocystis* sp. PCC 6803 full-length *hik2* gene (slr1147) encoding a polypeptide of 435 amino acids. The clones were then over-expressed and purified as described in materials and methods section (chapter 2). Figure 4.1.A, lane 3 shows the overexpressed Hik2 protein is present mainly in the soluble cell fraction, and can be purified using nickel affinity chromatography. The C-terminal His-tagged Hik2 protein migrated on reducing 12 % SDS-PAGE with an apparent molecular mass of 50 kDa.

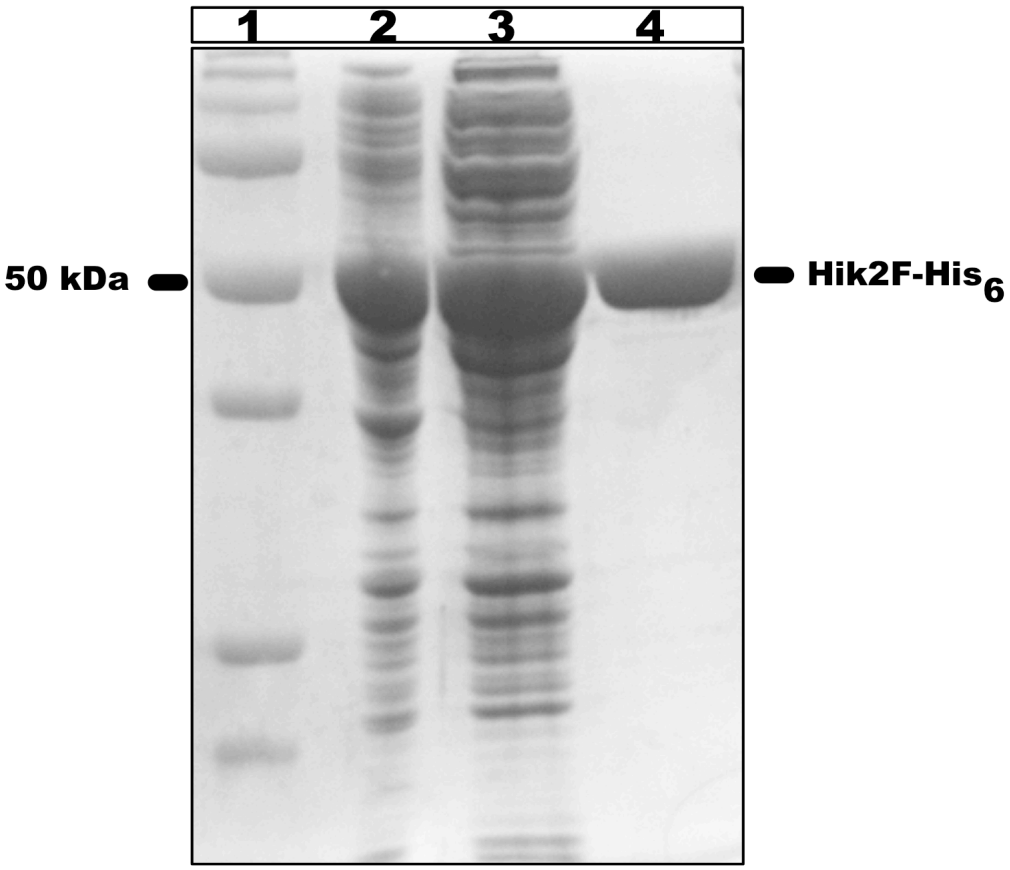

Figure 4.1 Over-expression and purification of recombinant Hik2 protein. Recombinant Hik2 was expressed and purified as indicated under the method and material section. 12% SDS-PAGE followed by staining with Coomassie blue of different cell fractions shows in lane 1 protein molecular weight markers in kDa; lane 2 is total cell fractions containing recombinant Hik2 protein; lane 3 is soluble fraction; and lane 4 is Hik2-His_6 eluted from nickel chromatography. The position of the 50 kDa molecular weight marker is indicated on the left. The position of Hik2 is indicated on the right

4.2.2. Sequence alignment of Hik2 shows conserved cysteine residues

Sequence alignment of Hik2 orthologous (figure 4.2) shows two conserved cysteine residues. The first conserved cysteine is found at the start of GAF domain. This cysteine residue is also conserved in algal and plants CSK protein (Puthiyaveetil *et al*, 2008). The second conserved cysteine residue is found at the end of the GAF sensor domain, just before the start of Kinase domain. This cysteine however is partially conserved and missing from *Microcystis*, *Microcoleus*, *Lyngbya Majuscula*, and *Cyanothece*.

4.2.3. Hik2 does not respond to redox agents *in vitro*

From the sequence alignment shown in figure 4.2 there are two conserved cysteine residues that are possibly involved in redox sensing. In order to investigate the effects of redox agents on the autophosphorylation activity of Hik2, the full-length recombinant Hik2 protein was incubated with different redox agents; Potassium ferricyanide, benzoquinone, hydroquinone, and DTT. I found that the untreated full-length Hik2 protein was autokinase active (figure.4.3, lane 1). Oxidising agents: potassium ferricyanide and benzoquinone had no effect on the activity of Hik2 (figure.4.3, lane 2 and 3, respectively**)**. Also, reducing agents, DTT did not affect the activity of Hik2 (figure.4.3, lane 4).

4.2.4. Na^+ ions regulates the autophosphorylation activity of Hik2

To investigate the effect of various types of salts on the autophosphorylation activity of Hik2, I incubated the purified Hik2 protein with NaCl, Na_2SO_4, $NaNO_3$ or KCl in the presence of 2.5 μCi of [γ ^{32}P] ATP. Figure 4.4 shows that NaCl, Na_2SO_4 or $NaNO_3$ inhibited the autophosphorylation activity of Hik2 (figure 4.4.A**,** lane 2, lane 3, and lane 4, respectively). However, KCl did not inhibit the autophosphorylation activity of Hik2. This result implies that the Na^+ ion and not the Cl^- ion is responsible for inhibition of the activity of Hik2. Figure.4.5 shows dose-response inhibition of Hik2 with an increase in concentration of NaCl. A 50 % inhibition of autophosphorylation of Hik2 was achieved at 0.25 M of NaCl.

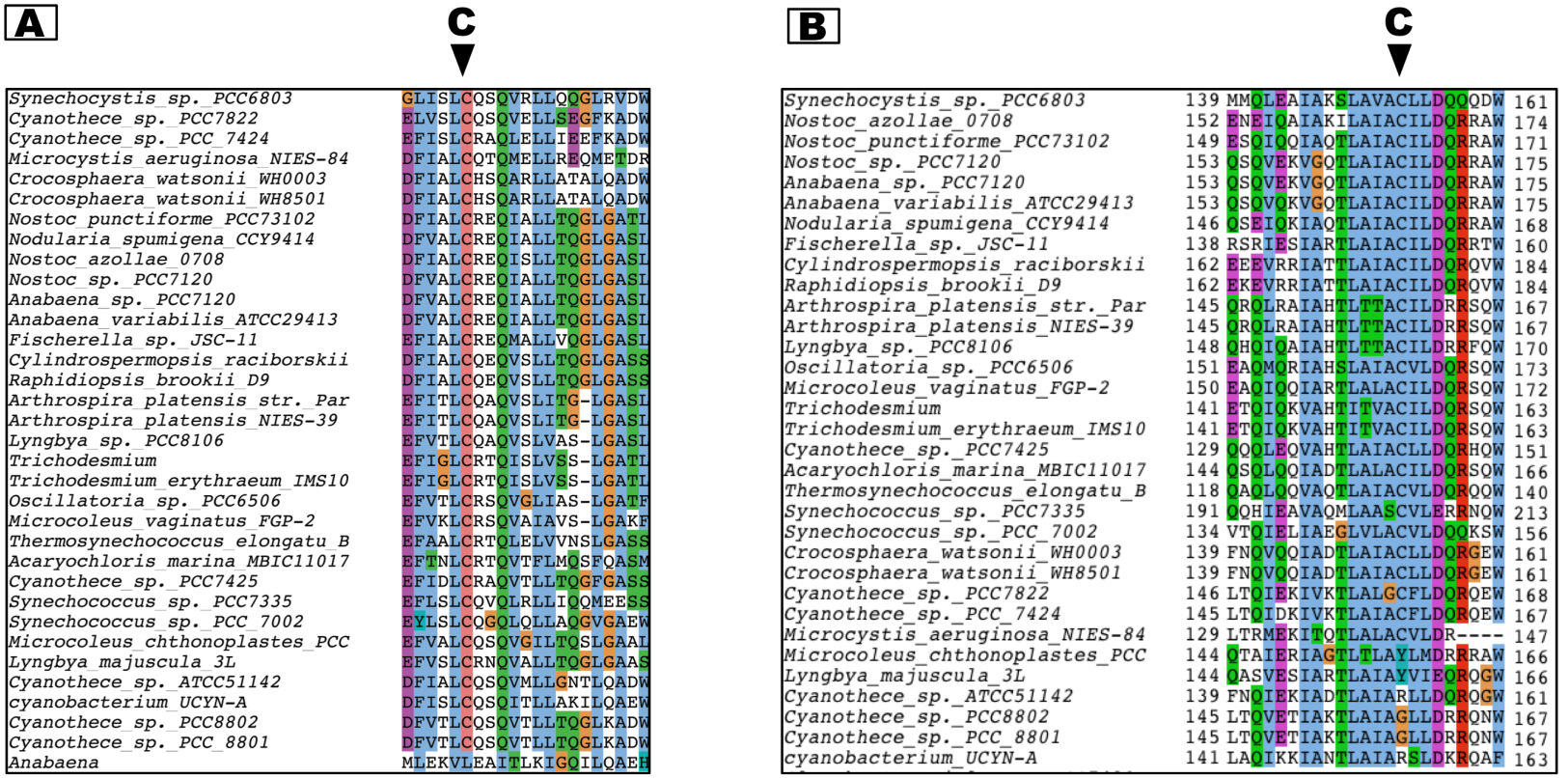

Figure 4.2 Sequence alignment of GAF domain of cyanobacterial Hik2 proteins. Amino acids are coloured according to their chemical properties and degree of conservation, and is the standard scheme of ClustalX (Chenna et al, 2003). Purple corresponds to acidic amino acids; blue, hydrophobic; green, polar and neutral; brown, glycine; and khaki, proline. A) Shows the first conserved cysteine residue located at the beginning of the GAF domain; B) shows the second conserved cysteine residue found at the end of the GAF domain. The conserved cysteine residues are indicated with an arrowhead.

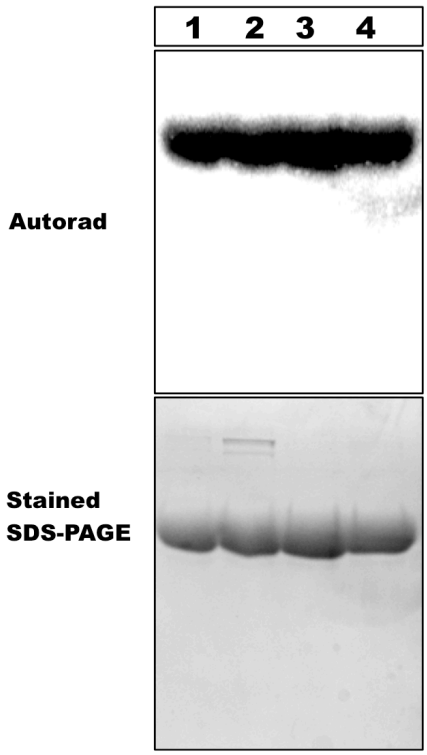

Figure 4.3 Effect of redox agents on the autophosphorylation activity of Hik2. 5 μM full-length recombinant Hik2 proteins were pre-equilibrated for 30 minutes in kinase reaction buffer containing: lane 1, dd.H_2O; lane 2 benzoquinone; lane 3, $K_3Fe(CN)_6$; and lane 4, DTT. Autophosphorylation activity of Hik2 initiated by addition of 2.5 μCi [γ^{32}-P] ATP and reaction was incubated at 22 ºC for 15 seconds before terminating the autophosphorylation reaction with 6 μl of 5 fold concentrated Laemmli sample buffer (Laemmli, 1970). Proteins were resolved on 12 % SDS-PAGE and the gel was exposed to autoradiography (autorad) overnight.

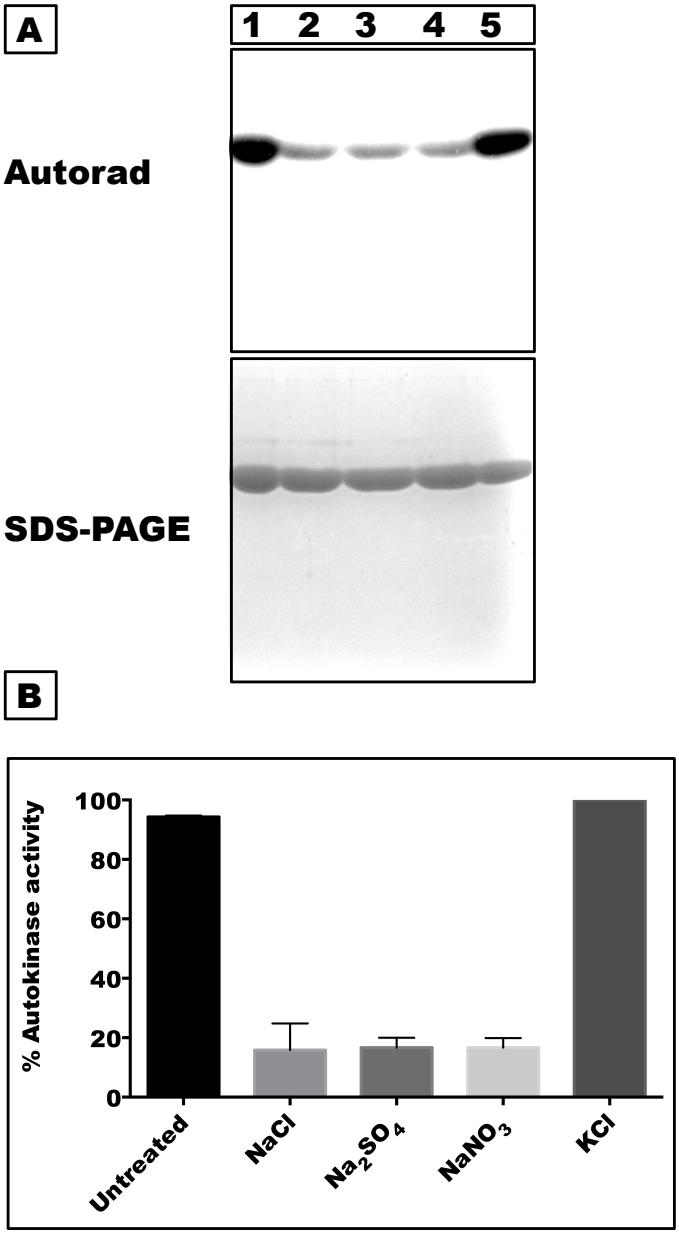

Figure 4.4 Effects of different salts on the autophosphorylation activity of full-length Hik2. A) 2.5 μM of full-length Hik2 protein was pre-equilibrated for 30 minutes with the following salts: lane 1, untreated sample; lane 2, treated with 0.3 M NaCl; lane 3, treated with 0.25 M Na_2SO_4; lane 4, treated with 0.3 M $NaNO_3$; lane 5, treated with 0.375 M KCl. Autophosphorylation was initiation by adding 2.5 μCi [γ^{32}P]ATP and incubated at 22 ºC for 20 seconds. Autophosphorylation was terminated with Laemmli sample buffer and proteins were resolved in 12 % SDS-PAGE. The SDS-PAGE was exposed to autoradiography (autorad) overnight. The above experiment was repeated at least three times. B) The intensity of bands from the autoradiograph was quantified using imageJ (Schneider *et al*, 2012) and data points were plotted using Prism 6 (Motulsky & Christopoulos, 2003). Each data represents the mean of three measurements ± S.E.

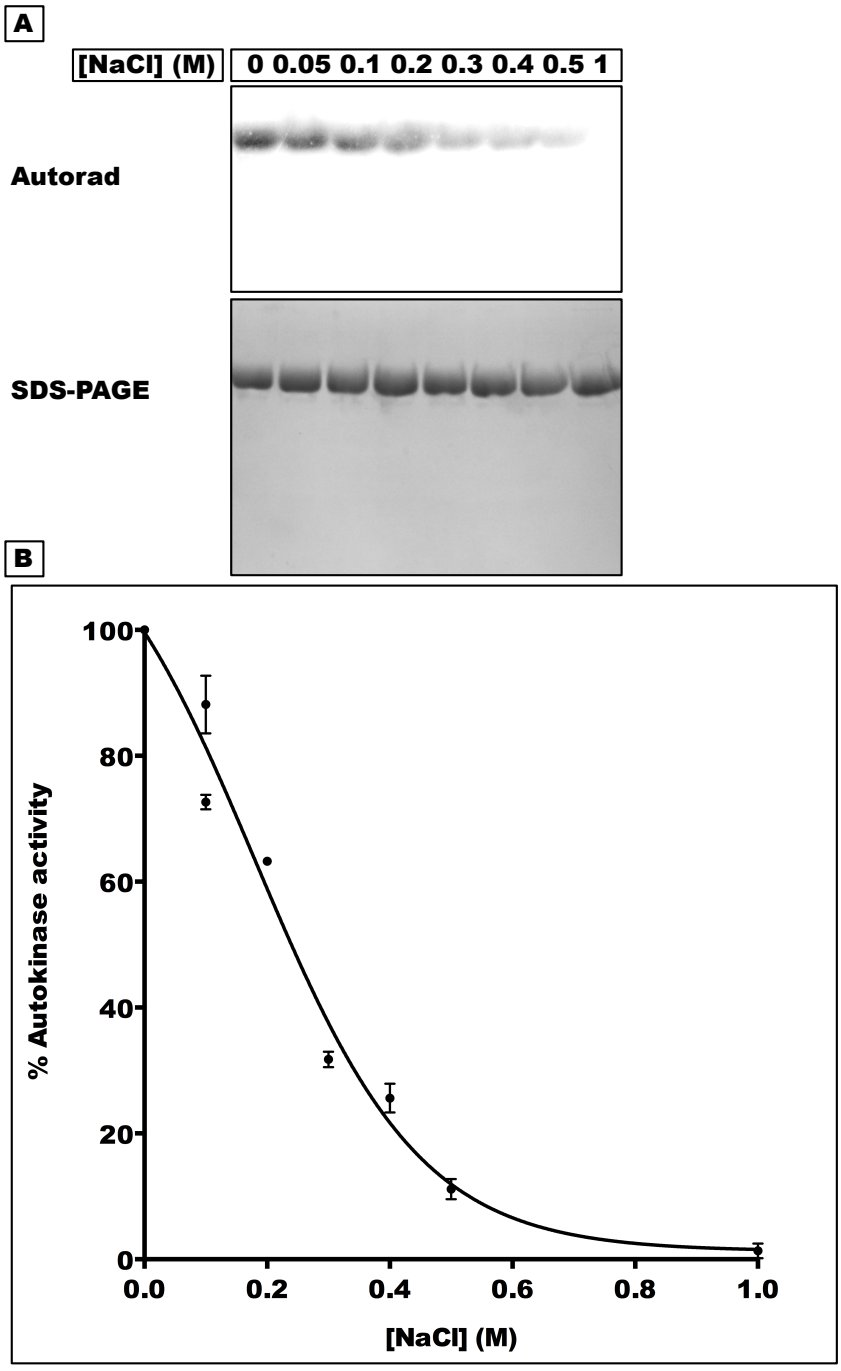

Figure 4.5 Concentration-Response of inhibition of Hik2. A) 5 μM of full-length Hik2 protein was pre-equilibrated for 30 minutes with 0 to 1 M NaCl in a final volume of 20 μL. Autophosphorylation was performed for 15 seconds as indicated under the materials and methods. Autophosphorylation was terminated with Laemmli sample buffer and proteins were then resolved on 12 % SDS-PAGE. B) Intensity of each band was quantified using ImageJ and data points were plotted using Prism 6. Each point represents the mean ± S.E of three measurements.

4.3. DISCUSSION

Most two-component proteins are not required for growth of cyanobacteria under laboratory conditions and therefore deletion of their genes is not lethal. However, inactivation of *hik2* gene was shown to be lethal (Paithoonrangsarid *et al*, 2004). I therefore used an *in vitro* approach to characterise the sensing mechanism of Hik2 protein. In this chapter, the full-length *hik2* gene (encoding for 435 amino acids) was successfully cloned and the polyhis-tagged recombinant Hik2 protein was purified from *E.coli*. The purified Hik2 protein migrated on a reduced SDS-PAGE with an apparent molecular weight of 50 kDa, which corresponds to Hik2 monomer (figure 4.1). Moreover, the purified Hik2 protein in solution was colourless, which indicates that the recombinant Hik2 protein does not contain coloured cofactors such as heme, FAD, or iron-sulfur cluster that are required for some sensor proteins to perceive redox signals. The lack of colour from the recombinant Hik2 protein was further supported by the primary amino acid sequence of Hik2, in which there is no obvious motifs for any known cofactor.

The predicted sensor domain of cyanobacterial, red and brown algal Hik2 protein is a GAF domain. But for green algal and higher plants, SMART database does not predict the nature of its sensor domain (Puthiyaveetil *et al*, 2008). Nevertheless, sequence alignment of the sensor domain of higher plants Hik2s with that of red algal and cyanobacteria show that they share strong similarities. In addition, bacterial purified recombinant Hik2 protein of higher plant *Arabidopsis thaliana* (see chapter 8) and the brown algal *Phaeodactylum tricornutum* were

also colourless in solution (Puthiyaveetil, unpublished data). *Arabidopsis* and *Phaeodactylum* Hik2 also lack obvious motifs required for binding cofactors. So it is not surprising to find that bacterial over-expressed and purified recombinant Hik2 protein is also colourless.

Cyanobacterial Hik2 was predicted to form a two-component pair with Rre1 (Puthiyaveetil & Allen, 2009). The Hik2 homologue, CSK co-occur with Rre1/Ycf29 in chloroplasts of brown and red algae, but not in higher plants. In plants, CSK is found as an orphan, modified histidine kinase. The Hik2-Rre1 two-component system pairs in cyanobacteria and chloroplasts of red algae are probably involved in regulation of gene(s) encoding components of the phycobilisome complex (Puthiyaveetil & Allen, 2009). Therefore, it is likely that Hik2 perceives its redox signal directly or indirectly from the electron transport chain. The fact that *Arabidopsis* CSK functions as a redox sensor implies that the cyanobacterial Hik2 could also be involved in redox sensing. CSK however relays the redox signal to the chloroplast genome through a modified route, using eukaryotic type serine/threonine catalytic mechanism and was proposed to act on regulatory components of plastid transcription (Puthiyaveetil *et al*, 2010).

Sequence alignment of cyanobacterial Hik2 proteins showed that there are two conserved cysteine residues that could be involved in redox sensing (figure 4.2). In particular, the first conserved cysteine residue is fully conserved in all cyanobacteria species and in all chloroplasts. However, our *in vitro* assay shown on figure 4.3 shows that Hik2 did not respond to different redox condition.

Therefore, at this stage the redox-sensing activity of cyanobacterial Hik2 is just speculative and based on: i) The *Arabidopsis* CSK perceives redox signal *in vivo* and ii) The function Rre1/Ycf29 is linked to control of genes encoding for phycobilisome.

In addition to redox sensing ability of Hik2, it was also predicted to be involved in sensing a hyperosmotic signal. The work presented in this chapter demonstrates that the recombinant Hik2 protein responds to salt signal, specifically to sodium ions (figure 4.4 and 4.5). The cyanobacterial genome encodes for five-histidine kinases Hik2, Hik10, Hik16, Hik33, and Hik34 that have been proposed to sense salt and hyperosmotic signals. All of the above histidine kinases likely to have one or more functions.

Bacterial cells exposed to high salt concentration have to cope with lower water potential and higher ionic potential, which can be toxic to cellular metabolism (Los *et al*, 2010). Increase in sodium ion concentration in the cytoplasm of the cell competes for potassium-binding sites in proteins and leads to inhibition by destabilising their tertiary structure. In cyanobacteria, an increase of sodium ion concentration results in efflux of potassium ions.

Salt stress also has profound effect on photosynthesis. Treatment of cyanobacteria with high concentrations of NaCl results in 40 % decrease of the D1 protein of photosystem II complex, and as a consequence, it results in a decrease in photosystem II mediated oxygen evolution activity. But it increases

expression of genes encoding subunits of the photosystem I reaction centre (Marin *et al*, 2003). Therefore, it is vital that cyanobacteria contain robust system(s) to regulate salt and osmotic homeostasis. Indeed, to date, five two-component pairs, including the putative Hik2-Rre1 pair, are involved in responding to salt and osmotic shock.

Paithoonrangasarid *et al* reported that in cyanobacteria, the Rre1 is required for transcription activation of some salt tolerance genes in a high salt or a hyperosmotic conditions. However, the work presented here shows that the autophosphorylation activity of Hik2 is inhibited by sodium ion, thus in high salt condition, Rre1 is no longer able to accept phosphoryl group from Hik2. It is therefore likely that the dephosphorylated form of Rre1 has transcription activation role for those genes that Paithoonrangasarid *et al* reported. Therefore, Hik2-Rre1 system acts as transcription repressor in active form, and the repression is removed in high salt condition, upon inhibition of Hik2 by sodium ion.

Chapter 5
Oligomeric states of Hik2

5.1. INTRODUCTION

Signal transduction typically initiates at the cell surface, where the stimulus (chemical ligand) is detected by membrane-spanning receptors; signal transduction then propagates through the transmembrane domain to the cytoplasm. In membrane bound histidine kinases, signalling molecules are detected thorough their extracellular sensor domain, which is located at the N-terminus of histidine kinase polypeptide. Both soluble and membrane-anchored histidine kinases exist predominantly as homodimers that are assisted by their conserved DHp domains. In addition, higher oligomeric order for membrane histidine kinases have been reported for Dcus (Scheu *et al*, 2010), RegB (Swem *et al*, 2003), AtoS (Filippou *et al*, 2008), KdpD (Heermann *et al*, 1998), and also for the chemotaxis receptor (Massazza *et al*, 2011). For the above histidine kinases, with exception of the chemotaxis receptor, higher order oligomerisation was promoted by intermolecular disulfide bond. But soluble histidine kinases have not been reported to form higher order oligomers. Instead, soluble histidine kinases are reported to exist only as an inactive monomer or an active dimer for EnvZ (EnvZc) (Cai *et al*, 2003), VirAc (Pan *et al*, 1993), and CheA (Surette *et al*, 1996).

Oligomeric states of proteins can be determined using several techniques, such with mass spectrometry, circular dichroism, fluorometric denaturation, chemical crosslinking, native-PAGE, and size exclusion chromatography. Native-PAGE and size exclusion chromatography are most suited for stable protein-protein interactions; therefore, they are not the best choice for proteins that have

transient or semi-stable interaction, as a result they lead to disruption of such interaction.

Alternatively, chemical crosslinking provides a more direct method of studying transient semi-stable protein-protein interaction. This technique involves formation of covalent bonds between two polypeptides that are in close proximity, for example, between two monomers in a dimer or between two dimers in a tetramer. This technique mimics near physiological conditions and has advantages for studying oligomerisation of semi-stable protein-protein interactions. In this chapter, I describe results obtained using crosslinker dithiobis (succinimidylpropionate) here described as DSP and size exclusion chromatography to study oligomeric states of full-length of *Synechocystis* sp PCC6803 Hik2 proteins.

DSP contain reactive N-hydroxysuccinimide functional groups at each ends of its spacer arm, which is formed of 6 carbons and 2 sulphides. The side chain of lysine and N-terminus of each polypeptide are targets for crosslinking by DSP functional groups. Figure 5.1 shows a theoretical chemical reaction between each monomer of two Hik2 polypeptides and functional groups of DSP. The product is detected using non-reducing SDS-PAGE.

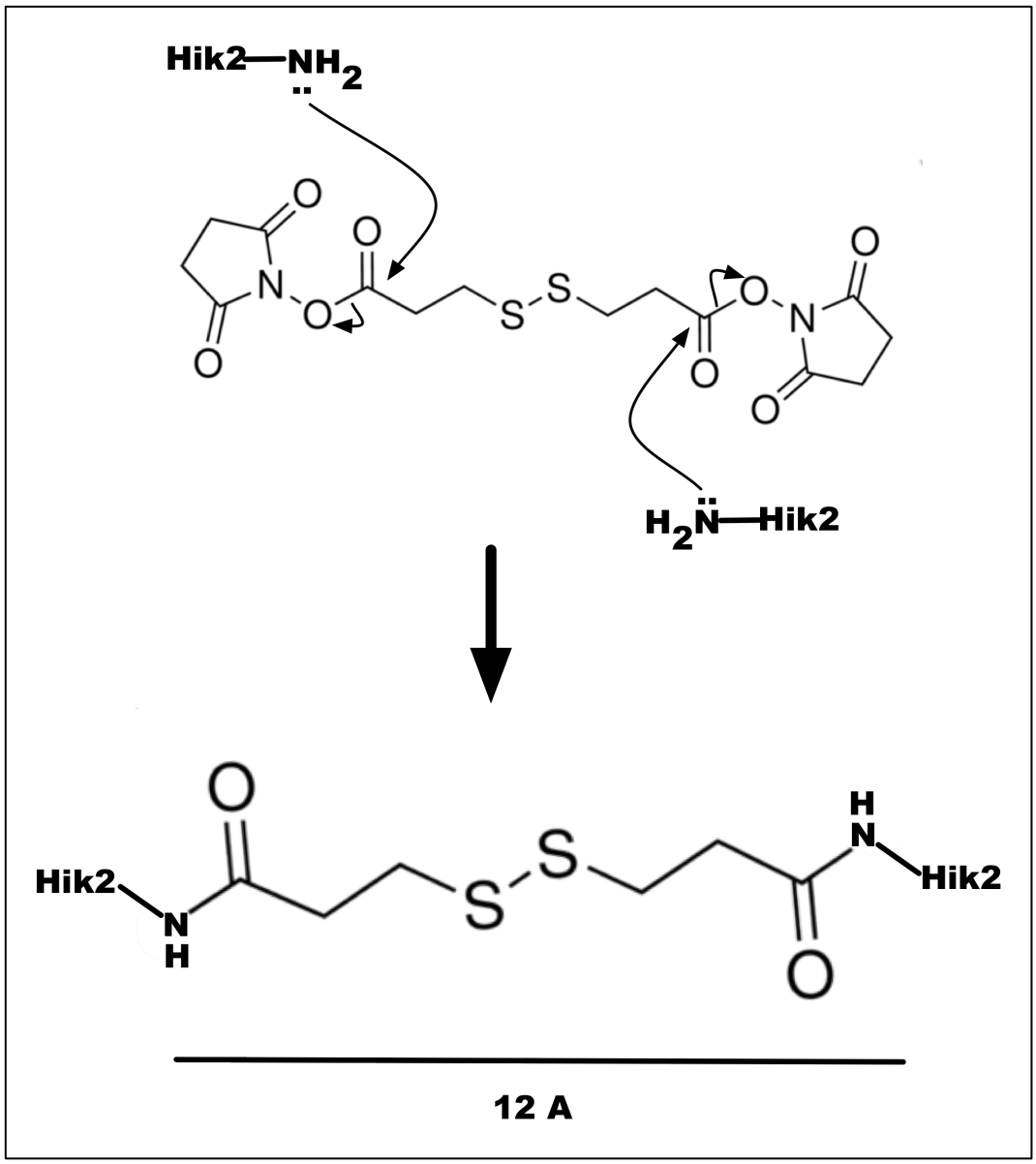

Figure 5.1 Theoretical reaction between DSP and Hik2 polypeptide. *A*, DSP and nucleophilic attack of the carbonyl group of DSP by an amino group of a Hik2 polypeptide. *B*, the product of the Hik2 oligomer. The distance of spacer arm is shown below the figure Å.

5.2. RESULTS

5.2.1. Hik2 exists predominantly as monomer and tetramer

In order to determine the oligomeric state of Hik2, recombinant Hik2 protein was incubated with varying concentration of crosslinker DSP for 5 minutes. Crosslinked products were then resolved on a non-reducing SDS-PAGE. Figure 5.2, lane 2 shows the untreated Hik2 protein that has migrated on a non-reducing SDS-PAGE with an apparent molecular weight of 50 kDa, corresponding to the monomeric form of Hik2. Figure 5.2, lane 3-10 shows chemical crosslinking produced two distinct protein bands at 50 kDa corresponding to monomeric form and a second band at 200 kDa corresponding to tetrameric form containing a dimer of dimers. Increasing the concentration of DSP from 0-9 mM (Figure.5.1, lane 3-10) had no effect on oligomerisation state of Hik2; so therefore, the monomeric form does not result from the shortage of crosslinker.

5.2.2. The oligomeric state of Hik2 is concentration dependent

I next investigated whether the oligomeric state of Hik2 depends on Hik2 protein concentration. Crosslinking was performed with varying concentrations of Hik2 proteins, ranging from 2-50 μM, while the concentration of DSP and incubation times were kept constant. Equal amounts of crosslinked Hik2 proteins were then analysed with non-reducing SDS-PAGE. Interestingly, there is no correlation between the monomeric state of Hik2 and protein concentration. But the

tetrameric form of Hik2 decreased with increase in protein concentration (Figure 5.3).

5.2.3. Hik2 exists as phosphorylated monomer and tetramer states:

In order to investigate functional states of Hik2-monomer and Hik2-tetramer, I carried out autophosphorylation of Hik2 before and after crosslinking. Figure 5.4, lane 2 shows Hik2 protein that was allowed to autophosphorylate and followed by crosslinking with DSP produced phosphorylated monomer and tetramer forms. Figure.5.4, lane 3 shows crosslinking followed by autophosphorylation produced inactive monomer and tetramer.

5.2.4. NaCl converts hexamer form of Hik2 into tetramer

On Superdex 200 column that calibrated with buffer lacking NaCl, the Hik2 was eluted as oxctamer and hexamer (figure 5.5A, blue line) forms. However, in the presence of 600 mM (figure 5.5A, red line), higher order oligomers (octamer and hexamer) were converted into tetramer.

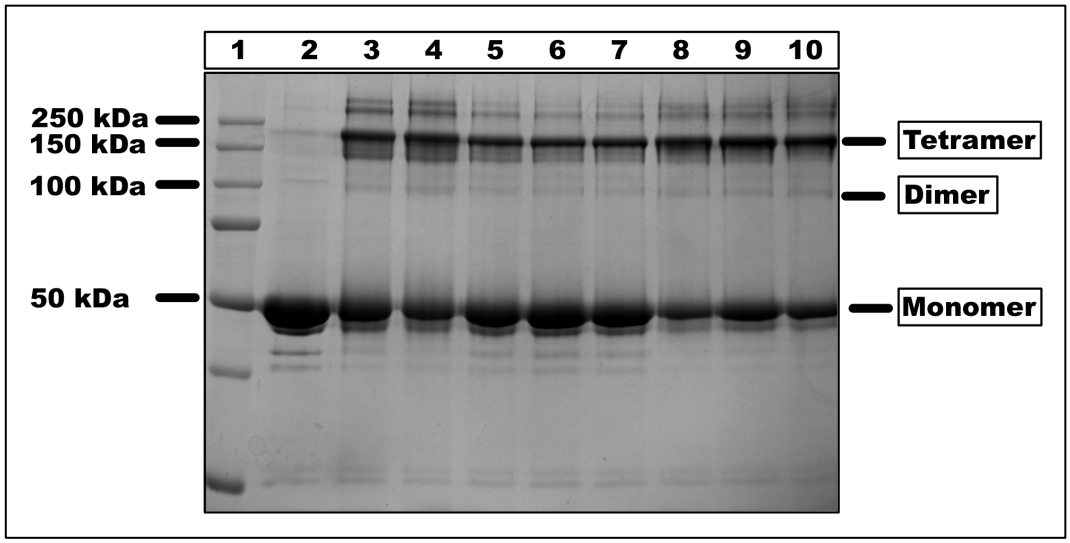

Figure 5.2 Effects of chemical crosslinking on the oligomeric state of Hik2. 5 μM of recombinant, His-tagged Hik2 protein was treated with various concentrations of DSP for 5 minutes at 23 ºC as indicated in the materials and methods (chapter 2). Lane 1 shows protein molecular weight in kDa; lane 2, shows untreated Hik2 protein (control); lane 3, Hik2 treated with 1 mM DSP; lane 4, Hik2 treated with 2 mM DSP; lane 5, Hik2 treated with 3 mM DSP; lane 6, Hik2 treated with 4 mM DSP; lane 7, Hik2 treated with 5 mM DSP; lane 8 Hik2 treated with 6 mM DSP; lane 9, Hik2 treated with 7 mM DSP; lane 10, Hik2 treated with 9 mM DSP. Samples were subjected to non-reducing 10 % SDS-PAGE. The molecular weight is shown on the left in a kDa. The oligomeric states of Hik2 are indicated on the right

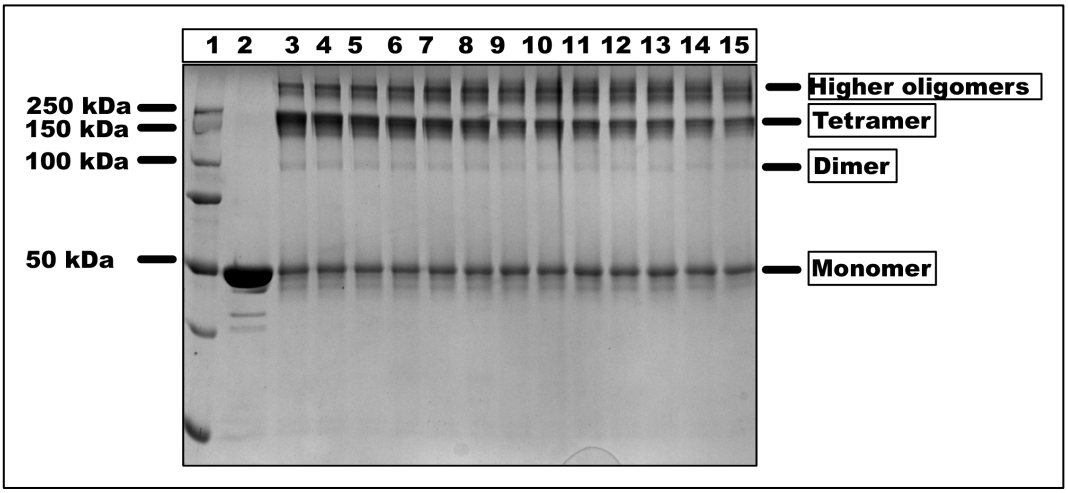

Figure 5.3 Effect of protein concentration and chemical crosslinking on the oligomeric state of Hik2. 2- 50 μM Hik2 proteins were treated with 2 mM DSP for 5 minutes and the crosslinking reaction was terminated with 50 mM Tris-HCl and 20 mM glycine. 2 μg of protein was loaded on non-reducing 10 % SDS-PAGE. Lane 1 shows protein molecular weight marker in kDa. Lane 2, 2 μM untreated Hik2 protein. Proteins in the following lanes were cross-linked and corresponds to the following protein concentrations: lane 3, 2 μM; lane 4, 3 μM; lane 5, 4 μM; lane 6, 5 μM; lane 7, 10 μM; lane 8, 15 μM; lane 9, 20 μM; lane 10, 25 μM; lane 11, 30 μM; lane 12, 35 μM; lane 13, 40 μM; lane 14, 45 μM; and lane 15, 50 μM. Protein molecular weight markers are shown on the left hand side in kDa. Different oligomeric states are labelled on the right hand side of the gel

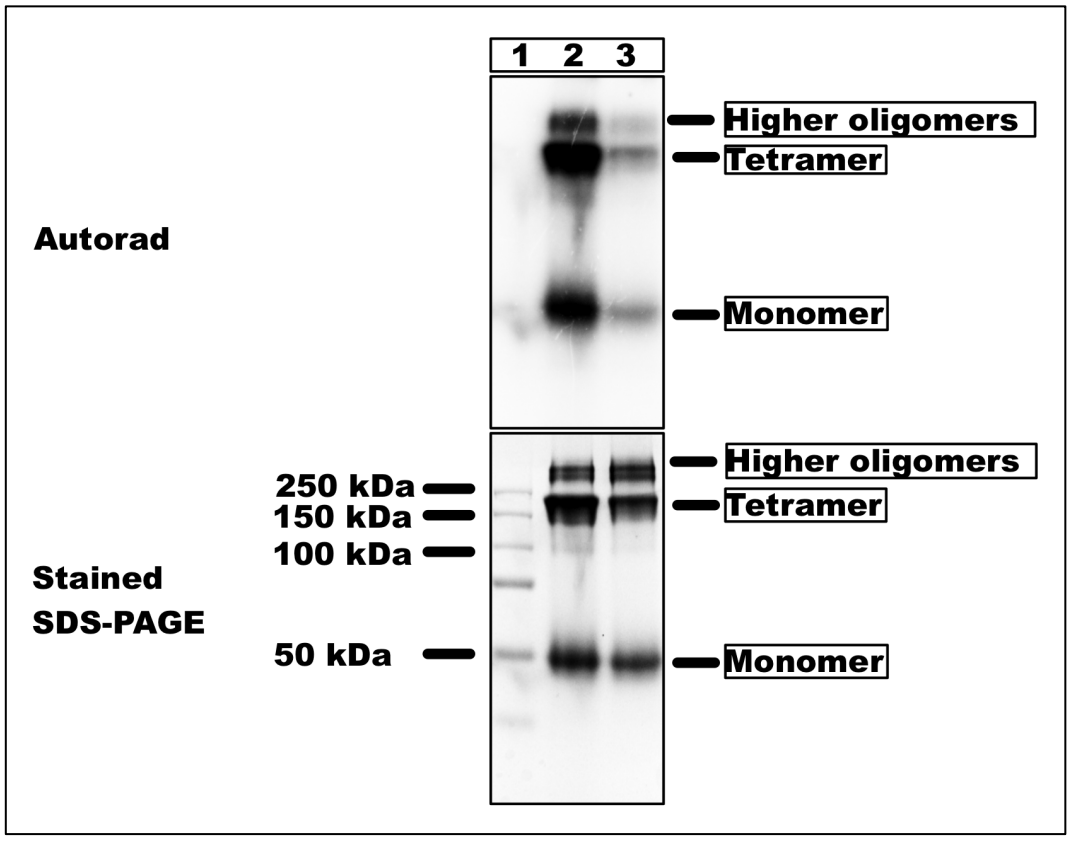

Figure 5.4 Functional characterisation of oligomeric states of Hik2. The effect of crosslinking on the autophosphorylation activity of Hik2 was tested with 2 mM DSP and 5 μM Hik2 protein. Lane 1 shows protein molecular weight marker in KDa; lane 2 shows result of Hik2 proteins that was allowed to autophosphorylate before crosslinking; lane 3 shows result of Hik2 protein that was first crosslinked and followed by autophosphorylation. Autophosphorylation products were then resolved on a 10 % non-reduced SDS-PAGE and the gel was then exposed to autoradiography (autorad). The gel was then stained with Coomassie Brilliant Blue (stained SDS-PAGE).

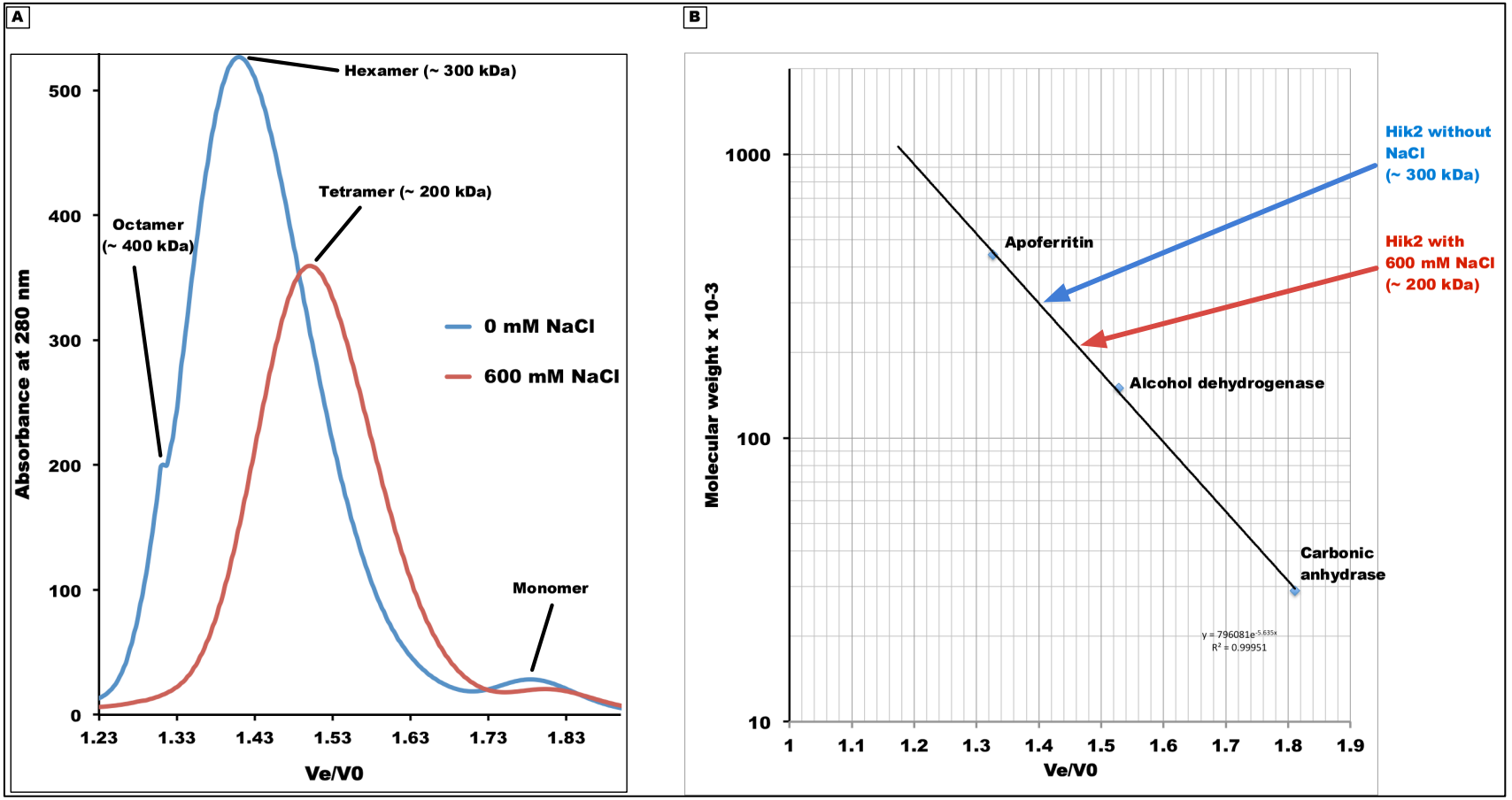

Figure 5.5. Chromatographic separation of Hik2 on Superdex 200. **A**) Typical elution profile of Hik2 on Superdex 200 eluted with buffer containing 50 mM Tris-HCl (pH 7.6) and 100 mM KCl (blue line) or with 50 mM Tris-HCl (pH 7.6) and 600 mM NaCl (red line). The elution positions of Hik2 without NaCl (400 and 300 kDa, consisting of an octamer formed of dimer of tetramers, a hexamer formed of trimer of dimers, respectively) and with 600 mM NaCl (200 kDa, consisting of dimer of dimer) are shown. **B**) Calibration curve of the Superdex 200 using standard proteins of known molecular weight: Apoferritin (443 kDa), Alcohol dehydrogenase (150 kDa), and Carbonic anhydrase (29 kDa). Blue dextran (2000 kDa) was used to determine the void volume (V0). The positions of Hik2 eluents from the Superdex 200 are shown by blue arrow (without NaCl) and by red arrow (with 600 mM NaCl), respectively.

5.3. DISCUSSION

This chapter describes an investigation into the *in vitro* oligomerisation states of Hik2 using the chemical crosslinker DSP. I show that the full-length Hik2 protein exists as monomeric and tetrameric forms (figure 5.3). Below, I discuss the possible functional roles of different oligomeric states of Hik2.

Eukaryotic protein kinases such as receptor tyrosine kinases oligomerise upon ligand binding. However, histidine kinases are programmed to become "auto" oligomers regardless of stimulation by signalling molecules, through their conserved dimerisation domain. Almost all known examples of histidine kinases are thought to exist as homodimers. But little is known about higher order oligomeric states of histidine kinases. Recent studies showed that at a low protein concentration, the CheA sensor kinase exists predominately as a monomer, while a dimer forms *in vitro*. The relative quantity of the dimeric state of CheA increases with an increase in CheA protein concentration (Surette *et al*, 1996). The data obtained by Surette *et al* implies that *in vivo*, the CheA most probably exist as inactive monomer and its dimerisation is probably stabilised upon its interaction with the chemotaxis receptor. The membrane anchored sensor kinase DcuS (dicarboxylate uptake sensor and regulator) from *E. coli* exists as monomer, dimer and tetramer both *in vitro* and *in vivo* (Scheu *et al*, 2010). The ArcB sensor kinase of *E.coli* contains two conserved redox-active cysteines that are regulated by the redox state of ubiquinone. Oxidation of these cysteines leads to

intermolecular disulfide formation between each monomer of ArcB and locks ArcB into a state inactive as a protein kinase. (Georgellis *et al*, 2001; Malpica *et al*, 2004). Anther example of regulatory oligomerisation is the RegB histidine kinase. For RegB, the active dimer form was converted into inactive tetramer form by intermolecular oxidation of its conserved cysteine (Swem *et al*, 2003). Like ArcB, oligomerisation of RegB disrupts its autokinase activity.

Like DcuS, chemical crosslinking showed that the Hik2 exists predominately as monomeric and tetrameric forms (figures 5.2 and 5.3). However, unlike CheA, DcuS, ArcB and RegB, the dimeric form of Hik2 could not be detected (figures 5.2, 5.3, and 5.5). For Hik2, chemical crosslinking produced higher-order oligomers such as tetramer, hexamer and octamer. Furthermore, gel filtration showed that the Hik2 is present predominantly as a hexameric and of octameric forms (figure 5.5A), and therefore likely that in vivo, the Hik2 might be present as higher order forms.

Functional characterisation of oligomeric state of Hik2 using autophosphorylation assay and chemical crosslinking showed that the monomeric and tetrameric forms of Hik2 were present as phosphorylated (autokinase active) forms (figure 5.4, lane 2). The absence of dimer and phosphorylation of the monomeric form of Hik2 is interesting because it was thought that dimerization activity of histidine kinases was universal and required for their trans-autophosphorylation activity; therefore, one would assume that the monomeric

form of Hik2 is autokinase inactive and Hik2 should only become active upon dimerisation. Although histidine kinases such as CheA and EnvZ are active upon dimerisation, it seems that this is not the case for Hik2. The present study shows that the Hik2 monomer is an active/autophosphorylated form (figure 5.4, lane2). This suggests two explanations; i) Hik2 uses a *cis*-autophosphorylation mechanism, therefore dimerisation may not be essential for its autophosphorylation activity; ii) the monomeric and tetrameric forms of Hik2 could be at equilibrium, thus the phosphorylated/active tetramer that formed of a dimer of dimers rapidly dissociates into monomers, giving the phosphorylated monomeric form that is observed in figure 5.4, lane 2. The ability for Hik2 to form tetramer and higher-order complexes could be part of its *in vivo* signal enhancing and transmission mechanism. Indeed, the Hik2 was highly active in its higher oligomeric form (figure 5.4); however, when it was treated with sodium ion, which converts the octamer and hexamer forms of Hik2 into tetramer (figure 5.5A), it becomes less active (chapter 4, figure 4.4 and 4.5). Thus suggesting that the autophosphorylation activity of Hik2 require cooperativity between dimers in hexamer and higher order oligomers.

Chapter 6

Characterisation of kinase domain of Hik2

6.1. INTRODUCTION

The core kinase domain of a histidine kinase has two conserved subdomains. The DHp and CA subdomains are important for autophosphorylation and phosphotransfer activities of histidine kinases. The conserve histidine kinase phosphorylation site is located in the DHp domain and can usually easily be determined from sequence alignment. However, direct determination of phosphorylation sites of peptides using conventional techniques employs an acid treatment of phosphorylated peptide followed by mass spectroscopy. This technique is most suitable for identification of acid-stable phosphoamino acids, those containing the phosphoester bond (P-O) (phosphoserine, phosphothreonine, and phosphotyrosine). It is, therefore, challenging to study acid labile phosphoamino acids such as those with acyl-phosphate bond (phosphoglutamate and phosphoaspartate) or those with a phosphoramidate bonds (phosphohistidine). Histidine kinases are known to autophosphorylate on the conserved histidine residue found in the H-box.

For experiments described in this chapter, I employed an acid-base stability assay and site-directed mutagenesis to characterise the nature of phosphoamino acids and the ATP-binding domain.

6.2. RESULT

6.2.1. Acid-base stability assay

Phosphoserine and phosphothreonine are stable under acidic conditions but labile under alkaline conditions. Conversely, proteins that are phosphorylated on basic residues (histidine, arginine, or lysine), their phosphoryl groups are acid labile but stable under basic conditions (Attwood *et al*, 2007). Those phosphorylated on acidic residues, such as aspartate or glutamate are susceptible to both acid and base hydrolysis (Attwood *et al*, 2011). The nature of the phosphoamino acid of Hik2 was investigated using acid-base stability assay. Figure 6.1 shows four replicates of autophosphorylated Hik2 proteins resolved on SDS-PAGE and blotted onto PVDF membrane. The PVDF membranes were then treated with buffers containing either 50 mM Tris-HCl (pH 7.4) (neutral), 1 M HCl (acidic), or 3 M NaOH (basic). The membranes were then incubated for 2.5 hours at 55 ºC while being gently agitated. Figure 6.1.A shows that the ^{32}P on untreated Hik2 (control) were relatively stable. Figure 6.1.B shows that the ^{32}P on Hik2 were relatively stable at pH 7.4, at 55 ºC for 2.5 hours. Figure 6.1.C shows that the ^{32}P on Hik2 were completely hydrolysed upon incubation in 1 M HCl, at 55 ºC for 2.5 hours. Figure 6.1.D shows that the ^{32}P on Hik2 were relatively stable when incubated in 3 M NaOH, at 55 ºC for 2.5 hours.

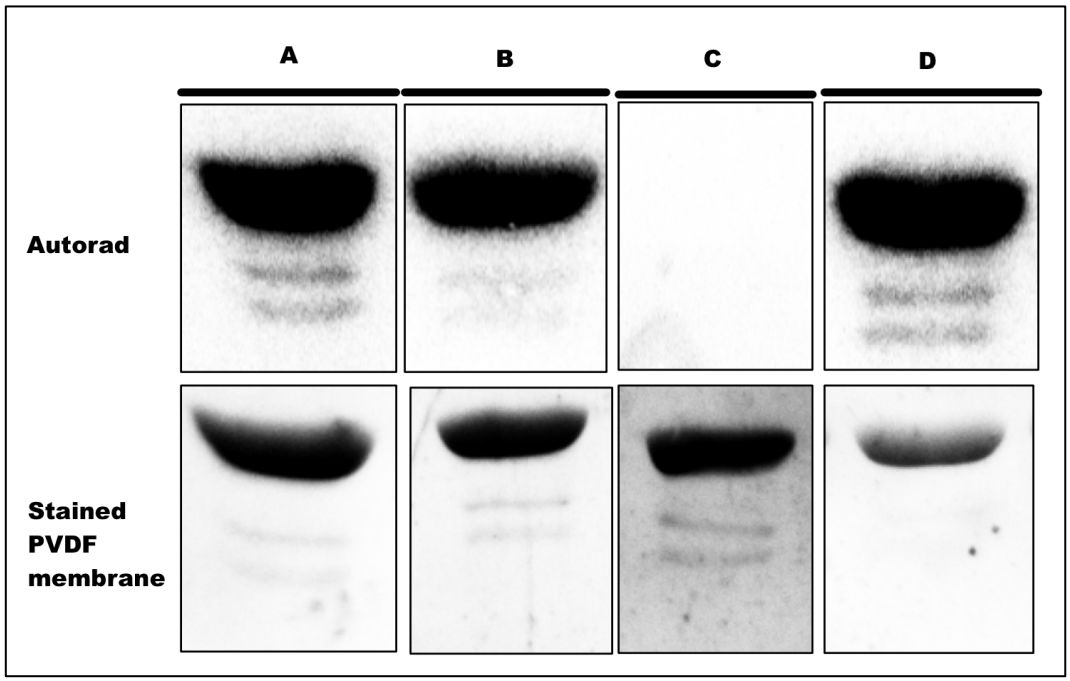

Figure 6.1. Acid-base stability assay. Four replicates of autophosphorylated Hik2 proteins were resolved on a 12 % SDS-PAGE and blotted to a PVDF membrane. The PVDF membrane was then cut and incubated either in 50 mM Tris-HCl (pH 7.4), 1 M HCl, or 3 M NaOH at 55 ºC for 2.5 hours. The hydrolysis of γ^{32}P was visualised using autoradiography. **A**, untreated; **B**, treated with 50 mM Tris-HCl (pH 7.4); **C**, treated with 1 M HCl. **D**, treated with 3 M NaOH.

6.2.2. Hik2 undergoes autophosphorylation on His185

The result shown in Figure 6.1 indicates that Hik2 was autophosphorylated on a histidine residue. I therefore mutated the conserved histidine residue located in the H-box of Hik2 to a glutamine to test its role in the autophosphorylation activity. The wild-type and putative phosphorylation site mutant recombinant proteins were purified and assayed as described in the materials and method (chapter 2). Figure 6.2 lane 2 shows histidine to glutamine mutation completely abolished the autophosphorylation activity of Hik2.

6.2.3. Characterisation of ATP-binding pocket of Hik2

The ATP-binding cavity of any histidine kinase contains conserved residues that are essential for its autophosphorylation. These include the G1 and G2 boxes, which have the characteristic signatures 'DxGxG' and 'GxGxG', respectively. Figure 6.3 shows sequence alignments of Hik2 orthologous shows that Hik2 contains typical histidine kinase G1 and G2 boxes. The conserved glycine residues in G1 and G2 boxes were then individually substituted to alanine residues in order to establish their role in autophosphorylation of Hik2. Figure 6.4 shows that the wild-type protein become autophosphorylated, however, substitution of the first or second conserved glycine residues in the G1-box abolished the autophosphorylation activity of Hik2 (Figure 6.4. lane 2 and 3). Similarly, substitution of any of the conserved glycine residues in the G2-box completely abolished the autophosphorylation of Hik2 (Figure 6.4. lane 4, 5 and 6).

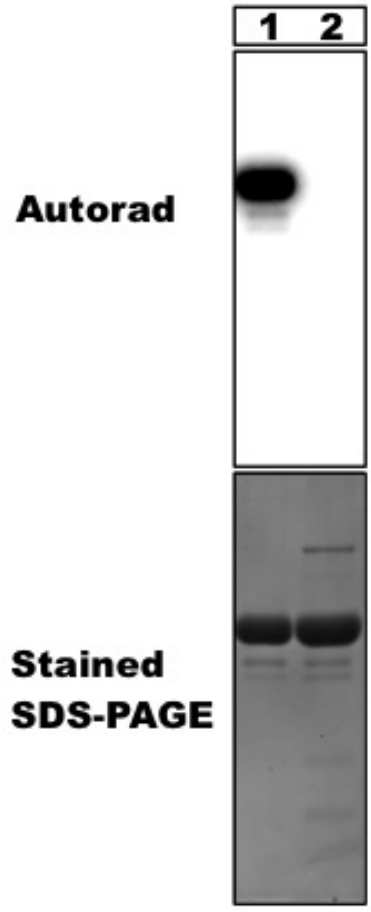

Figure 6.2 Effects of H185Q mutation on the autokinase activity of Hik2. The conserved histidine residue in the H-box was substituted to a glutamine as instructed in the method and material section. 2 μM of purified variant of Hik2 protein was assayed in the presence of 2.5 μCi ATP at 22 ºC. proteins were then resolved on a 12 % SDS-PAGE and the gel was exposed to an autoradiography overnight. Lane 1 shows the wild-type Hik2 protein. Lane 2 shows H185Q mutant protein.

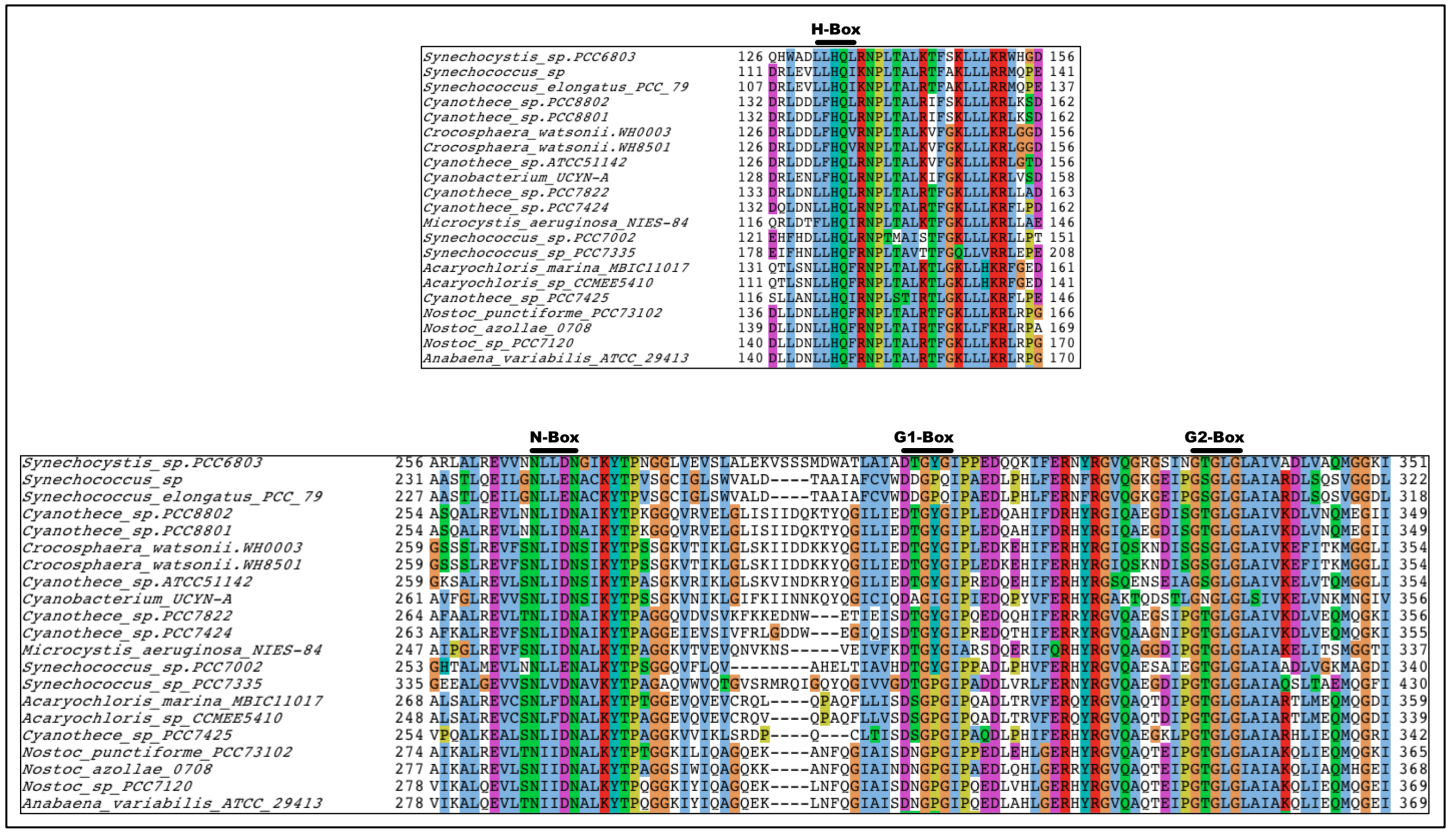

Figure 6.3 Conserved features of kinase domain of cyanobacterial Hik2 protein. Amino acids are coloured according to their chemical properties and degree of conservation, and is the standard scheme of ClustalX (Chenna et al, 2003). Purple corresponds to acidic amino acids; blue, hydrophobic; green, polar and neutral; brown, glycine; and khaki, proline. A) DHp domain. The conserved H-box of Hik2 is shown above the sequence. B) CA domain. The conserved N, G1, and G2 boxes are shown above the sequence.

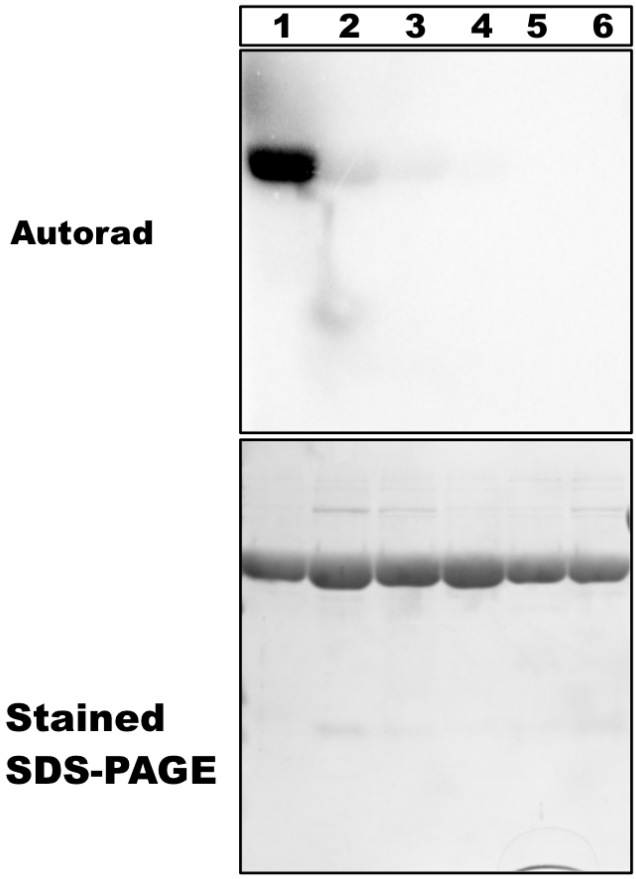

Figure 6.4 Effects of G1 or G2 box mutation on the autokinase activity of Hik2. The first two conserved glycine residues in the G1-box and all three conserved glycine residues in the G2-box were substituted individually to alanine. Purified variant of Hik2 proteins were assayed as indicated in materials and methods (chapter2). Lane 1, wild type Hik2 protein; lane 2, G1-box mutant G359A; lane 3, G1-box mutant G361A; lane 4, G2-box mutant G386A; lane 5, G2-box mutant G388A; lane 6, G2-box mutant G390A. The autophosphorylation reaction was allowed to proceed for 15 seconds at 22 ºC. The autophosphorylation reaction was quenched with 6 μl of Laemmli sample buffer. Proteins were separated on a SDS-PAGE 12 % and the incorporated γ^{32}-P was visualized using autoradiography.

6.3. DISCUSSION

Histidine kinases possess unique kinase core domain that sets them apart from serine/threonine or tyrosine kinases. Their core catalytic domain consists of conserved motifs that are also referred to as boxes. These conserved boxes – H, N, G1, F, G2, and G3 are directly involved in binding and the hydrolysis of an ATP molecule. Here, I show that Hik2 has a typically bacterial histidine kinase catalytic domain.

Histidine kinases are known to be autophosphorylated on a conserved histidine residue that is located in their H-box. I confirmed the nature of the phosphoamino acid of Hik2 using an acid-base stability assay. Figure 6.1 shows that the phosphoamino acid of Hik2 was acid labile and base stable, which indicates that Hik2 is autophosphorylated on histidine, arginine, or lysine residue(s). I then investigated the role of conserved histidine residue (H185) of Hik2 by substituting it with glutamine. My mutational study as shown in figure 6.2 rendered Hik2 into an inactive form (figure 6.3).

The kinase core domain of Hik2 contains a typical histidine kinase CA (Catalytic and ATP-binding) domain, which consists of conserved sequence motifs N, G1 (DxGxG), F, G2 (GxGxG), and G3 boxes (Puthiyaveetil & Allen, 2009; Puthiyaveetil *et al*, 2008). The CA domain is essential for binding an ATP molecule and for priming the gamma phosphate of ATP for a nucleophile attack

by the conserved histidine residue that is located within the H-box. Therefore, mutation within the G1 or G2 box is not possible without disrupting the structure of the nucleotide-binding pocket and it leads to inactivation of the autokinase reaction. Indeed, mutation within G1 or G2 boxes for several histidine kinases abolishes their autokinase activity (Chen *et al*, 2009; Gamble *et al*, 1998). Similarly, substitution of any of the glycine residues in the G1 or G2 boxes of Hik2 abolished its autophosphorylation activity (figure 6.4). Here, it is also important to note that for EnvZ or CheA kinases, mutation of the first conserved residues in G2 boxes is non-inhibitory. However, this was not the case for Hik2, where it was not possible to substitute any of the conserved residues within the G2-box without disrupting the activity of Hik2. This may indicate that G2-box found in Hik2 has a different fold to those found in EnvZ or CheA proteins. The G1-box plays an important role in conferring specificity to ATP. In particular, a conserved aspartic acid in the G1-box is involved in forming hydrogen bond with amino nitrogen 6 of an ATP molecule. But nucleotides such as GTP contain an oxygen molecule in place of the amino group of ATP; therefore, they are easily discriminated.

Chapter 7

Characterisation of response regulators

7. INTRODUCTION

In bacteria, sensor histidine kinases and their corresponding response regulators are often encoded in the same operon (Alm et al, 2006). Therefore, given genome sequences, identifying functional partners in bacterial two-component system can be straightforward. However, some histidine kinases and their response regulator partners are not encoded in the same operon and identifying two-component pairs using purely a genomic approach is not straightforward.

In cyanobacteria, genes encoding Hik2 and its putative response regulators are not found in the same operon. As the result, we could not identify conjugate response regulator partner(s) of Hik2 using the conventional genomic approach. However, Hik2 and its putative response regulators were identified in large-scale protein-protein interaction studies by (Sato et al, 2007). In these studies, Hik2 was observed to interact with Rre1 (Response regulator 1) and RppA (Regulator of photosynthesis and photopigment-related gene expression), *in vivo*, in a yeast two-hybrid assay. However, it is important to note that protein-protein interaction in the yeast two-hybrid assay most often leads to false positives because of random, non-specific interactions arising from over-expression of bait and prey proteins. Therefore, data obtained from yeast two-hybrid assays should always taken with caution, unless otherwise supported with further evidence from pull-down assays, *in vivo* Bimolecular Fluorescence Complementation (BiFC) interaction, and/or *in vivo/vitro* functional interaction. But such important supporting evidence for Hik2-Rre1 or Hik2-RppA is not yet available.

In this chapter, I therefore describe systematic characterisation of the interaction of various response regulators with Hik2 using *in vitro* phosphotransfer kinetics, with the aim of deducing the functional partner(s) of Hik2.

7.2. Possible candidate response regulator partners of Hik2

In order to determine the response regulator partner(s) of Hik2, I selected the following four *Synechocystis sp*. PCC 6803 response regulators for screening: Rre1 (slr1783), RppA (sll0797), RpaA (regulator of phycobilisome-associated A, sll0797), and RpaB (regulator of phycobilisome-associated B, slr0115).

These response regulators were selected on the basis that Rre1/Ycf29 and RpaB/Ycf27B response regulators co-occur with Hik2 in all cyanobacteria and in chloroplasts of non-green algae (Ashby & Houmard, 2006; Lopez-Maury et al, 2002; Puthiyaveetil & Allen, 2009; Puthiyaveetil et al, 2008). The genome of the red alga, *Cyanidioschyzon merolae* encodes only for one histidine kinase, which is a Hik2 homologue, and the gene product is then targeted to chloroplasts. The chloroplast genome of *Cyanidioschyzon merolae* also encodes for two response regulators, Rre1/Ycf29 and RpaB/ycf27B (Matsuzaki et al, 2004; Puthiyaveetil & Allen, 2009; Puthiyaveetil et al, 2008). Therefore, it seems very likely that Hik2-

Rre1 and Hik2-RpaB form two-component pairs in cyanobacteria and in the chloroplasts. Finally, Rre1 was observed to interact with Hik2 in a yeast two-hybrid assay (Sato et al, 2007).

In cyanobacteria, RppA forms a two-component pair with RppB – a nickel-responsive histidine kinase that regulates nickel responsive genes (Lopez-Maury et al, 2002). In addition to its role in nickel homeostasis, Li *et al* reported that RppA regulates transcription of photosynthetic genes in response to the redox state of PQ pool through unknown sensor histidine kinase (Li & Sherman, 2000). Therefore, it was interesting that RppA was observed to interact with Hik2 in yeast (Sato et al, 2007).

RpaA forms a conjugate response regulator pair with the KaiC-interacting histidine kinase, SasA (Li & Sherman, 2000; Wu & Bauer, 2010). SasA is a histidine kinase that interacts with KaiC. The autophosphorylation activity of SasA is controlled by KaiC. In *Synechococcus elongateus,* the circadian rhythm is generated by an oscillator consisting of the KaiA, KaiB and KaiC. The circadian clock receives an input from the redox state of plastoquinone pool through CikA (Circadian Input Kinase A) and also through direct interaction of KaiA with the oxidised form of PQ (Ivleva et al, 2006; Wood et al, 2010). In this model, the SasA-RpaA two-component system forms the primary clock output pathway.

Since there is no evidence for Hik2-RpaA interaction, RpaA is used here to serve as a negative control in the Hik2 phosphotransfer experiments described.

7.3. RESULT

7.3.1. Conserved sequence motifs of putative response regulator partners of Hik2

Figure 7.1 shows conserved sequence features of the receiver domains of Rre1, RpaA, RpaB, and RppA from *Synechocystis* sp. PCC 6803. The D2-box shown in figure 7.1.A is responsible for binding Mg^{2+} ions. The D1-box shown on figure 7.1.A was reported to be a phosphorylation site for multiple response regulators, and to be required for dephosphorylation of histidine kinases. In addition to these conserved sequence motifs, a conserved cysteine residue is present in RppA, RpaB, and RpaA, but not in Rre1 (figure 7.1.B).

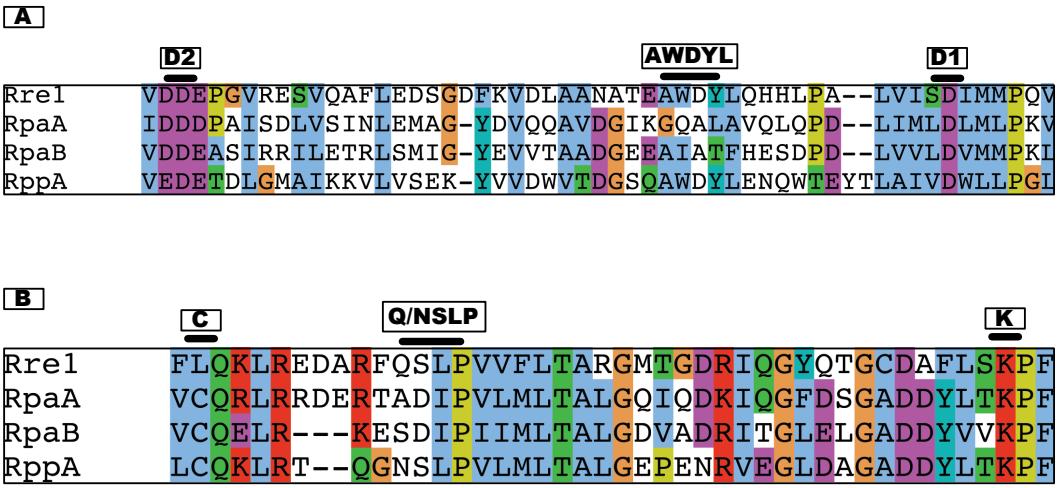

Figure 7.1 Conserved features of receiver domain of putative response regulators of HIK2. The sequences aligned are for receiver domains corresponding to amino acid positions from and between the following segments of the full-length protein: A) Rre, 62-114; RpaA, 6-57; RpaB, 2-53; RppA, 6-59. B) Rre, 119-162; RpaA, 62-105; RpaB, 58-98; RppA, 64-105. The residue colour scheme is the same as in Figure 4.2. The conserved acidic residues (D2 and D1 boxes) and K-box are shown. Sequence similarities that are shared only between Rre1 and RppA (AWDLY and Q/NSLP) are also shown.

7.3.2. Hik2-Rre phosphotransfer kinetics reveal that Hik2 transfers phosphate to Rre1 and RppA

Hik2 interacts with Rre1 and RppA in yeast two-hybrid assay. This indicates that Rre1 and RppA are potential response regulators for Hik2. To further confirm Hik-Rre1 and Hik-RppA two-component systems, I cloned genes encoding the receiver domains of Rre1, RppA, and RpaB. Genes were cloned into pET-30a(+). The gene encoding the full-length RpaA protein was cloned into pET-21b.

In order to allow faithful signal transmission between functional two-component pairs, there is specificity between the kinase and the response regulator, and therefore they should exhibit faster phosphotransfer kinetics than non two-component pairs. The autophosphorylation reaction of full-length Hik2 was performed as indicated in materials and methods (chapter 2). For the phosphotransfer reaction, 67.5 μL of autophosphorylated Hik2 are mixed with 67.5 μL of response regulator reaction mix and incubated for 0, 20, 40, 60, or 90 minutes before terminating the reaction with SDS-sample buffer. Results shown on figure 7.2.B indicate that the phosphotransfer between Hik2-Rre1 was the fastest when compared to that between Hik2-RppA, Hik2-RpaB, and Hik2-RpaA. In just 20 minutes, Rre1 removed approximately 45 % of phosphate and over 90 % of phosphate was removed within 90 minutes. There was a delay in the phosphotransfer activity of Hik2-RppA. However, between 20 minutes and 90 minutes, the kinetics increased rapidly. In contrast, RpaA and RpaB showed

similar kinetics to Hik2 alone, and therefore RpaA and RpaB did not remove phosphate from Hik2.

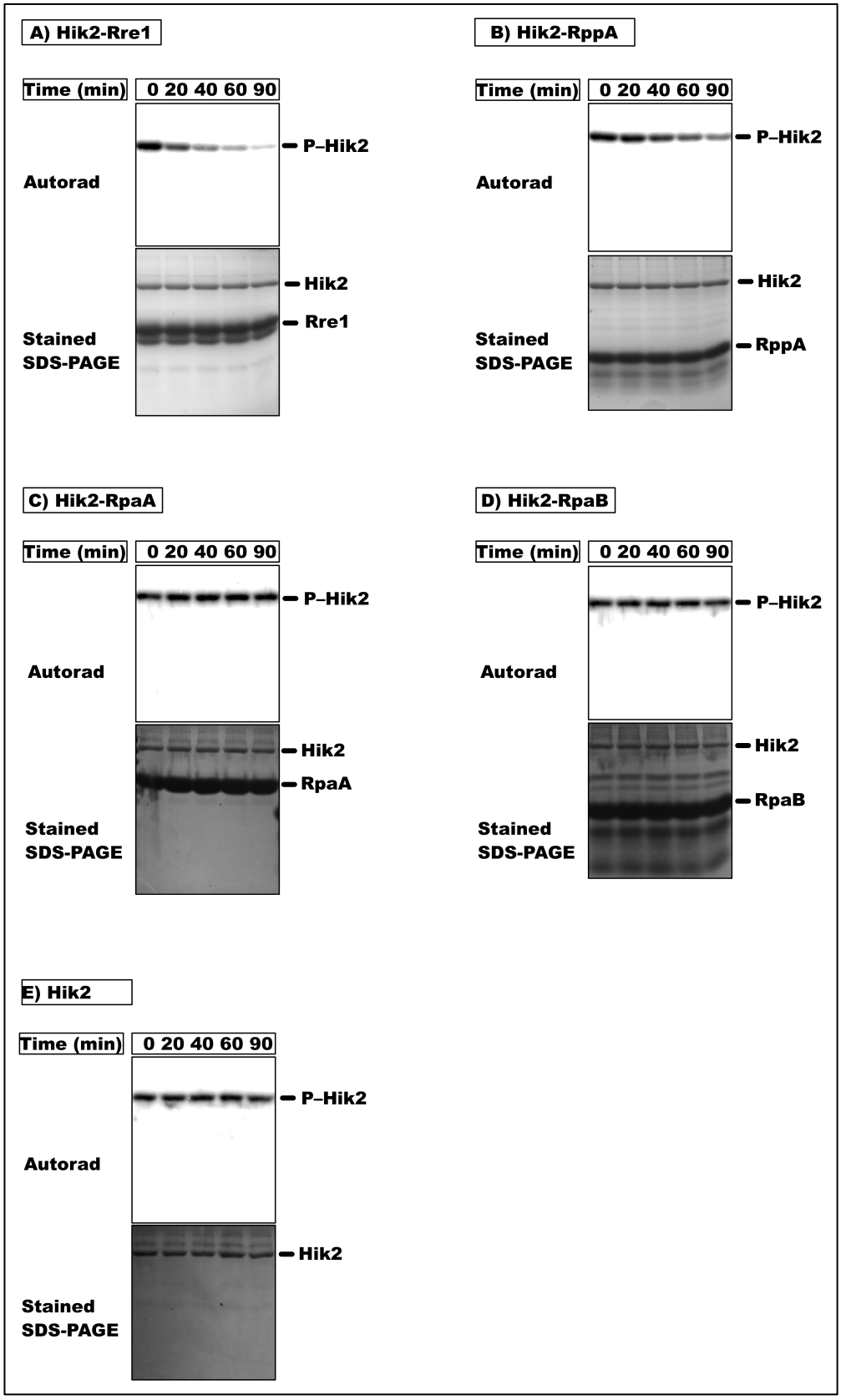
A) Hik2-Rre1
Time (min)
0 20 40 60 90
Autorad
P–Hik2
Stained SDS-PAGE
Hik2
Rre1
B) Hik2-RppA
Time (min)
0 20 40 60 90
Autorad
P–Hik2
Stained SDS-PAGE
Hik2
RppA
C) Hik2-RpaA
Time (min)
0 20 40 60 90
Autorad
P–Hik2
Stained SDS-PAGE
Hik2
RpaA
D) Hik2-RpaB
Time (min)
0 20 40 60 90
Autorad
P–Hik2
Stained SDS-PAGE
Hik2
RpaB
E) Hik2
Time (min)
0 20 40 60 90
Autorad
P–Hik2
Stained SDS-PAGE
Hik2

Figure 7.2.A Time-course of phosphotransfer from P-Hik2 to Rre, RppA, RpaA, and RpaB. 1 μM of autophosphorylated Hik2 (P-Hik2) was mixed with 5 μM of the following response regulators that were already preequilibrated in kinase reaction buffer: A) Rre1; B) RppA; C) RpaA; D) RpaB; and E) Control (no response regulator mix) in 25 μL final volume. The phosphotransfer reaction was allowed to proceed for 0, 20, 40, 60, and 90 minutes. Reaction was terminated at the indicated time, and proteins were resolved on 15 % SDS-PAGE. The SDS-PAGE exposed for autoradiography overnight. The above experiments were repeated at least three times with fresh protein samples.

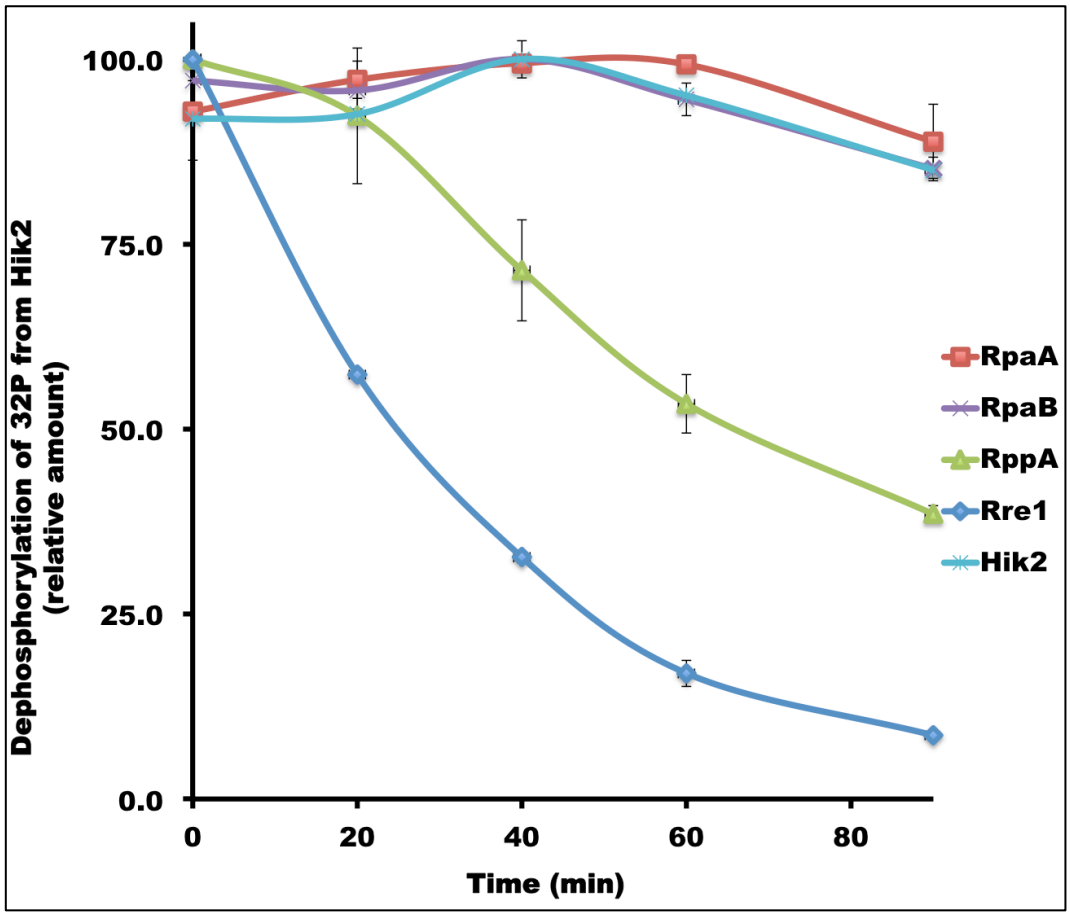

Figure 7.2.B Kinetics of phosphotransfer from P-Hik2 to Rre1 and Hik2. The intensity of bands from the autoradiography (fig.7.2.A) was quantified using the programme ImageJ and the percentage activity was plotted as a function of time (in minutes). Data for Hik2-RpaA are shown with a red line; purple line shows data for Hik2-RpaB; green line shows data for Hik2-RppA; blue line shows data for Hik2-Rre1; and cyan line shows data for Hik2 alone. An error bar indicates standard error of the mean value of three independent experiments.

8. DISCUSSION

Response regulators contain a conserved receiver domain and a variable output domain that serves as a DNA binding domain, or, in some cases, is involved in regulation of protein-protein interactions such as in chemotaxis or methyltransferase activities. As shown on figure 7.1, the receiver domains of putative response regulators of Hik2, the Rre1, RppA, RpaA, and RpaB contain a conserved divalent-binding motif (D2) and a putative phosphorylation site (D1). In addition, the receiver domain is responsible for conferring specificity to the true two-component pair (Skerker et al, 2008). This prevents crosstalk between non-conjugate two-component pairs. Specificity is achieved by conserved residues having coevolved in the functional two-component pairs. Here, figure 7.1 shows Rre1 and RppA shares some common conserved features that are unique to them but missing from RpaA and RpaB response regulators. Both response regulators contain AWDVL, and Q/NSLP (figure 7.1), however, it appears that these sequences are not found in other cyanobacterial Rre1 and RppA proteins. The second conserved feature of these putative response regulators of Hik2 is that a conserved cysteine residue is present in RppA, RpaA, and RpaB, but not in Rre1. The presence of a conserved cysteine residue is interesting because it is probably required for additional control of response regulators activity. DNA-binding activities of response regulators are regulated by phosphorylation. However, the presence of conserved cysteine residues in RpaA, RpaB, and RppA indicates that in addition to phosphorylation, their DNA binding activities could be regulated directly by the redox state of the electron transport chain, for example, by the

redox state of the ferredoxin-thioredoxin system. At night, in darkness, Fd is present predominantly as its oxidised form, whereas in day-light, it is reduced by photosynthesis through PSI. The redox state of ferredoxin-thioredoxin system regulates several Calvin cycle enzymes.

A recent study by Hanke *et al* showed that RpaA interacts with ferredoxin (Fd) in a redox dependent manner (Hanke et al, 2011). The RpaA-Fd interaction was observed to be the strongest under reducing conditions, which implies that, in cyanobacteria, RpaA interacts with Fd in the day-time when Fd is in its reducing form (Matsuzaki et al, 2004). Moreover, a previous study suggested that the SasA-RpaA system is activated by Kai proteins during the day-time (Taniguchi et al, 2010). Tangiuchi *et al* reported that RpaA receives inputs from two distinct pathways. One input comes from the circadian clock proteins, through KaiC-SasA system, and a second input from a non-circadian pathway, from an unknown regulator (Taniguchi et al, 2010). More importantly, their findings show that both inputs exert their effects on RpaA only in the day-time. Furthermore, Tangiuchi *et al* propose that, at night, the histidine kinases CikA and LabA together inhibit the activity of RpaA. However, in light of the new finding obtained by Hanke *et al*, and from the presence of conserved cysteine residue in RpaA (figure 7.1.B), it is likely that RpaA, RpaB, and RppA are regulated by a light-dark cycle. In this cycle, during the day, these response regulators are activated by the Fd system, whereas at night they become inactive because oxidation of their conserved cysteine by Fd. It is therefore likely that CikA and LabA may not play any part at

all in the inactivation of RpaA at night. The role of conserved cysteine residues of RppA and RpaB most probably play similar roles as in RpaA, but further experiments are required to explore their interaction with Fd, also using mutational study to confirm the role of this conserved cysteine.

Interaction of the above response regulators with Hik2 was confirmed using *in vitro* phosphotransfer kinetics. Phosphotransfer kinetics showed that Rre1 had the highest phosphotransfer activity, followed by RppA (figure 2.A and figure 2.B). This finding is consistent with the data obtained in yeast-two hybrid assay (Sato et al, 2007). Interestingly, the rate of dephosphorylation of Hik2 by RppA was low for the first 20 minutes; however, it increased between 20 and 90 minutes. The delay in phosphotransfer activity between Hik2-RppA could have a functional role. RppA has been reported to regulate transcription of genes encoding for photosystems in response to the redox state of PQ pool, that usually a long-term acclimatory process usally takes place in minutes, hours or days.

In cyanobacteria and chloroplasts, the redox state of the PQ pool controls redistribution of excitation energy between photosystem II and I by a process known as state transitions. The redox state of PQ pool also controls transcription of the chloroplast genes that encode reaction-center proteins of photosystem II and I, initiating a long term acclimatory process known as photosystem stoichiometry adjustment (Pfannschmidt et al, 1999). In cyanobacteria, the redox

state of the PQ pool controls reaction-center gene transcription (Fujita, 1997; Murakami et al, 1997) and this process has been suggested to involve the RppA two-component signal transduction system (Li & Sherman, 2000). The finding of an interaction of RppA with Hik2 by Sato *et al*, and the fact that RppA can accept phosphate from autophosphorylated Hik2 (figures 7.2.A and 7.2.B) is therefore interesting.

As shown in chapter four, the autophosphorylation activity of Hik2 is negatively regulated by salt, and it is therefore likely that Hik2 acts as a negative regulator of salt tolerance genes through Rre1. Most bacterial transcriptional activators can have both transcriptional activator or repressor roles. The NarL transcriptional activator, for example, requires phosphorylation for its DNA binding activity and for transcriptional activation (Browning et al, 2004; Maris et al, 2002). A truncated form of NarL that has a deletion of the receiver domain binding DNA is similar to its phosphorylated form, but DNA binding activity alone is not sufficient for transcription initiation. Transcriptional activation seems to require cooperativity between two or more transcriptional activators (Barnard et al, 2004; Browning et al, 2004).

Rre1 controls many genes, including those involved in temperature and salt tolerance, and possibly genes encoding for the photosynthetic light-harvesting antenna system. Recent studies also showed that the *Synechocystis* Sp. PCC 6803

Rre1 protein binds specifically to the promoter region of *adhA* gene and regulates its transcription (Vidal et al, 2009). Similar to FNR and NarL, Rre1 may interact with other regulatory proteins in order for it to have dual function as a transcriptional activator and repressor. Furthermore, transcriptional activation or repression by a response regulator is governed by the location of its DNA binding with site respect to the transcriptional initiation site. If the DNA binding site is located upstream to the site of transcriptional initiation, then response regulators will have transcriptional activator roles, whereas if the binding site is located downstream to the gene, then they will have transcriptional inhibition role (Barnard et al, 2004). It is therefore important to identify the location of Rre1 and RppA binding sites to further understand their roles as transcription activators or inhibitors.

Chapter 8
Chloroplast Sensor Kinase

8.1. INTRODUCTION

Chloroplasts were once free-living cyanobacteria and they had their own complete genome. However, after cyanobacteria became endosymbionts, they lost vast numbers of genes to their hosts nuclear genetic system. The small portion of genes that were retained by the chloroplast encode core components of reaction centres, enzymes that are involved in fatty acid synthesis, and genes that encode bacterial type transcription machineries (Allen *et al*, 2011; Delannoy *et al*, 2011). So, why are these small portion of genes were kept by the organelle? What makes those genes special? Many hypotheses have been devised to answer these questions. In particular, a process of CES (for control by epistasy of synthesis) and Co-location for redox regulation (CoRR) hypotheses seem to stand out from the rest in explaining why chloroplasts have "cherry-picked" certain genes for retention.

CES states that those small portions of genes are important for autoregulation of assembly and assembly factors (Zerges, 2002). Indeed, CES was demonstrated for genes encoding core proteins of PS II and Cyt b_6f (Choquet et al, 2003; de Vitry et al, 1989; Erickson et al, 1989). However, PS I genes does not obey the CES rule. Instead, PS I genes were shown to be under the control of redox reaction. The process of CES was also not observed in cyanobacteria, and therefore, probably arose with endosymbiosis.

CoRR states that co-location of genes and gene products in the same compartment is needed to facilitate rapid and direct regulation by the redox signal generated by photosynthesis in the chloroplast or by respiration in the mitochondrion (Allen, 1993; Allen, 2003). CoRR predicted the presence of bacterial type signalling system in chloroplasts, which would function as a redox sensor and redox response regulator to link the redox state of electron transport chain to chloroplast transcriptional control. Evidence in support of CoRR emerged for the first time in 1999, where it was demonstrated that the redox state of PQ pool regulates genes encoding the core components of reaction centre complexes (Pfannschmidt *et al*, 1999). Recently, Puthiyaveetil and Allen discovered a bacterial-type redox sensor, termed Chloroplast Sensor Kinase (CSK), in algal and higher plants. CSK couples the redox signal from the photosynthetic electron transport chain to chloroplast transcription (Puthiyaveetil *et al*, 2008).

8.2. RESULT

8.2.1. CSK binds DBMIB

CSK was shown to control transcription of *psaA/B* genes in response to light that favours oxidation of the PQ pool, and it is, therefore possible that the CSK senses the PQ pool directly. Here, we investigated interaction of CSK with PQ analogue, DBMIB, using a fluorometric technique. The intrinsic fluorescence of protein is mainly due to tryptophan residues. This fluorescence is sensitive to small structural changes, and therefore tryptophan fluorescence quenching is used to study conformational changes in polypeptides. I titrated DBMIB with CSK as described under the materials and methods section and measured fluorescence emission at 340 nm. Fluorescence emission was plotted as a function of free DBMIB concentration. Figure 8.1 shows that the CSK binds DBMIB with increasing concentration of DBMIB. A K_d value of 3.66 μM was obtained by fitting data to nonlinear curve as described under the materials and methods section (chapter 2)

8.2.2. CSK does not autophosphorylate, *in vitro*

We next examined *in vitro* autophosphorylation of CSK in the present of different redox agents. Figure 8.2, lane 1 shows that untreated CSK is inactive. Figure 8.2, lane 2, 3, 4, and 5 were treated with $K_3Fe(CN)_6$, DTT, benzoquinone, and hydroquinone, respectively. Similar to the untreated CSK sample (figure 8.2, lane

1), treatment of CSK with different redox agents did not yield CSK autokinase activite (Figure 8.2, lane 2-5). Interestingly, benzoquinone and hydroquinone treated CSK proteins migrated as two bands on 12 % SDS-PAGE (figure 8.2, lane 4 and 5)

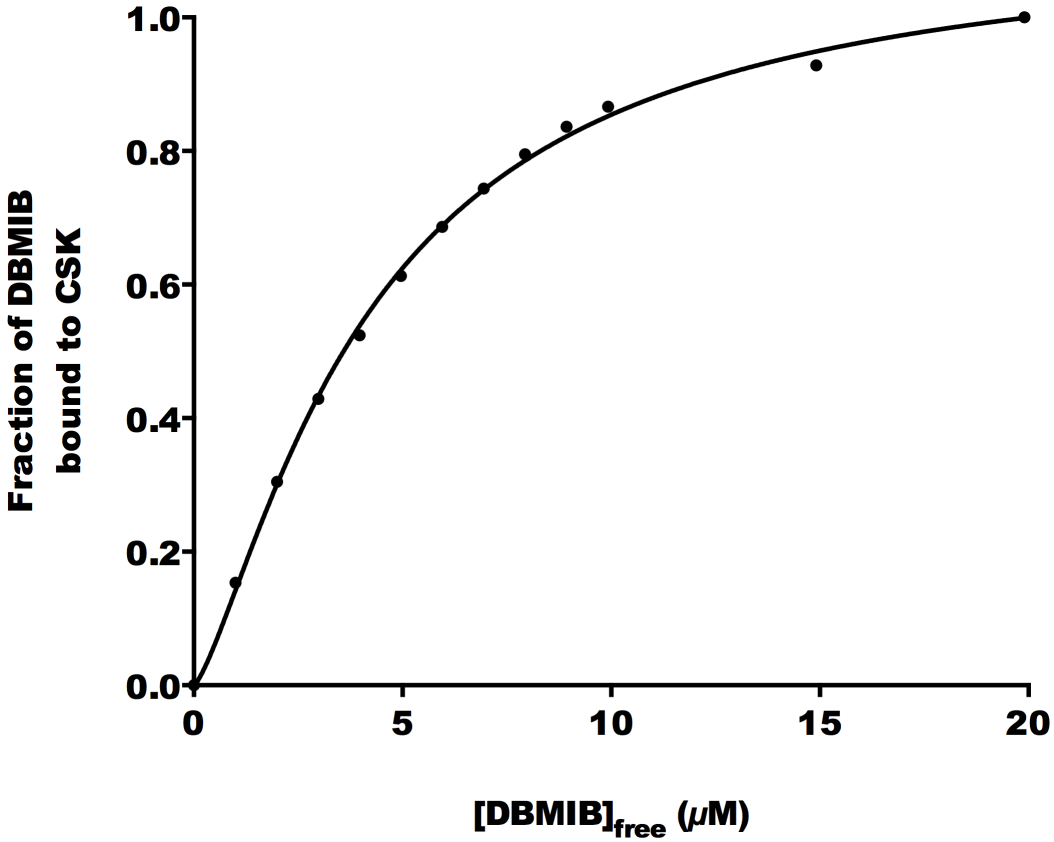

Figure 8.1 Fluorometric binding titration of DBMIB to CSK. Varying concentrations of DBMIB were added to CSK at 0.1 μM final in a total volume of 3 mL, and titration was performed at 25 ºC. CSK protein was excited at 280 nm and fluorescence emission was measured at 340 nm. Data were converted to free DBMIB concentration as indicated under the materials and methods section (chapter 2) and data were plotted as the function of free DBMIB concentration.

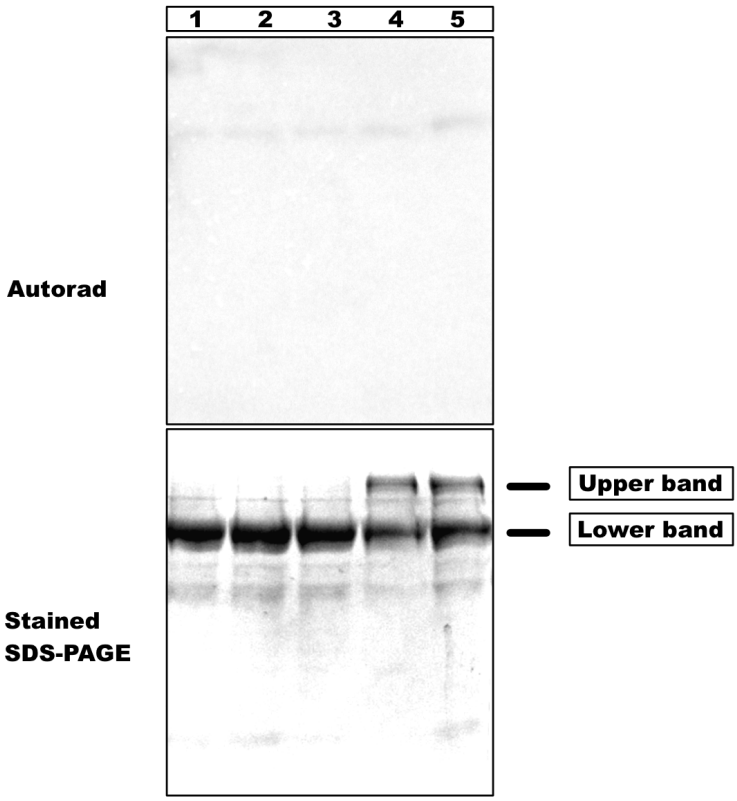

Figure 8.2 Effect of different redox agents on the activity of CSK. Purified recombinant CSK proteins were pre-treated with: lane 1, nothing; lane 2, 2 mM $K_3Fe(CN)_6$; lane 3, 6 mM DTT ; lane 4, 0.5 mM benzoquinone; lane 5, 0.5 mM hydroquinone. Autophosphorylation was initiated by addition of [γ^{32}-P] ATP and the reaction mixture was then incubated at 30 ºC for 60 minutes. The reaction was terminated by adding 6 μL of 5-fold concentrated sample buffer and proteins were resolved on a 12 % SDS-PAGE.

8.2.3. CSK has a modified CA domain

The ATP binding cavity of histidine kinases contains conserved residues that are essential for its autophosphorylation (see chapter 6). These residues includes G1 and G2 boxes, which have characteristic signatures "DxGxG" and "GxGxG", respectively. Sequence alignment of CSK homologues shows that CSK in green plants has a modified ATP-binding domain. In higher plants, only the first conserved glycine residue is retained, and the second conserved glycine residue in the G1-box is replaced by an aspartic acid (figure 8.3). Moreover, the first two conserved glycine residues in the G2-box are replaced by an asparagine and a valine, respectively. Only the third conserved glycine residue of the G2-box is retained in higher plants (figure 8.3).

8.2.4. Secondary structural prediction of the ATP-lid of CSK and Hik2

Figure 8.4 shows, with exception of *Cynidioschzon merolae* CSK, the cyanobacterial Hik2 and chloroplasts CSKs all have similar predicted secondary structure of the ATP-lid. In secondary structure, the ATP-lid is located between the G1-box and the G2-box forms a coil-coil. *Cynidioschyzon merolae* CSK contains an unusually large sequence between the G1 and G2 boxes, perhaps suggesting a larger ATP-lid. Furthermore, *Arabidopsis* and *Phaeodactylum* CSKs do not have the conserved G2-motif.

Figure 8.3 Conserved sequence features of CA-domain of CSK. Sequence alignment of higher plant CSK and its bryophyte, algal and cyanobacterial homologues. The residue colours scheme is the same as in Fig.4.2. The N, G1, and G2 boxes are shown above the sequence.

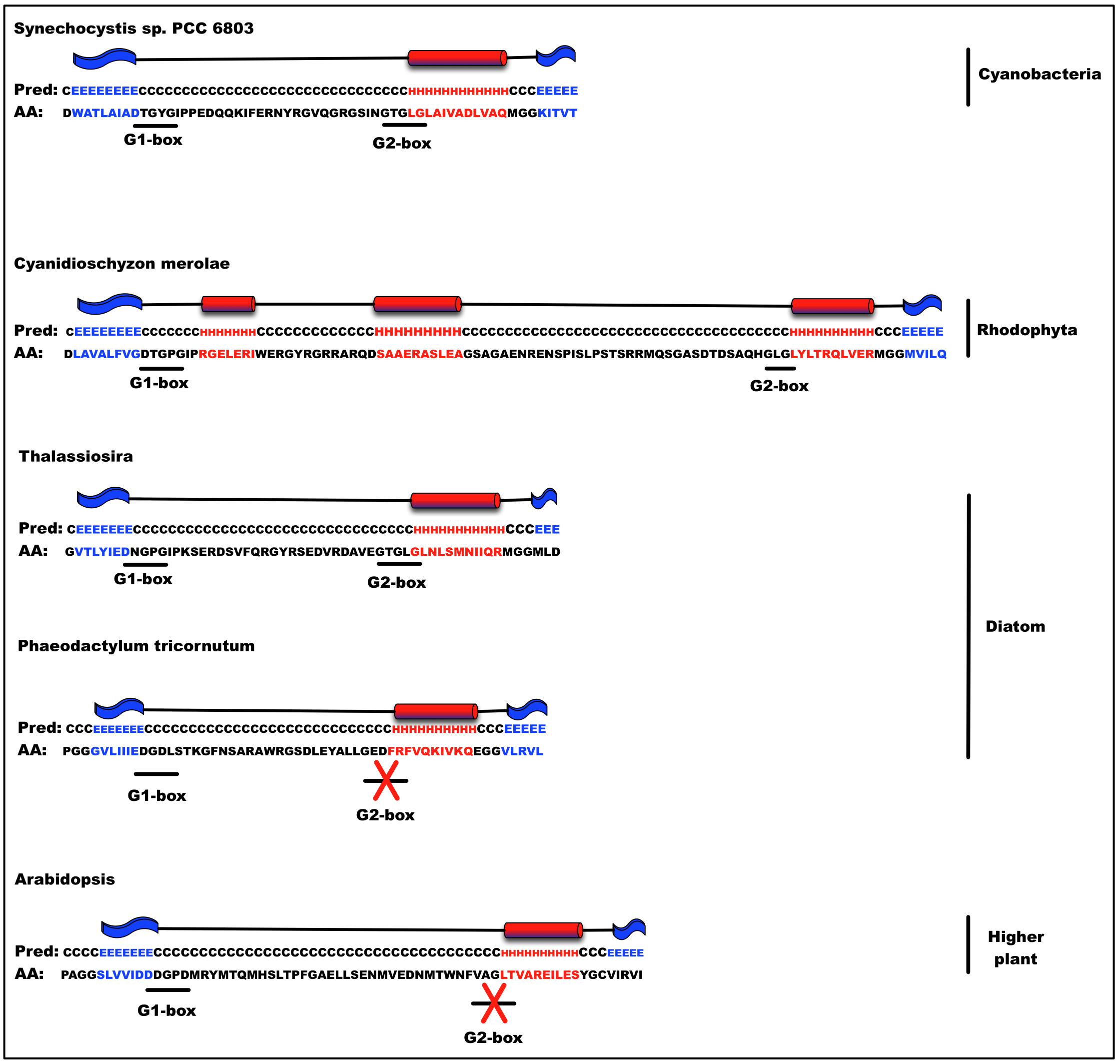

Figure 8.4 Predicted secondary structure of the ATP-lid of CSK homologues. Secondary structure of ATP-lid of Cyanobacterial Hik2 and of CSK of *Cyanidoschzon merolae, Thalassiorira, Phaeodactylum tricornutum, and Arabidopsis thaliana* CSK protein predicted using programme PSIPRED (http://bioinf.cs.ucl.ac.uk/psipred/). The conserved motif of G1 and G2 boxes is shown. Where the motif is missing, this is indicted by the red cross. AA stands for a target sequence; Pred stands for predicated secondary structure; coil is shown with black line; helix is shown with red oval shape; strand is shown with blue.

8.2.5. **TNP-ATP binding**

Based on the sequence alignment shown on figure 8.3, CSK is predicted to contain a modified ATP binding cavity. Furthermore, the recombinant CSK protein was inactive in autophosphorylation *in vitro* (figure 8.2). In order for CSK to function as a protein kinase, it must first have the ability to bind an ATP molecule, and then it must catalyse substrate phosphorylation. Here, I investigated the ATP binding activity of *Arabidopsis* CSK using a fluorescent ATP derivative TNP-ATP. TNP-ATP contain a trinitrophenyl group, which upon being exposed to a hydrophobic pocket such as an ATP binding cavity, it becomes more fluorescent. The result shown on figure 8.4 the fluorescence emission spectrum of TNP-ATP changed in the presence of 2 μM CSK (figure 8.5, blue line), indicating that TNP-ATP-CSK complex is formed. Fluorescence emission at 540 nm is increased by more than two-fold in the presence of CSK. The TNP-ATP from CSK was displaced with addition of an excess natural ATP (figure 8.5, green line).

8.2.6. **TNP-ATP binding constant**

We next investigated binding affinity of TNP-ATP to CSK by varying the concentration of TNP-ATP in the presence of CSK and 1 mM natural ATP. The fluorescence emission increase at 540 nm was measured and data was fitted to nonlinear regression to calculate K_d for TNP-ATP. Figure 8.6 shows that a K_d value of 1.1 μM was obtained.

8.2.7. **TNP-ATP dissociation constant**.

TNP-ATP dissosciation constant was determined by titrating against ATP in the presence of 1 μM TNP-ATP and the resulting fluorescence decrease was measured. Figure 8.7 shows that a K_d value of 7.5 mM for ATP was calculated by fitting data using nonlinear regression. This study indicates that CSK binds TNP-ATP better than it binds ATP.

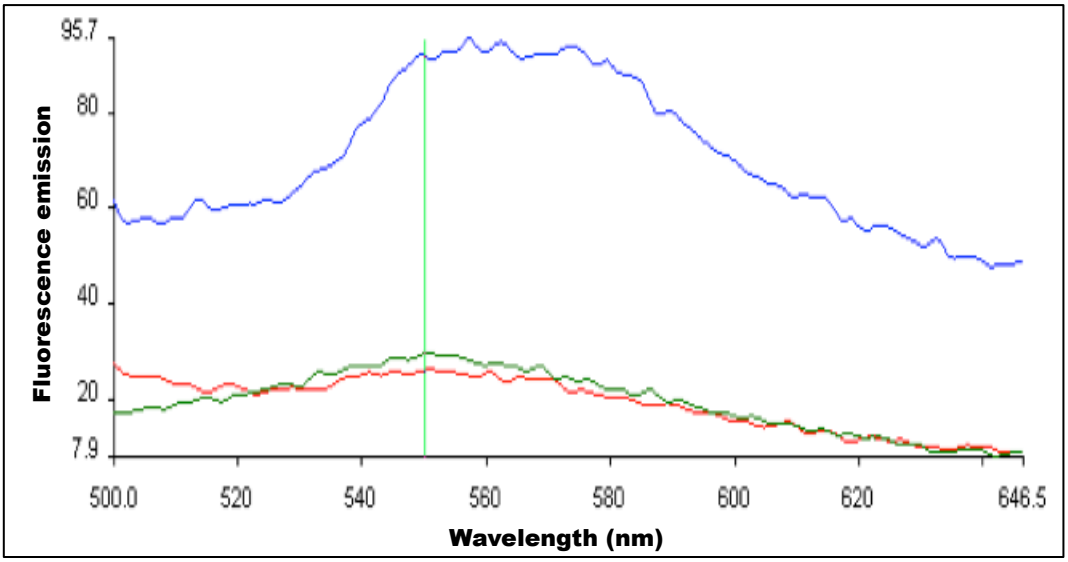

Figure 8.5 Binding equilibrium of TNP-ATP to *Arabidopsis* CSK using fluorescence spectroscopy. TNP-ATP was excited at 410 nm and excitation emission was measured between 500 to 646 nm. Fluorescence emission spectra of 1 μM TNP-ATP is shown by red line (—**)**; fluorescence spectra of 1 μM TNP-ATP in the presence of 2 μM CSK is shown by blue line (—); and fluorescence spectra of 1 μM TNP-ATP in the presence of 2 μM CSK and 40 mM natural ATP is shown by green line (—).

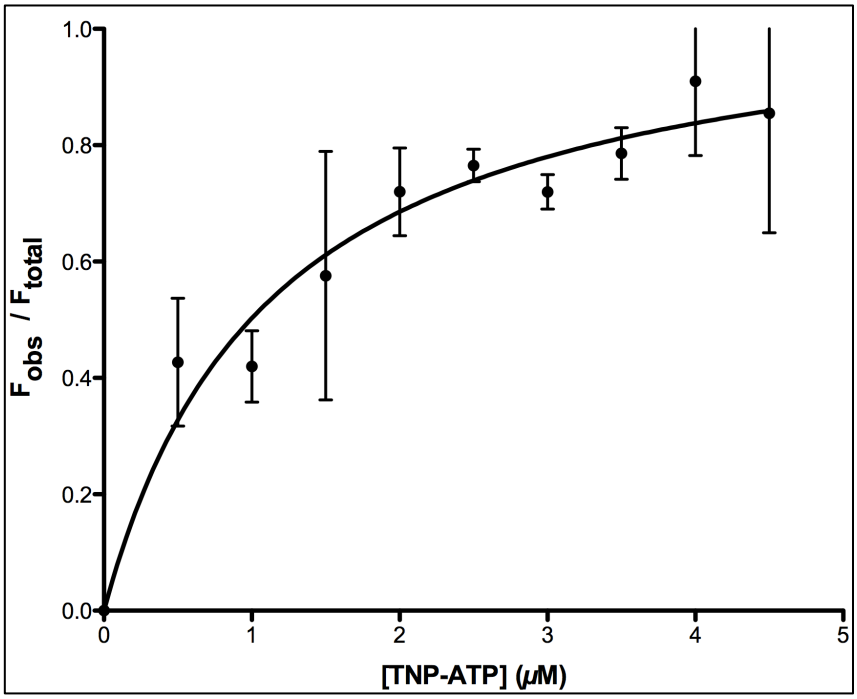

Figure 8.6 Titration of *Arabidopsis* CSK with TNP-ATP. TNP-ATP binding titration was performed with varying concentration of TNP-ATP in the presence of 2 μM CSK and 1μM ATP. TNP-ATP was excited at 410 nm and excitation emission at 540 nm was monitored. Correction to background TNP-ATP fluorescence was made by subtracting values for buffer plus TNP-ATP from CSK plus TNP-ATP and data were then plotted using Prism 5 (Motulsky & Christopoulos, 2003). Each data point represents the mean ± S.E of three measurements. Dissociation constant (K_d) for TNP-ATP was calculated by nonlinear regression curve fitting of data.

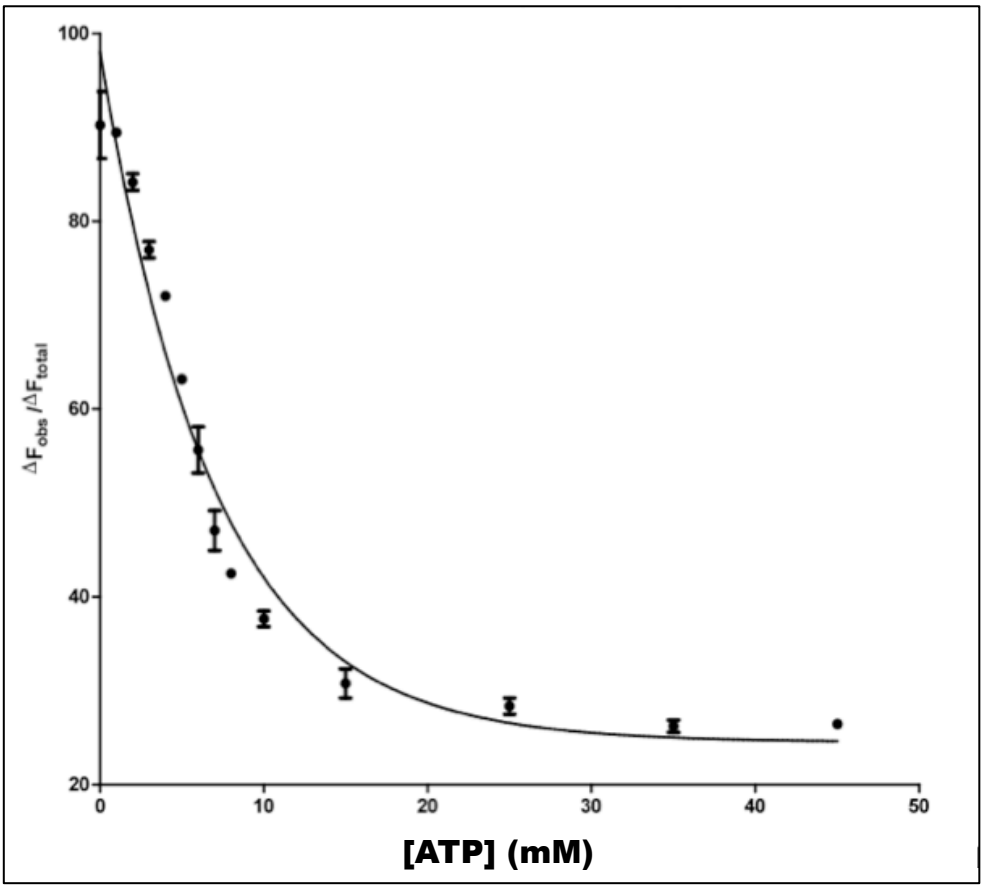

Figure 8.7 Displacement of TNP-ATP from *Arabidopsis* CSK. TNP-ATP displacement titration was performed with varying concentration of ATP to a sample that was pre-equilibrated with 1 μM TNP-ATP and 1 μM CSK. Decrease in intensity of emission at 540 nm was measured. Data was plotted as function of ATP concentration and data were plotted using Prism 5 (Motulsky & Christopoulos, 2003). Each data point represents the mean ± S.E of three measurements. The dissociation constant (K_d) for TNP-ATP was calculated by nonlinear regression curve fitting of data.

8.3. DISCUSSION

CSK has been proposed to link the redox state of the PQ pool to chloroplast gene transcription (Puthiyaveetil *et al*, 2008). But it is not yet clear whether CSK receives a direct signal from the PQ pool. Here, using a fluorometric assay, I exploit the interaction of a PQ analogue, DBMIB with the full-length *Arabidopsis* CSK protein. Our result shown in figure 8.1 demonstrates that CSK binds DBMIB directly. This observation further supports the proposal that CSK acts as a PQ pool sensor.

The PQ pool has a standard midpoint potential of + 50 mV, n = 2 (Silverstein *et al*, 1993b; Silverstein *et al*, 1993c) and an effective redox potential that changes with fluctuating light distribution between the photosystems. These fluctuations may affect a specific redox sensor. For example, the redox state of the PQ pool controls the light-dependent phosphorylation of chloroplast light-harvesting complex II (LHC II) (Allen, 1992; Allen et al, 1981). The LHCII kinase (Stn7/Stt7) is responsible for phosphorylation of LHC II (Bellafiore et al, 2005; Depege et al, 2003; Rochaix, 2007). LHCII kinase has a midpoint of potential of + 48 mV, which is similar to that of PQ pool midpoint potential (Silverstein *et al*, 1993a). But some quinone pool sensors do not use its redox signal. The RegB for example interacts with the reduced and oxidised form of ubquinone with a similar affinity, and only the oxidised form of ubquinone seems

to inactivate the autophosphorylation activity of RegB (Wu & Bauer, 2010). However, the autophosphorylation activity of RegB is regulated through an allosteric effect triggered by binding of ubquinone/ubiquinol rather than oxidation by ubiquinone (Wu & Bauer, 2010). In contrast, the result shown here in figure 8.2 that CSK does not respond to different redox reagents. The fact that CSK binds DBMIB indicates that CSK could also employ similar sensing mechanism to RegB. We also noted that benzoquinone–and hydroquinone–treated CSK protein migrated as two bands on the SDS-PAGE gel that is both denaturing and reducing (figure 8.2, lanes 4 and 5). Cysteine residue in enzymes are known to react with quinones to form quinone-cysteine adducts that cannot be broken with reducing agents, for example by DTT used in our sample buffer (Li *et al*, 2005). Cysteine residues in CSK could be forming a thioether-quinone adduct. This observation further strengthens quinone-binding activity of CSK. However, it is not yet clear whether the adduct formation is part of the signalling mechanism of CSK.

Loss of a gene encoding a conjugate response regulator partner of histidine kinases usually leads to loss of gene encoding the sensor kinase. For example, the Ycf26 and the Ycf27 are known to form conjugate pairs in cyanobacteria are also present in chloroplasts of most red algae (Ashby *et al*, 2002; Seki *et al*, 2007). But Ycf26 and Ycf27 are absent from green lineages. The chloroplast genome of the ancient red alga *C. merolae* encodes for Ycf27 and Ycf29 response regulators; however, the *ycf26* gene is absent from this alga. Instead, the nuclear encoded

CSK functionally replaces Ycf26 function in *C. merolae* (Puthiyaveetil & Allen, 2009).

The CSK of the green algal and land plant lineage has lost the conserved histidine residue that is a site for autophosphorylation and that is also needed for phosphotransfer; Therefore, this modified CSK cannot function as a typical histidine kinase. Instead, the conserved histidine residue in CSK is replaced by tyrosine or glutamine in green algae and by glutamate in higher plants (Puthiyaveetil & Allen, 2009; Puthiyaveetil *et al*, 2008). Comparably, there is an equivalent modification in the CA domain of those modified CSKs (figure.8.3 and 8.4). However, this modification has not affected the ATP binding activity of *Arabidopsis* CSK (figure 8.5, 8.6, and 8.7). The binding affinity of CSK for the fluorescent analogue of ATP (TNP-ATP) is 1.1 μM, a result that is comparable to that of bacterial histidine kinases. The EnvZ and CheA have K_d value for TNP-ATP of 1.9 μM and 1.7 μM, respectively (Plesniak *et al*, 2002; Stewart *et al*, 1998). Furthermore, TNP-ATP can be displaced from CSK using ATP (figure 8.7).

Although modification within the ATP binding domain of CSK did not affect its ATP binding activity, we could not detect autophosphorylation of CSK *in vitro* (figure 8.2.). This suggests that the CSK in chloroplasts has a different catalytic mechanism from that of its cyanobacterial homologue. Perhaps this

modification is need for CSK to integrate new catalytic mechanism. Since Ycf29 and Ycf27 are missing from chloroplasts of green lineages, CSK must undergo modification in order to rewire into an existing signal transduction pathway of chloroplasts. Indeed, Puthiyaveetil *et al* (Puthiyaveetil *et al*, 2010) have shown that *Arabidopsis* CSK protein interacts with two plastid transcription machineries, including sigma factor 1 (SIG1), a transcriptional initiation factor that has prokaryotic origin. SIG1 is required to initiate *psbA* and *psaAB* genes transcription (Shimizu et al, 2010). The second protein that CSK interact with is the plastid transcription kinase (PTK). Interestingly, Shimizu *et al* (Shimizu *et al*, 2010) showed that transgenic *Arabidopsis* plants, lacking the putative SIG1 phosphorylation site were unable to regulate transcription of *psaAB* genes in light condition that favours the oxidation of PQ pool. This is interesting because transgenic plants that lack the *csk* gene also have the same phenotype as SIG1 mutant plants (Puthiyaveetil *et al*, 2008).

Histidine kinases do not transfer the γ-phosphate group directly from an ATP molecule to their substrate. Instead, they use the higher energy of the phosphoramide bond to facilitate the transfer of their phosphate to an aspartate residue of the response regulator. However, Phospho-serine/threonines are thermodynamically more stable than phosphoramide or acyl-phosphate; therefore they cannot passively transfer phosphate groups. Indeed, several modified histidine kinases, such as ETR2 (Moussatche & Klee, 2004), plant phytochrome (Fankhauser *et al*, 1999), α-keto dehydrogenase kinase (Lasker *et al*, 2002), and

pyruvate dehydrogenase kinase (PDK) (Thelen *et al*, 2000) have lost the ability to catalyse His-Asp phosphotransfer. Instead, they have acquired a catalytic mechanism that is similar to serine/threonine kinases, and they now phosphorylate their substrates on serine or threonine residues. In addition to a serine/threonine kinase activity, PDK was observed to autophosphorylate on multiple histidine residues. But PDK does not catalyse His-Asp phosphotransfer (Thelen *et al*, 2000)**.** Energetically, it is also possible to transfer phosphate from His or Asp to serine/threonine. Indeed, in the CheA-CheY two-component system, disruption of the conserved aspartate residue of CheY resulted in the transfer of phosphate from the conserve histidine of CheA to a serine residue of CheY (Bourret *et al*, 1990). The glutamate residue replacing the histidine in the H-box of modified CSKs possibly work in such way as to transfer phosphate to its substrate. However, it is not yet clear whether the modified CSKs are autophosphorylated on a glutamate residue.

Chapter 9
General discussion

9.1. Final conclusion and summary

The work presented in this thesis provides insight into an autophosphorylation mechanism of full-length Hik2 protein and its phosphotransfer activity to its response regulator partners, Rre1 and RppA.

In chapter 3, I showed evidence that the gene encoding for Hik2 protein is distributed in all 49 cyanobacterial species that I had looked at. Furthermore, in 12 cyanobacteria genomes, Hik2 is present as a truncated form, a finding that is also in agreement with Ashby *et al* (Ashby & Houmard, 2006). The full-length Hik2 protein of *Synechocystis* sp. PCC 6803 is autokinase active in its ground state and its activity was inhibited by sodium ions (chapter 4, figures 4.4 and 4.5). Furthermore, Hik2 protein seems to exist as a monomer, a tetramer and as higher-order oligomers that are probably at equilibrium with each other (chapter 5.1-5.3). Analysis of autophosphorylation activity of Hik2 revealed that the monomeric and oligomeric forms of Hik2 are autophosphorylated (chapter 5.4). For Dcus and ArcA, higher-order oligomers seem to be a mechanism of inhibiting their autokinase activities (Malpica et al, 2004; Scheu et al, 2010). However, the role of higher-order oligomerisation of Hik2 has yet to be elucidated.

Mutational studies of conserved motifs of the core kinase domain of Hik2 revealed that the Hik2 uses similar ATP-binding and autophosphorylation mechanisms to those of typical histidine kinases, such as EnvZ (chapter 6, figures 6.1-6.3). However, the Hik2 homologue in chloroplasts, CSK is found as a modified histidine kinase. Firstly, the conserved histidine residue that is required for autophosphorylation activity is replaced in CSK by a glutamine or tyrosine in green algae and by a glutamate in higher plants (Puthiyaveetil et al, 2008). Secondly, the ATP binding-cavity of modified CSKs contains mutations within key motifs that are important for stabilising an ATP molecule upon binding, and are required for the release of the ADP molecule from its binding cavity (chapter 8, figure 8.3). Nevertheless, these mutations did not abolish the protein ATP-binding abilities. The striking difference between Hik2 and CSK is that the recombinant CSK protein is inactive in autophosphorylation, *in vitro*. Perhaps the modified CSK had lost its autophosphorylation activity or it may require a signal to activate autophosphorylation. However, CSK is active in chloroplasts, and couples the redox state of PQ pool to chloroplast gene transcription. As shown in chapter 8, figure.8.1, CSK interacts with the PQ analogue, DBMIB. This finding further support CSK as PQ pool redox sensor. However, we have yet to demonstrate the kinase activity of CSK either *in vitro* or *in vivo*.

9.2. A model for Hik2 control of gene expression in *Synechocystis*

Figure.9.1 proposes our current working model of transcription control mediated by Hik2 two-component signal transduction system in the cyanobacterium *Synechocystis* sp. PCC 6803, and is based on the following observations. Firstly, Hik2 interacts with Rre1 and RppA *in vivo,* in a yeast two-hybrid assay (Sato et al, 2007). Secondly, Rre1 and RppA were implicated in regulation of transcription of genes encoding components of photosynthetic machineries; also, Rre1 was reported to control salt tolerance genes (Li & Sherman, 2000; Paithoonrangsarid et al, 2004). Thirdly, the Hik2 homologue CSK controls chloroplast gene transcription in response to changes in the redox state of PQ pool (Puthiyaveetil et al, 2008). Finally, Hik2 transfers a phosphoryl group to Rre1 and RppA *in vitro* (chapter 7, figures 7.2.A and 7.2.B). In these model presented in figure 9.1, autophosphorylated Hik2 transfers a phosphoryl group to Rre1 and RppA. Phosphorylated Rre1 activates genes encoding phycobilisome and genes coding for photosystems, thereby balancing the redistribution of electrons between PS II and PS I. Conversely, phosphorylated Rre1 represses salt tolerance genes. Phosphorylated RppA activates transcription of genes encoding core components of photosynthetic reaction centres (Li & Sherman, 2000). Upon salt or hyperosmotic shock, autophosphorylation of Hik2 will be inhibited (chapter 4, figure.4.3 and 4.5). Rre1 and RppA are then no longer phosphorylated, thus Rre1 no longer acts as a transcription inhibitor for salt tolerance genes.

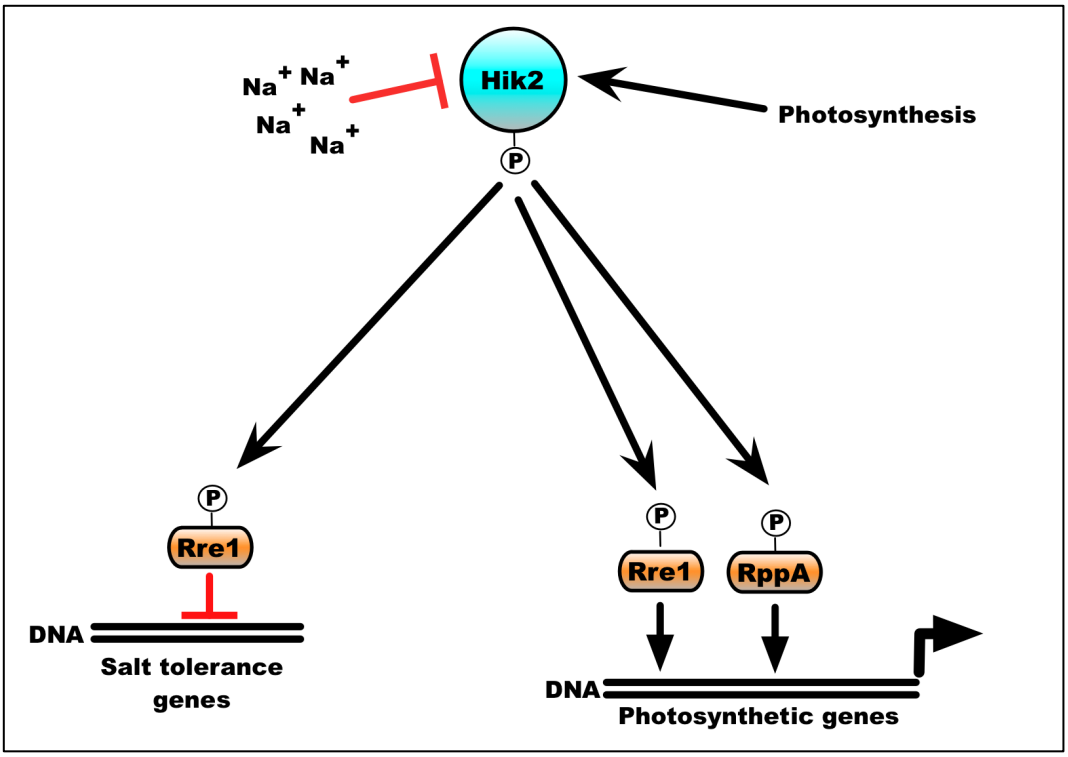

Figure 9.1 The proposed signal transduction pathways of the Hik2 two-component system. The autophosphorylation activity of Hik2 is regulated by signals from photosynthesis and by sodium ion (Na^{2+}). Red arrow an indicates inhibitory effect. Black arrow indicates activation. Autophosphorylated (active) Hik2 transfers phosphoryl group to Rre and RppA. Phosphorylated Rre1 and RppA activate genes encoding for photosynthetic reaction centres. In addition, phosphorylated Rre1 acts as a negative regulator for salt tolerance genes. Under high salt condition, Na^{2+} inhibits the autophosphorylation of Hik2, thus removing repression from salt tolerance genes.

9.3. A model for CSK control of gene expression in chloroplasts

It is thus proposed that in light 1 conditions, CSK acts as the SIG1 kinase and repress *psaA* transcription, and thereby regulates the stoichiometry of photosystems (Puthiyaveetil et al, 2010). This proposal (Puthiyaveetil et al, 2010) is based on the following two key observations. Firstly, CSK and SIG1 interact (Puthiyaveetil et al, 2010). Secondly, both CSK knockout mutants and the phosphorylation site mutant of SIG1 have the same signalling phenotype – neither shows wild-type repression of *psaA/B* transcription in photosystem I light (light 1) – suggesting they are part of the same signal transduction pathway. The demonstration that CSK binds the PQ analogue, DBMIB (chapter 8, figure 8.1 and figure 8.2, lanes 4 and 5) further clarifies some important points in the CSK signal transduction pathway. First of all, it reveals the crucial gene regulatory signal from the photosynthetic electron transport chain as oxidised PQ (figure 9.2.A). In photosystem II light – light 2 – (figure 9.2.B), the PQ pool becomes reduced and CSK is likely to become inactive as a protein kinase because PQH_2 inactivates CSK. In light 2, a putative phospho-SIG1 phosphatase is predicted to dephosphorylate the phosphorylated SIG1 (Puthiyaveetil et al, 2012; Puthiyaveetil et al, 2010), and thereby remove repression of *psaA/B* genes transcription. The dephosphorylated SIG1 can now transcribe *psaA/B* and *psbA/D* genes efficiently, increasing the PS I/PS II ratio in light 2 (Puthiyaveetil et al, 2012; Puthiyaveetil et al, 2010).

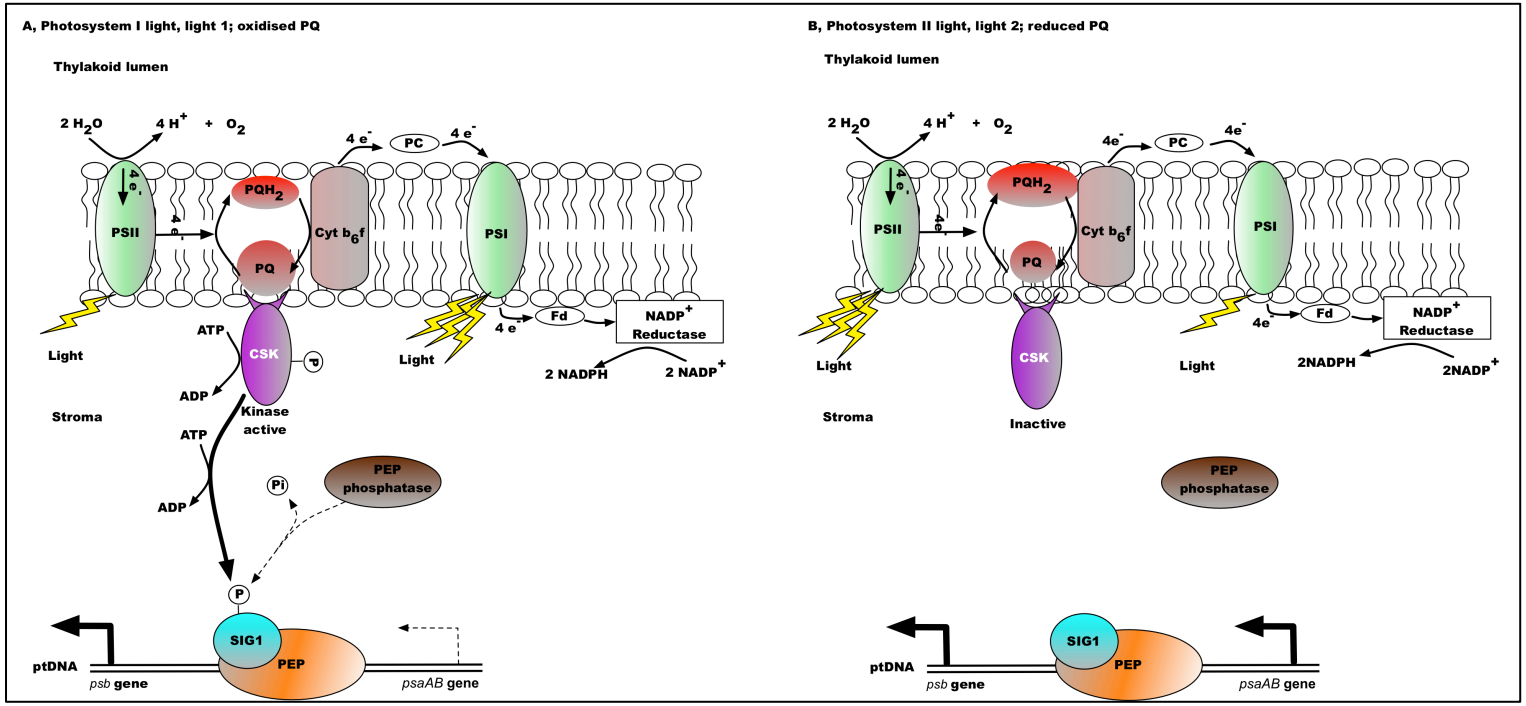

Figure 9.2 A model showing Chloroplast Sensor Kinase (CSK) coupling the redox signal from the PQ pool to chloroplast gene transcription. **A) Activation of CSK**. When PS I is preferentially excited, the PQ pool becomes oxidised. The oxidised PQ pool then activates the autophosphorylation and kinase activity of CSK. The active CSK can then act as a protein kinase for Sigma Factor 1 (SIG1) (green) (Puthiyaveetil et al, 2012; Puthiyaveetil et al, 2010). Phosphorylated SIG1 cannot transcribe the *psaA* gene efficiently (shown by a dotted line), but transcription rate for *psb* gene is unaffected (Shimizu et al, 2010). **B) Inactivation of CSK**. When PSII is selectively exited (light 2), the PQ pool becomes reduced and PSI becomes the rate-limiting step. In this condition, any autokinase and protein kinase activities of CSK are suppressed. In light 2 conditions, a phosphoprotein phosphatase is predicted to act on plastid-encoded polymerase (PEP) to dephosphorylate Phospho-SIG1 (Puthiyaveetil et al, 2012; Puthiyaveetil et al, 2010), and thereby remove repression of the *psaA* gene

9.4. Future directions

9.4.1. Determination of protein-protein and protein DNA interactions in Hik2-RR two-component system

As discussed in chapter 7, Hik2 forms a two-component pair with Rre1 and RppA. However, the functional interaction that presented in this thesis is based on an *in vitro* phosphotransfer assay. This work would greatly benefit from *in vivo*, in cyanobacterium, functional protein-protein interaction between Hik2-Rre1 and Hik2-RppA using techniques such as Bimolecular Fluorescence Complementation (BiFC). The principle of BiFC employs tagging protein A and protein B with N-terminal and C-terminal YFP fragments, respectively. Interaction between protein A and B brings the two half fragments of YFP in close proximity, which allows it to reform into its native structure and emit fluorescence upon excitation (Hu et al, 2002). In this study, protein A represents Hik2 and protein B represents Rre1 or RppA.

Further interaction of Hik2 with its partners could be studied *in vitro* using isothermal titration calorimetry and Biacore. These two techniques will allow us to determine binding affinities (K_d) between Hik2-Rre and Hik2-RppA, and also will allow us to determine the binding mechanism employed in the Hik2-RR two-component system.

In order to identify promoter region(s) that Rre1 and RppA bind, chromatin immunoprecipitation (ChiP), and gel electrophoreses mobility shift followed by DNase I footprinting could be employed. Once binding regions are identified, one could look at the condition(s) under which the transcriptional factor binds to the promoter region, and at its role as transcription activator or repressor. Since ChiP technique involves crosslinking of DNA-protein complexes, the technique can be used to identify further interacting factors that are probably required for Rre1 and RppA transcriptional activation or inactivation using mass spectroscopy.

9.4.2. Deletion and overexpression of *hik2*, *rre1*, and *rppA* genes

Disruption of genes in cyanobacteria involves homologous recombination and insertion of antibiotic resistance gene. Success of complete segregation of the recombinant genes is determined using the PCR technique. Single and double mutant strains of Rre1 and RppA could be generated to further characterise the Hik2-RR system. Mutant and wild-type cell lines will be treated with different conditions such as high-light, low-light, and light conditions that favour the oxidation or reduction of PQ pool. Transcript levels for various genes encoding for photosynthetic and respiratory complexes will be analysed using a RT-PCR and/or a Northern blotting. Alternately, DNA-microarrays can be used to look at global transcription effects to determine genes that are under Hik2-Rre1 and Hik2-RppA control. Since disruption of the *hik2* gene is lethal, one could overexpress Hik2 and as well as Rre1 and RppA proteins in *Synechocystis sp*.

PCC 6803 under different stress conditions and that determine under which condition Hik2 is phosphorylated or dephosphorylated.

9.4.3. Structure determination of CSK and Hik2

Hik2 and the unmodified CSK proteins contain typical histidine kinase motifs and are therefore predicted to employ the His-Asp phosphotransfer mechanism. However, the modified form of CSK lacks several conserved motifs that are found in histidine kinases. First of all, it lacks the conserved histidine residue that is required for phosphorylation. Therefore, the modified CSK employs a different catalytic mechanism than unmodified CSK and Hik2. Structure determination of Hik2 and the modified CSK, followed by structural comparison will reveal insight into the catalytic mechanism of Hik2 and CSK. Furthermore, since there is no structure available for a full-length histidine kinase in the protein databank, elucidation of full-length structure of CSK and/or Hik2 will shed light into the mechanism of a signal propagation from the sensor domain of histidine kinase to its kinase domain.

Appendix

Protein overexpression and purification

Figure 2 shows the result of protein overexpression of the full-length and the truncated forms of *Arabidopsis* CSK protein. Figure 2, lane 2 shows that the full-length CSK protein is mainly present in the insoluble cell fraction, and present in a low quantity in the soluble cell fraction. The purified CSK_F migrated on SDS-PAGE with an apparent molecular mass of 75 kDa. The truncated form of CSK, containing the core kinase domain of CSK, migrated on SDS-PAGE with an apparent molecular mass of 37 kDa.

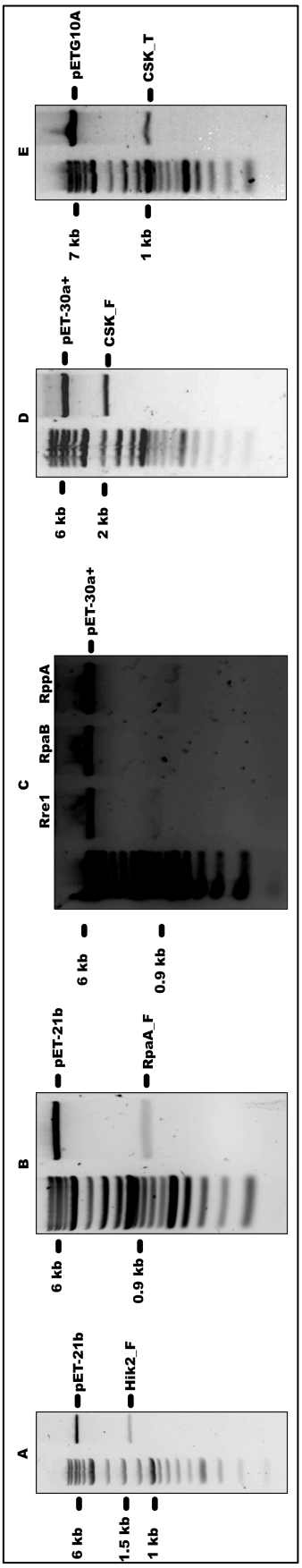

Figure 1 Recombinant plasmid containing the following clones: A) Hik2_F; B) RpaA; C) Rre1, RpaB, and RppA; D); CSK_F; E) CSK_T were double-digested with the appropriate restriction enzymes indicated in the material and method section. DNA size markers are shown on the lift in kb. DNA fragment corresponding to the vector and insert are shown on the right.

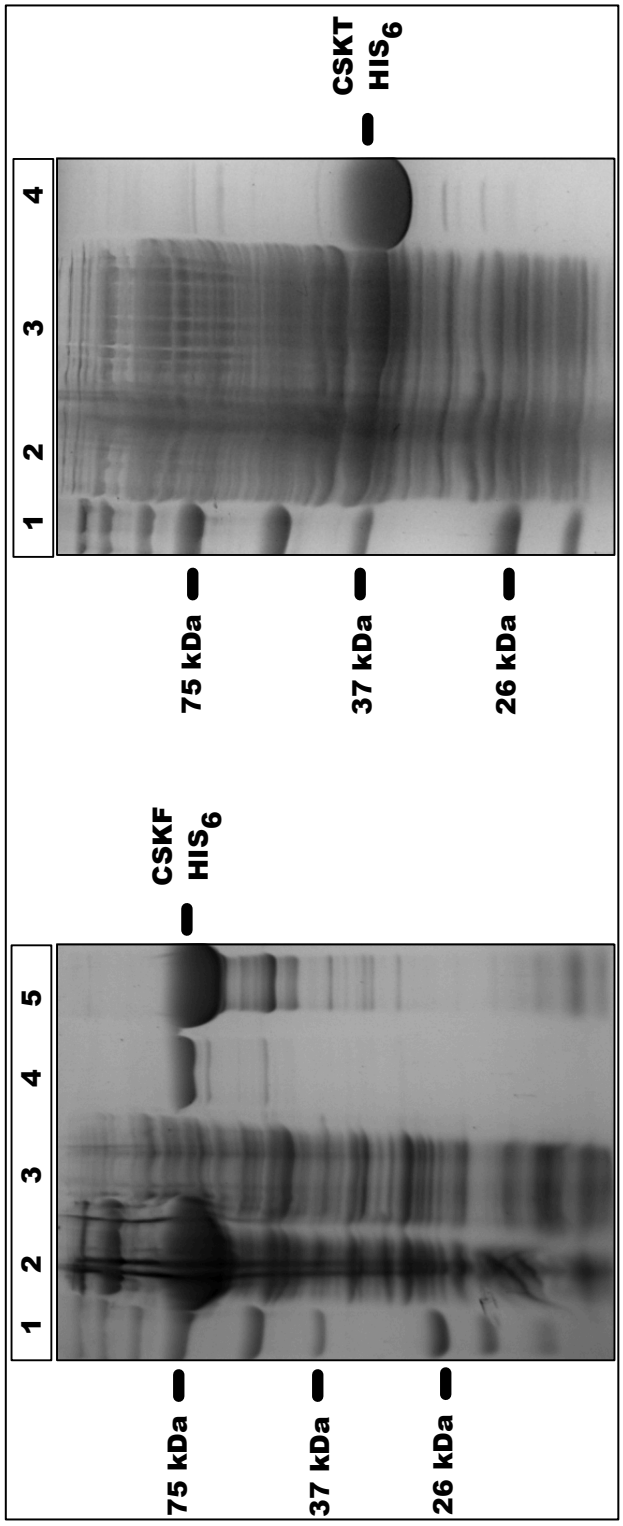

Figure 2. Protein overexpression and purification. The full-length CSK protein was overexpressed and purified as described in the experimental section. The following samples were loaded on a SDS-PAGE 12 %. Lane 1, protein molecular weight marker; lane 2, total cell lysate; lane 3, soluble cell fraction; lane 4 and 5 are elution fraction1. On the left, protein molecular weight markers are shown in kDa. The positions of the overexpressed CSK_F and CSK_T are indicated on the right.

Reference

REFERENCES

Ali JA, Orphanides G, Maxwell A (1995) Nucleotide binding to the 43-kilodalton N-terminal fragment of the DNA gyrase B protein. *Biochemistry* **34:** 9801-9808

Allen JF (1992) Protein-phosphorylation in regulation of photosynthesis. *Biochimica Et Biophysica Acta* **1098:** 275-335

Allen JF (1993a) Control of gene expression by redox potential and the requirement for chloroplast and mitochondrial genomes. *Journal of Theoretical Biology* **165:** 609-631

Allen JF (1993b) Redox control of transcription: sensors, response regulators, activators and repressors. *FEBS Letter* **332:** 203-207

Allen JF (2003a) Botany. State transitions–a question of balance. *Science* **299:** 1530-1532

Allen JF (2003b) The function of genomes in bioenergetic organelles. *Philosophical Transactions of the Royal Society of London Series B, Biological Sciences* **358:** 19-37; discussion 37-18

Allen JF, Bennett J, Steinback KE, Arntzen CJ (1981) Chloroplast protein phosphorylation couples plastoquinone redox state to distribution of excitation energy between photosystems. *Nature* **291:** 25-29

Allen JF, de Paula WB, Puthiyaveetil S, Nield J (2011a) A structural phylogenetic map for chloroplast photosynthesis. *Trends in Plant Sciences* **16:** 645-655

Allen JF, Santabarbara S, Allen CA, Puthiyaveetil S (2011b) Discrete redox signaling pathways regulate photosynthetic light-harvesting and chloroplast gene transcription. *PLoS One* **6:** e26372

Alm E, Huang K, Arkin A (2006) The evolution of two-component systems in bacteria reveals different strategies for niche adaptation. *PLoS computational biology* **2:** e143

Altschul SF, Gish W, Miller W, Myers EW, Lipman DJ (1990) Basic local alignment search tool. *Journal of Molecular Biology* **215:** 403-410

Anand GS, Goudreau PN, Stock AM (1998) Activation of methylesterase CheB: evidence of a dual role for the regulatory domain. *Biochemistry* **37:** 14038-14047

Ashby MK, Houmard J (2006) Cyanobacterial two-component proteins: structure, diversity, distribution, and evolution. *Microbiology and Molecular Biology Reviews* **70:** 472-509

Ashby MK, Houmard J, Mullineaux CW (2002) The ycf27 genes from cyanobacteria and eukaryotic algae: distribution and implications for chloroplast evolution. *FEMS microbiology letters* **214:** 25-30

Attwood PV, Besant PG, Piggott MJ (2011) Focus on phosphoaspartate and phosphoglutamate. *Amino acids* **40:** 1035-1051

Attwood PV, Piggott MJ, Zu XL, Besant PG (2007) Focus on phosphohistidine. *Amino Acids* **32:** 145-156

Ban C, Junop M, Yang W (1999) Transformation of MutL by ATP binding and hydrolysis: a switch in DNA mismatch repair. *Cell* **97:** 85-97

Barnard A, Wolfe A, Busby S (2004) Regulation at complex bacterial promoters: how bacteria use different promoter organizations to produce different regulatory outcomes. *Current Opinion in Microbiology* **7:** 102-108

Bellafiore S, Barneche F, Peltier G, Rochaix JD (2005) State transitions and light adaptation require chloroplast thylakoid protein kinase STN7. *Nature* **433:** 892-895

Bleecker AB, Schaller GE (1996) The Mechanism of Ethylene Perception. *Plant Physiology* **111:** 653-660

Bottcher B, Graber P (2008) Structure of the H+ ATP Synthase from Chloroplasts In *Photosynthetic Protein Complexes: A Structural Approach*, Fromme P (ed), 9, pp 201-216. Germany: Wiley-VCH Verlag GmbH & Co.

Bourret RB, Hess JF, Simon MI (1990) Conserved aspartate residues and phosphorylation in signal transduction by the chemotaxis protein CheY. *Proceedings of the National Academy of Sciences of USA* **87:** 41-45

Browning DF, Cole JA, Busby SJ (2004) Transcription activation by remodelling of a nucleoprotein assembly: the role of NarL at the FNR-dependent Escherichia coli nir promoter. *Molecular Microbiology* **53:** 203-215

Cai SJ, Khorchid A, Ikura M, Inouye M (2003) Probing catalytically essential domain orientation in histidine kinase EnvZ by targeted disulfide crosslinking. *Journal of Molecular Biology* **328:** 409-418

Chakraborty S, Li M, Chatterjee C, Sivaraman J, Leung KY, Mok YK (2010) Temperature and Mg2+ sensing by a novel PhoP-PhoQ two-component system for regulation of virulence in Edwardsiella tarda. *Journal of Biological Chemistry* **285:** 38876-38888

Chan C, Paul R, Samoray D, Amiot NC, Giese B, Jenal U, Schirmer T (2004) Structural basis of activity and allosteric control of diguanylate cyclase. *Proceedings of the National Academy of Sciences of USA* **101:** 17084-17089

Chen T, Liu J, Lei G, Liu YF, Li ZG, Tao JJ, Hao YJ, Cao YR, Lin Q, Zhang WK, Ma B, Chen SY, Zhang JS (2009) Effects of Tobacco Ethylene Receptor mutations on receptor kinase activity, plant growth and stress responses. *Plant & Cell Physiology* **50:** 1636-1650

Chenna R, Sugawara H, Koike T, Lopez R, Gibson TJ, Higgins DG, Thompson JD (2003) Multiple sequence alignment with the Clustal series of programs. *Nucleic Acids Research* **31:** 3497-3500

Cheung J, Hendrickson WA (2010) Sensor domains of two-component regulatory systems. *Current Opinion in Microbiology* **13:** 116-123

Choquet Y, Zito F, Wostrikoff K, Wollman FA (2003) Cytochrome f translation in Chlamydomonas chloroplast is autoregulated by its carboxyl-terminal domain. *Plant Cell* **15:** 1443-1454

Clamp M, Cuff J, Searle SM, Barton GJ (2004) The Jalview Java alignment editor. *Bioinformatics* **20:** 426-427

Cramer WA, Baniulis D, Yamashita E, Zhang H, Zatsman AI, Hendrich MP (2008) Cytochrome b6f Complex, Colon Structure, Spectroscopy, and Function of Heme cn: n-Side Electron and Proton Transfer Reactions. In *Photosynthetic Protein Complexes: A Structural Approach*, Fromme P (ed), 7, pp 155-179. Germany: Wiley-VCH Verlag GmbH & Co.

Delannoy E, Fujii S, Colas des Francs-Small C, Brundrett M, Small I (2011) Rampant gene loss in the underground orchid Rhizanthella gardneri highlights evolutionary constraints on plastid genomes. *Molecular Biology and Evolution* **28:** 2077-2086

Depege N, Bellafiore S, Rochaix JD (2003) Role of chloroplast protein kinase Stt7 in LHCII phosphorylation and state transition in Chlamydomonas. *Science* **299:** 1572-1575

Dereeper A, Guignon V, Blanc G, Audic S, Buffet S, Chevenet F, Dufayard JF, Guindon S, Lefort V, Lescot M, Claverie JM, Gascuel O (2008) Phylogeny.fr: robust phylogenetic analysis for the non-specialist. *Nucleic Acids Research* **36:** W465-469

Erickson JM, Pfister K, Rahire M, Togasaki RK, Mets L, Rochaix JD (1989) Molecular and biophysical analysis of herbicide-resistant mutants of Chlamydomonas reinhardtii: structure-function relationship of the photosystem II D1 polypeptide. *Plant Cell* **1:** 361-371

Fankhauser C, Yeh KC, Lagarias JC, Zhang H, Elich TD, Chory J (1999) PKS1, a substrate phosphorylated by phytochrome that modulates light signaling in Arabidopsis. *Science* **284:** 1539-1541

Ferreira KN, Iverson TM, Maghlaoui K, Barber J, Iwata S (2004) Architecture of the photosynthetic oxygen-evolving center. *Science* **303:** 1831-1838

Filippou PS, Kasemian LD, Panagiotidis CA, Kyriakidis DA (2008) Functional characterization of the histidine kinase of the E. coli two-component signal transduction system AtoS-AtoC. *Biochimica et Biophysica Acta* **1780:** 1023-1031

Finn RD, Mistry J, Schuster-Bockler B, Griffiths-Jones S, Hollich V, Lassmann T, Moxon S, Marshall M, Khanna A, Durbin R, Eddy SR, Sonnhammer EL, Bateman A (2006) Pfam: clans, web tools and services. *Nucleic Acids Research* **34:** D247-251

Fujita Y (1997) A study on the dynamic features of photosystem stoichiometry: Accomplishments and problems for future studies. *Photosynthesis Research* **53:** 83-93

Gamble RL, Coonfield ML, Schaller GE (1998) Histidine kinase activity of the ETR1 ethylene receptor from Arabidopsis. *Proceedings of the National Academy of Sciences of USA* **95:** 7825-7829

Gao R, Stock AM (2009) Biological insights from structures of two-component proteins. *Annual Review of Microbiology* **63:** 133-154

Georgellis D, Kwon O, Lin ECC (2001) Quinones as the redox signal for the Arc two-component system of bacteria. *Science* **292:** 2314-2316

Grabbe R, Schmitz RA (2003) Oxygen control of nif gene expression in Klebsiella pneumoniae depends on NifL reduction at the cytoplasmic membrane by electrons

derived from the reduced quinone pool. *European Journal of Biochemistry* **270:** 1555-1566

Gupta RS (2009) Protein signatures (molecular synapomorphies) that are distinctive characteristics of the major cyanobacterial clades. *International Journal of System Evolutionary Microbiology* **59:** 2510-2526

Hanke GT, Satomi Y, Shinmura K, Takao T, Hase T (2011) A screen for potential ferredoxin electron transfer partners uncovers new, redox dependent interactions. *Biochimica et Biophysica Acta* **1814:** 366-374

Heermann R, Altendorf K, Jung K (1998) The turgor sensor KdpD of Escherichia coli is a homodimer. *Biochimica Et Biophysica Acta-Biomembranes* **1415:** 114-124

Heermann R, Jung K (2010) The complexity of the 'simple' two-component system KdpD/KdpE in Escherichia coli. *FEMS microbiology letters* **304:** 97-106

Hu CD, Chinenov Y, Kerppola TK (2002) Visualization of interactions among bZIP and Rel family proteins in living cells using bimolecular fluorescence complementation. *Molecular Cell* **9:** 789-798

Ibrahim I (2009) Characterizing chloroplast sensor kinase. *Bioscience Horizons* **2:** 191-196

Inoue H, Tsuchiya T, Satoh S, Miyashita H, Kaneko T, Tabata S, Tanaka A, Mimuro M (2004) Unique constitution of photosystem I with a novel subunit in the cyanobacterium Gloeobacter violaceus PCC 7421. *FEBS Lett* **578:** 275-279

Ioanoviciu A, Yukl ET, Moenne-Loccoz P, de Montellano PR (2007) DevS, a heme-containing two-component oxygen sensor of Mycobacterium tuberculosis. *Biochemistry* **46:** 4250-4260

Ivleva NB, Gao T, LiWang AC, Golden SS (2006a) Quinone sensing by the circadian input kinase of the cyanobacterial circadian clock. *Proceedings of the National Academy of Sciences of USA* **103:** 17468-17473

Ivleva NB, Gao TY, LiWang AC, Golden SS (2006b) Quinone sensing by the circadian input kinase of the cyanobacterial circadian clock. *Proceedings of the National Academy of Sciences of USA* **103:** 17468-17473

Kaneko T, Sato S, Kotani H, Tanaka A, Asamizu E, Nakamura Y, Miyajima N, Hirosawa M, Sugiura M, Sasamoto S, Kimura T, Hosouchi T, Matsuno A, Muraki A, Nakazaki N, Naruo K, Okumura S, Shimpo S, Takeuchi C, Wada T, Watanabe A, Yamada M, Yasuda M, Tabata S (1996) Sequence analysis of the genome of the unicellular cyanobacterium Synechocystis sp. strain PCC6803. II. Sequence determination of the entire genome and assignment of potential protein-coding regions (supplement). *DNA Research* **3:** 185-209

Kraus N, . (2008) structure of cyanobacterial photosystem I In *Photosynthetic Protein Complexes: A Structural Approach*, Fromme P (ed), 2, pp 24-65. Germany: Wiley-VCH Verlag GmbH & Co.

Kurisu G, Zhang H, Smith JL, Cramer WA (2003) Structure of the cytochrome b6f complex of oxygenic photosynthesis: tuning the cavity. *Science* **302:** 1009-1014

Laemmli UK (1970) Cleavage of structural proteins during assembly of head of bacteriophage-T4. *Nature* **227:** 680-685

Lapid C, Gao Y. (2011) PrimerX. http://www.bioinformatics.org/primerx/index.htm.

Lasker MV, Thai P, Besant PG, Bui CD, Naidu S, Turck CW (2002) Branched-chain 6-ketoacid dehydrogenase kinase: A mammalian enzyme with histidine kinase activity. *Journal of Biomolecular Techniques* **13:** 238-245

Li H, Sherman LA (2000) A redox-responsive regulator of photosynthesis gene expression in the cyanobacterium Synechocystis sp strain PCC 6803. *Journal of Bacteriology* **182:** 4268-4277

Li WW, Heinze J, Haehnel W (2005) Site-specific binding of quinones to proteins through thiol addition and addition-elimination reactions. *Journal of the American Chemical Society* **127:** 6140-6141

Lopez-Maury L, Garcia-Dominguez M, Florencio FJ, Reyes JC (2002) A two-component signal transduction system involved in nickel sensing in the cyanobacterium Synechocystis sp. PCC 6803. *Molecular Microbiology* **43:** 247-256

Los DA, Zorina A, Sinetova M, Kryazhov S, Mironov K, Zinchenko VV (2010) Stress sensors and signal transducers in cyanobacteria. *Sensors* **10:** 2386-2415

Malpica R, Franco B, Rodriguez C, Kwon O, Georgellis D (2004) Identification of a quinone-sensitive redox switch in the ArcB sensor kinase. *Proceedings of the National Academy of Sciences of USA* **101:** 13318-13323

Marin K, Suzuki L, Yamaguchi K, Ribbeck K, Yamamoto H, Kanesaki Y, Hagemann M, Murata N (2003) Identification of histidine kinases that act as sensors in the perception of salt stress in Synechocystis sp PCC 6803. *Proceedings of the National Academy of Sciences of USA* **100:** 9061-9066

Marina A, Mott C, Auyzenberg A, Hendrickson WA, Waldburger CD (2001) Structural and mutational analysis of the PhoQ histidine kinase catalytic domain. Insight into the reaction mechanism. *The Journal of Biological Chemistry* **276:** 41182-41190

Maris AE, Sawaya MR, Kaczor-Grzeskowiak M, Jarvis MR, Bearson SM, Kopka ML, Schroder I, Gunsalus RP, Dickerson RE (2002) Dimerization allows DNA target site recognition by the NarL response regulator. *Nature Structure Biology* **9:** 771-778

Mary I, Vaulot D (2003) Two-component systems in Prochlorococcus MED4: genomic analysis and differential expression under stress. *FEMS microbiology letters* **226:** 135-144

Mascher T, Helmann JD, Unden G (2006) Stimulus perception in bacterial signal-transducing histidine kinases. *Microbiology and Molecular Biology Review* **70:** 910-938

Massazza DA, Parkinson JS, Studdert CA (2011) Cross-Linking Evidence for Motional Constraints within Chemoreceptor Trimers of Dimers. *Biochemistry* **50:** 820-827

Matsuzaki M, Misumi O, Shin-I T, Maruyama S, Takahara M, Miyagishima SY, Mori T, Nishida K, Yagisawa F, Nishida K, Yoshida Y, Nishimura Y, Nakao S, Kobayashi T, Momoyama Y, Higashiyama T, Minoda A, Sano M, Nomoto H, Oishi K, Hayashi H, Ohta F, Nishizaka S, Haga S, Miura S, Morishita T, Kabeya Y, Terasawa K, Suzuki Y, Ishii Y, Asakawa S, Takano H, Ohta N, Kuroiwa H, Tanaka K, Shimizu N, Sugano S, Sato N, Nozaki H, Ogasawara N, Kohara Y, Kuroiwa T (2004) Genome sequence of the ultrasmall unicellular red alga Cyanidioschyzon merolae 10D. *Nature* **428:** 653-657

Miyatake H, Mukai M, Park SY, Adachi S, Tamura K, Nakamura H, Nakamura K, Tsuchiya T, Iizuka T, Shiro Y (2000) Sensory mechanism of oxygen sensor FixL from Rhizobium meliloti: crystallographic, mutagenesis and resonance Raman spectroscopic studies. *Journal of Molecular Biology* **301:** 415-431

Moglich A, Yang X, Ayers RA, Moffat K (2010) Structure and function of plant photoreceptors. *Annual Review of Plant Biology* **61:** 21-47

Motulsky H, Christopoulos A (2003) *Fitting models to biological data using linear and nonlinear regression. A practical guide to curve fitting*, San Diego, CA: GraphPad Software Inc, http://www.graphpad.com.

Moussatche P, Klee HJ (2004) Autophosphorylation activity of the Arabidopsis ethylene receptor multigene family. *The Journal of Biological Chemistry* **279:** 48734-48741

Moxley MA, Tanner JJ, Becker DF (2011) Steady-state kinetic mechanism of the proline:ubiquinone oxidoreductase activity of proline utilization A (PutA) from Escherichia coli. *Archives of Biochemistry and Biophysics* **516:** 113-120

Muller P, Li XP, Niyogi KK (2001) Non-photochemical quenching. A response to excess light energy. *Plant Physiology* **125:** 1558-1566

Murakami A, Kim SJ, Fujita Y (1997) Changes in photosystem stoichiometry in response to environmental conditions for cell growth observed with the cyanophyte Synechocystis PCC 6714. *Plant and Cell Physiology* **38:** 392-397

Nelson N, Ben-Shem A (2004) The complex architecture of oxygenic photosynthesis. *Nature Review Molecular Cell Biology* **5:** 971-982

Ortiz de Orue Lucana D, Groves MR (2009) The three-component signalling system HbpS-SenS-SenR as an example of a redox sensing pathway in bacteria. *Amino Acids* **37:** 479-486

Paithoonrangsarid K, Shoumskaya MA, Kanesaki Y, Satoh S, Tabata S, Los DA, Zinchenko VV, Hayashi H, Tanticharoen M, Suzuki I, Murata N (2004) Five histidine kinases perceive osmotic stress and regulate distinct sets of genes in Synechocystis. *The Journal of Biological Chemistry* **279:** 53078-53086

Pan SQ, Charles T, Jin SG, Wu ZL, Nester EW (1993) Preformed Dimeric State of the Sensor Protein Vira Is Involved in Plant-Agrobacterium Signal-Transduction. *Proceedings of the National Academy of Sciences of USA* **90:** 9939-9943

Panaretou B, Prodromou C, Roe SM, O'Brien R, Ladbury JE, Piper PW, Pearl LH (1998) ATP binding and hydrolysis are essential to the function of the Hsp90 molecular chaperone in vivo. *EMBO Journal* **17:** 4829-4836

Pfannschmidt T (2003) Chloroplast redox signals: how photosynthesis controls its own genes. *Trends in Plant Science* **8:** 33-41

Pfannschmidt T, Nilsson A, Allen JF (1999) Photosynthetic control of chloroplast gene expression. *Nature* **397:** 625-628

Plesniak L, Horiuchi Y, Sem D, Meinenger D, Stiles L, Shaffer J, Jennings PA, Adams JA (2002) Probing the nucleotide binding domain of the osmoregulator EnvZ using fluorescent nucleotide derivatives. *Biochemistry* **41:** 13876-13882

Puthiyaveetil S, Allen JF (2009) Chloroplast two-component systems: evolution of the link between photosynthesis and gene expression. *Proceedings of the Royal Society B-Biological Sciences* **276:** 2133-2145

Puthiyaveetil S, Ibrahim IM, Allen JF (2012) Oxidation-reduction signalling components in regulatory pathways of state transitions and photosystem stoichiometry adjustment in chloroplasts. *Plant, Cell and Environment* **35:** 347–359

Puthiyaveetil S, Ibrahim IM, Jelicic B, Tomasic A, Fulgosi H, Allen JF (2010) Transcriptional control of photosynthesis genes: the evolutionarily conserved regulatory mechanism in plastid genome function. *Genome Biology and Evolution* **2:** 888-896

Puthiyaveetil S, Kavanagh TA, Cain P, Sullivan JA, Newell CA, Gray JC, Robinson C, van der Giezen M, Rogers MB, Allen JF (2008) The ancestral symbiont sensor kinase CSK links photosynthesis with gene expression in chloroplasts. *Proceedings of the National Academy of Sciences of USA* **105:** 10061-10066

Roca J, Wang JC (1992) The capture of a DNA double helix by an ATP-dependent protein clamp: a key step in DNA transport by type II DNA topoisomerases. *Cell* **71:** 833-840

Rochaix JD (2007) Role of thylakoid protein kinases in photosynthetic acclimation. *FEBS Letter* **581:** 2768-2775

Ryjenkov DA, Tarutina M, Moskvin OV, Gomelsky M (2005) Cyclic diguanylate is a ubiquitous signaling molecule in bacteria: insights into biochemistry of the GGDEF protein domain. *Journal of Bacteriology* **187:** 1792-1798

Sato S, Shimoda Y, Muraki A, Kohara M, Nakamura Y, Tabata S (2007) A large-scale protein protein interaction analysis in Synechocystis sp. PCC6803. *DNA Research* **14:** 207-216

Scheu PD, Liao YF, Bauer J, Kneuper H, Basche T, Unden G, Erker W (2010) Oligomeric sensor kinase DcuS in the membrane of Escherichia coli and in proteoliposomes: chemical cross-linking and FRET spectroscopy. *Journal of Bacteriology* **192:** 3474-3483

Schneider CA, Rasband WS, Eliceiri KW (2012) NIH Image to ImageJ: 25 years of image analysis. *Nature Methods* **9:** 671-675

Schultz J, Milpetz F, Bork P, Ponting CP (1998) SMART, a simple modular architecture research tool: identification of signaling domains. *Proceedings of the National Academy of Sciences of USA* **95:** 5857-5864

Seki A, Hanaoka M, Akimoto Y, Masuda S, Iwasaki H, Tanaka K (2007) Induction of a group 2 sigma factor, RPOD3, by high light and the underlying mechanism in Synechococcus elongatus PCC 7942. *The Journal of Biological Chemistry* **282:** 36887-36894

Sevvana M, Vijayan V, Zweckstetter M, Reinelt S, Madden DR, Herbst-Irmer R, Sheldrick GM, Bott M, Griesinger C, Becker S (2008) A ligand-induced switch in the periplasmic domain of sensor histidine kinase CitA. *Journal of Molecular Biology* **377:** 512-523

Shi L (2004) Manganese-dependent protein O-phosphatases in prokaryotes and their biological functions. *Frontiers in Bioscience* **9:** 1382-1397

Shimizu M, Kato H, Ogawa T, Kurachi A, Nakagawa Y, Kobayashi H (2010) Sigma factor phosphorylation in the photosynthetic control of photosystem stoichiometry. *Proceedings of the National Academy of Sciences of USA* **107:** 10760-10764

Silverstein T, Cheng L, Allen JF (1993a) Chloroplast thylakoid protein phosphatase reactions are redox-independent and kinetically heterogeneous. *FEBS Letter* **334:** 101-105

Silverstein T, Cheng LL, Allen JF (1993b) Redox titration of multiple protein phosphorylations in pea chloroplast thylakoids. *Biochimica Et Biophysica Acta* **1183:** 215-220

Skerker JM, Perchuk BS, Siryaporn A, Lubin EA, Ashenberg O, Goulian M, Laub MT (2008) Rewiring the specificity of two-component signal transduction systems. *Cell* **133:** 1043-1054

Stewart RC, VanBruggen R, Ellefson DD, Wolfe AJ (1998) TNP-ATP and TNP-ADP as probes of the nucleotide binding site of CheA, the histidine protein kinase in the chemotaxis signal transduction pathway of Escherichia coli. *Biochemistry* **37:** 12269-12279

Steyn AJ, Joseph J, Bloom BR (2003) Interaction of the sensor module of Mycobacterium tuberculosis H37Rv KdpD with members of the Lpr family. *Molecular Microbiology* **47:** 1075-1089

Stock AM, Mottonen JM, Stock JB, Schutt CE (1989) Three-dimensional structure of CheY, the response regulator of bacterial chemotaxis. *Nature* **337:** 745-749

Stock AM, Robinson VL, Goudreau PN (2000) Two-component signal transduction. *Annual Review of Biochemistry* **69:** 183-215

Surette MG, Levit M, Liu Y, Lukat G, Ninfa EG, Ninfa A, Stock JB (1996) Dimerization is required for the activity of the protein histidine kinase CheA that mediates signal transduction in bacterial chemotaxis. *Journal of Biological Chemistry* **271:** 939-945

Swem LR, Kraft BJ, Swem DL, Setterdahl AT, Masuda S, Knaff DB, Zaleski JM, Bauer CE (2003) Signal transduction by the global regulator RegB is mediated by a redox-active cysteine. *EMBO Journal* **22:** 4699-4708

Taniguchi Y, Takai N, Katayama M, Kondo T, Oyama T (2010) Three major output pathways from the KaiABC-based oscillator cooperate to generate robust circadian kaiBC expression in cyanobacteria. *Proceedings of the National Academy of Sciences of USA* **107:** 3263-3268

Thelen JJ, Miernyk JA, Randall DD (2000) Pyruvate dehydrogenase kinase from Arabidopsis thaliana: a protein histidine kinase that phosphorylates serine residues. *Biochemical Journal* **349:** 195-201

Trajtenberg F, Grana M, Ruetalo N, Botti H, Buschiazzo A (2010) Structural and Enzymatic Insights into the ATP Binding and Autophosphorylation Mechanism of a Sensor Histidine Kinase. *Journal of Biological Chemistry* **285:** 24892-24903

Vidal R, Lopez-Maury L, Guerrero MG, Florencio FJ (2009) Characterization of an alcohol dehydrogenase from the Cyanobacterium Synechocystis sp. strain PCC 6803 that responds to environmental stress conditions via the Hik34-Rre1 two-component system. *Journal of Bacteriology* **191:** 4383-4391

Vitry de C, Olive J, Drapier D, Recouvreur M, Wollman FA (1989) Posttranslational events leading to the assembly of photosystem II protein complex: a study using

photosynthesis mutants from Chlamydomonas reinhardtii. *Journal of Cell Biology* **109:** 991-1006

Volkman BF, Nohaile MJ, Amy NK, Kustu S, Wemmer DE (1995) Three-dimensional solution structure of the N-terminal receiver domain of NTRC. *Biochemistry* **34:** 1413-1424

Volz K, Matsumura P (1991) Crystal structure of Escherichia coli CheY refined at 1.7-A resolution. *Journal of Biological Chemistry* **266:** 15511-15519

Wang LC, Morgan LK, Godakumbura P, Kenney LJ, Anand GS (2012) The inner membrane histidine kinase EnvZ senses osmolality via helix-coil transitions in the cytoplasm. *The EMBO journal* **31:** 2648-2659

Wood TL, Bridwell-Rabb J, Kim YI, Gao T, Chang YG, LiWang A, Barondeau DP, Golden SS (2010) The KaiA protein of the cyanobacterial circadian oscillator is modulated by a redox-active cofactor. *Proceedings of the National Academy of Sciences of USA* **107:** 5804-5809

Wu JA, Bauer CE (2010) RegB Kinase Activity Is Controlled in Part by Monitoring the Ratio of Oxidized to Reduced Ubiquinones in the Ubiquinone Pool. *Mbio* **1**

Zerges W (2002) Does complexity constrain organelle evolution? *Trends in Plant Science* **7:** 175-182

Zhou YF, Nan B, Nan J, Ma Q, Panjikar S, Liang YH, Wang Y, Su XD (2008) C4-dicarboxylates sensing mechanism revealed by the crystal structures of DctB sensor domain. *Journal of Molecular Biology* **383:** 49-61